UNIVERSITÀ
DEGLI STUDI
FIRENZE

DOTTORATO DI RICERCA IN
AREA DEL FARMACO E TRATTAMENTI INNOVATIVI

CICLO XXXVII

Novel pharmacological options for cardiac hypertrophy: a functional study in human myocardium

Settore Scientifico Disciplinare
BIOS-11/A

Dottoranda
Dott.ssa Musumeci Monica

Supervisore
Prof.ssa Sartiani Laura

Co-Supervisore
Dott. Coppini Raffaele

Coordinatore
Prof. Di Cesare Mannelli Lorenzo

ANNO: 2023/2024

INDEX

1. INTRODUCTION **1**

1.1. Cardiac hypertrophy 1

1.1.1. Concentric and eccentric hypertrophy 3

1.2. Mechanisms of physiological hypertrophy 4

1.3. Mechanisms of pathological hypertrophy 6

1.4. Cardiac hypertrophy is a result of different tissue components 9

1.4.1. Hypertrophy at cardiomyocyte level 10

1.4.1.1. Ca^{2+} handling 10

1.4.2. Inflammation and pro-inflammatory cytokines 12

1.5. Extracellular matrix and fibrosis 13

1.5.1. Fibroblast 15

1.5.2. Myofibroblast 17

1.6. Primary hypertrophy and Secondary hypertrophy 20

1.6.1. Primary hypertrophy 20

1.6.1.1. Hypertrophic Cardiomyopathy 20

1.6.1.2. Fibrosis in HCM 28

1.6.1.3. Diagnosis 28

1.6.2. Secondary hypertrophy 30

1.6.2.1. Diagnosis 34

1.7. Pharmacological treatments 40

1.7.1. Primary hypertrophy 40

1.7.2. Secondary hypertrophy 43

2. AIM **49**

3. MATERIALS AND METHODS **51**

3.1. Cardiomyocytes isolation from human surgical samples 51

3.1.1. Electrophysiological evaluation using patch clamp measurements 53

3.1.2. Ca^{2+} handling evaluation using fluorescence dyes 55

3.2. Long-term culture and characterization of human cardiac fibroblasts 56

3.3. Fibroblasts differentiation protocol from pluripotent stem cells 57

4. RESULTS **59**

4.1. Electrophysiological evaluation of human ventricular cardiomyocytes from patient whit primary and secondary hypertrophy 59
4.2. Evaluation of Cibenzoline in patients with HCM 67
4.3. Evaluation of Dapagliflozin in patients with HCM and AoS 82
4.4. Studies on human cardiac fibroblasts from hypertrophic myocardial samples 90

5. DISCUSSION 97

5.1. Electrophysiological evaluation of human ventricular cardiomyocytes from patient whit primary and secondary hypertrophy 97
5.2. Evaluation of Cibenzoline in patients with HCM 99
5.3. Evaluation of Dapagliflozin in patients with HCM and AoS 101
5.4. Studies on human cardiac fibroblasts from hypertrophic myocardial samples 102

REFERENCES 105

1.INTRODUCTION

1.1Cardiac hypertrophy

The main function of the heart is to maintain perfusion of peripheral organs, adapting blood flow to their demand under both normal and stress conditions. To work efficiently, the heart tissue has a complex structure and architecture; fibres alignment, cell to cell interactions, cardiomyocytes organization and extracellular matrix composition made the heart the most complex and efficient unit of the human body.

Cardiac hypertrophy is a condition that may affect the entire heart and usually occurs as a response to high blood requirement by peripheral organs, increased preload or afterload, which are able to induce the heart tissue and in particular the cardiomyocytes to undergo enlargement (Nakamura M. et al., 2018). Despite cardiomyocytes play a fundamental role in the development of cardiac hypertrophy, other cardiac cell phenotypes are usually involved, such as fibroblasts, endothelial cells and smooth muscle cells, which are all fundamental for cardiac function and are also responsible for pathologic alterations of the cardiac architecture (Gupta S. et al., 2007).

As previously mentioned, cardiac hypertrophy is a reactive condition to increased cardiac workload or stress. It initially enhances cardiac contractility by adding sarcomeric units in parallel; the consequent increased thickness of left ventricular wall is able to reduce wall stress, thereby preserving cardiac efficiency.

Cardiac hypertrophy can be classified as physiological, when associated with normal cardiac function, or as pathological when associated with cardiac dysfunction (Shimizu I. et al., 2016). Physiological enlargement of the heart occurs through hypertrophy of cardiomyocytes in response to body growth or physical exercise. This process, known as physiological hypertrophy, is characterized by a proportional increase in the size of cardiomyocytes (cardiac muscle cells) and their structural components, without significant alterations in cardiac function or heart architecture. This form of adaptation is considered a healthy and reversible response, which enhances the heart ability to temporary handle increases of workload. Therefore, physiological hypertrophy is not associated with an increased risk of heart failure or other cardiovascular complications. Conversely, pathological hypertrophy represents a maladaptive response of the heart to chronic stress conditions, such as hypertension or valvular heart diseases. This type of hypertrophy is characterized by a heterogeneous increase of cardiomyocyte size, with alterations of

structural proteins, mitochondrial dysfunction, increase of interstitial fibrosis with increased levels of type I collagen, activation of myofibroblasts and changes in gene expression. Moreover, pathological hypertrophy can lead to adverse cardiac remodelling, with thickening and stiffening of the ventricular walls, which impairs heart ability to fill and pump blood effectively. This condition is associated with a significantly increased risk of developing heart failure, arrhythmias, myocardial ischemia, and sudden cardiac death. In particular, the cardiac phenotype of pathological hypertrophy may manifest as heart failure with preserved ejection fraction (HFpEF) or heart failure with reduced ejection fraction (HFrEF) (Shimizu I. et al., 2016).

The development of either physiological or pathological hypertrophy is determined by the specific nature of upstream stimuli and signalling mechanisms, rather than the duration of cardiac stress. For instance, intermittent pressure overload leads to pathological hypertrophy, whereas physical training, which is also an intermittent stimulus, results in physiological hypertrophy.

From a physiological perspective, cardiac growth is observed postnatally, during pregnancy, and in athletes. Physiological hypertrophy can often reverse, thus preventing cardiac remodelling and failure. Pathological hypertrophy, on the other hand, is triggered by chronic conditions such as hypertension, aortic stenosis, mitral or aortic regurgitation, myocardial infarction (MI), storage diseases (including lipid, glycogen and misfolded protein storage diseases) and genetic cardiomyopathies caused by mutations in sarcomere protein genes, such as hypertrophic cardiomyopathy (HCM). In developed countries, obesity and diabetes mellitus are significant comorbidities associated with the development of pathological hypertrophy (Nakamura M. et al., 2018).

The hypertrophic response of the cardiac tissue can manifest in different forms, depending on the nature and duration of the underlying causes leading to distinct patterns: concentric and eccentric hypertrophy.

1.1.1 Concentric and eccentric hypertrophy

The cardiac tissue has a precise structure and organization that allow blood flow through the chambers to the main vessels; change of size or number of cardiomyocytes modify also the dynamic of the blood flow through the cardiovascular system. When cardiac hypertrophy occurs, the specific type of cardiac tissue alteration is determined by the initial pathological stimulus (Shimizu I. et al., 2016). In fact, the geometry of hypertrophy is determined by the direction of cardiomyocyte enlargement, adding sarcomeres in parallel or in series. In the first case the hypertrophy is eccentric, cardiac walls are thinned, and chamber volume is increased, while adding sarcomere in series leads to wall thickening and chamber volume reduction. Chronic left ventricular (LV) pressure overload causes mainly concentric hypertrophy, while chronic LV volume overload is characterised by chamber enlargement and an eccentric pattern of hypertrophy. In aortic stenosis and hypertension, we observe a concentric hypertrophic growth, while eccentric hypertrophy occurs in aortic or mitral insufficiency, whereas asymmetric hypertrophy is a characteristic feature of genetic determined hypertrophy.

Since concentric hypertrophy refers to an increase in cardiac mass and a reduction of chamber volumes, eccentric hypertrophy refers to an increase in sarcomere length and chamber volumes, responsible for chamber dilatation. These are typical conditions of a disease called dilated cardiomyopathy (Grossman et al., 1975).

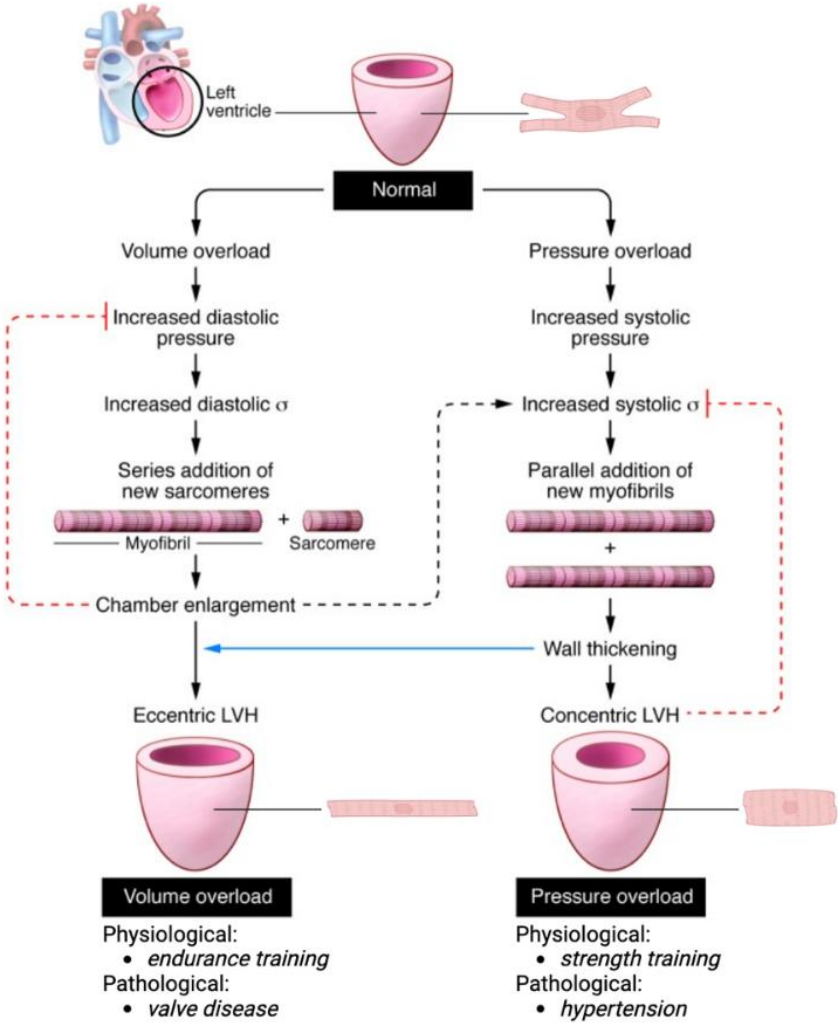

Figure 1: *Schematic overview of the development of concentric and eccentric hypertrophy (modified by Grossman W., Paulus WJ., 2013).*

1.2 Mechanisms of physiological hypertrophy

As previously mentioned, hypertrophic stimuli, such as exercise and pregnancy, influence the development of physiological hypertrophy. To this aim, a central role is played by the physiological increase of oxygen demand from peripheral organs that triggers different responses such as increased energy production and efficiency, proliferation and regeneration of cardiomyocytes, cell survival, angiogenesis, changes in mitochondrial function, metabolism and antioxidant systems.

Pregnancy-induced cardiac hypertrophy is a consequence of increased circulating volume and higher cardiac output during mid-to-late pregnancy. Hypertrophic remodelling in an uncomplicated pregnancy is a reversible event after the newborn birth. During pregnancy, the body increased metabolic demands lead to changes in both circulating substrates and

heart metabolism. Levels of free fatty acids, triglycerides, ketone bodies, and lactate rise, resulting in greater uptake and utilization of these substances by cardiac metabolism; conversely, glucose metabolism in the heart decreases during this period (Fulghum KL. et al., 2022).

Cardiac metabolic changes associated with adaptation to chronic physical exercise differ significantly from those observed during short periods of intense physical activity, with most research focusing on the latter context. Exercise-induced cardiac hypertrophy is correlated with an improvement in mitochondrial function. Although studies on cardiac substrate metabolism post-exercise have given heterogeneous results, a consistent finding is glucose oxidation. Additionally, changes are observed in the increase and decrease of fatty acid oxidation (FAO) in response to chronic exercise (Qiu Y. et al., 2022).

Several growth factors are reported to regulate physiological cardiac hypertrophy, and comprise a multitude of endogenous molecules including insulin-like growth factor 1 (IGF-1), hepatocyte growth factor (HGF), vascular endothelial growth factor (VEGF), platelet-derived growth factor (PDGF), and neuregulin-1 (NRG1) (Koziris LP.et al., 2022; Bersell K. et al., 2009).

Insulin and insulin-like growth factor 1 (IGF-1) are proteins with a crucial role in metabolism and cell growth. They regulate different signalling pathways in the heart, including apoptosis, contractility, metabolism, proliferation and differentiation (Yoshida T. et al., 2020). Alterations of IGF-1 concentrations in serum are associated with an increased risk of cardiovascular disease. For instance, heart failure is correlated with insulin resistance; IGF-1, which structure is similar to insulin, is synthesized in the liver in response to growth hormone. Insulin resistance or deficiency cause dysregulation of these processes and lead to an increase of fasting and postprandial glucose, as well as of lipid blood levels. Insulin increases glucose uptake into cells by stimulating the translocation of the glucose transporter GLUT4 from intracellular sites to the cell surface. Furthermore, IGF-1 is generally recognized for its cardioprotective role. Many studies have demonstrated that IGF-1 can protect cardiomyocytes from oxidative stress and improve cardiac function following myocardial infarction. Specifically, IGF-1 has been observed to reduce cardiomyocyte apoptosis and promote cardiac tissue regeneration, thereby contributing to the recovery of cardiac function after infarction (Bass-Stringer S. et al., 2021). Additionally, IGF-1 facilitates the activation of signalling pathways that enhance cell survival and reduce

oxidative damage, supporting the heart resilience to ischemic and oxidative insults. These properties make IGF-1 a promising therapeutic target for the protection and recovery of the heart under pathological stress conditions (Vinciguerra M. et al., 2010).

Vascular endothelial growth factor (VEGF) is crucial for the development and maintenance of cardiac hypertrophy, especially for its role in promoting angiogenesis and the formation of new blood vessels. This process is essential to support the increase in cardiac mass with proper vascularization, thereby ensuring a sufficient supply of oxygen and nutrients to the cardiomyocytes. During physiological cardiac hypertrophy, VEGF facilitates vascular adaptation by promoting the growth of new capillaries in cardiac tissue (Gogiraju R. et al., 2019). Furthermore, under hypoxic conditions, which are common in pathological cardiac hypertrophy, VEGF is positively regulated by transcription factors such as HIF-1 (hypoxia-inducible factor 1), which stimulates its production to improve tissue perfusion and reduce hypoxic stress (Ferrara, 2004). Thus, VEGF plays a protective and adaptive role in physiological cardiac hypertrophy, differing significantly from the mechanisms involved in pathological hypertrophy, a condition where angiogenesis may be dysfunctional (Izumiya et al., 2006). Finally, VEGF has a key role in the adaptation of the heart to exercise-induced increased workload, promoting both angiogenesis and cardiomyocyte survival, and is critical for cardiovascular health during physiological cardiac hypertrophy.

Platelet-derived growth factor (PDGF) also plays a key role in physiological cardiac hypertrophy. PDGF is involved in the regulation of cellular processes critical for the maintenance of cardiac function. Specifically, PDGF promotes proliferation and survival of cardiac fibroblasts and myocytes, facilitating structural and functional adaptations of cardiac muscle. Through its signalling pathways, PDGF contributes to extracellular matrix remodelling and maintenance of proper myocardial architecture, which supports increased cardiac mass and workload. This growth factor helps ensure that the heart remains well vascularized and able to meet high metabolic demands, thus preventing the transition from physiological to pathological hypertrophy (Qiu Y. et al., 2022).

1.3 Mechanisms of pathological hypertrophy

Since, physiological cardiac hypertrophy is characterized by a reversible adaptation of the heart to physiological stimuli, prolonged cardiac stress can lead to an apparently irreversible cardiac hypertrophy that became pathological. Moreover, excessive activation of neuro-

humoral mechanisms is associated with cardiac dysfunction and is referred to as "pathological hypertrophy." In this context, the proteins that act as mechano-transductors are crucial and their dysregulation promote the occurrence of pathological hypertrophy (Shimizu I. et al., 2016).

Events that lead to remodelling of the heart tissue and cause heart failure are associated with alterations in intracellular calcium (Ca^{2+}) homeostasis and changes in electrophysiological properties. Prominent morphological alterations associated with these events include increased apoptosis, fibrosis and dilatation of the chamber. These alterations are similarly observed in aortic stenosis and specific types of inherited forms of cardiomyopathy, such as hypertrophic and dilated cardiomyopathy, suggesting the occurrence of similar mechanisms (Hill JA., 2008).

The increase of Ca^{2+} levels in cardiomyocytes, trigger the activity of several Ca^{2+}-dependent signalling pathways, including the calcineurin/nuclear factor of activated T cells (NFAT) signalling and calmodulin-dependent kinase II signalling.

Calcineurin is a protein phosphatase that acts on serine and threonine and is activated by Ca^{2+} ions. This enzyme dephosphorylates NFAT in the cytoplasm, leading to its translocation into the nucleus and stimulating the expression of genes involved in hypertrophy. Activation of the calcineurin/NFAT signalling pathway alone is sufficient to induce pathological cardiac hypertrophy (Wilkins BJ et al., 2004).

Other main actors are transient receptor potential cation channel (TRPC). TRP channels are a subset of the TRP ion channel family, known for their permeability to Ca^{2+} and other cations. These channels can be activated by a variety of stimuli, such as changes in Ca^{2+} levels and second messengers like diacylglycerol (DAG). In the context of pathological cardiac hypertrophy, TRPC channels often become upregulated or hyperactivated, leading to increased Ca^{2+} influx into cardiomyocytes. This influx contributes to cellular growth and hypertrophy. The activation of TRPC channels is frequently associated with mechanical and biochemical stress signals, including those from the Angiotensin II receptor and other pro-hypertrophic pathways. Additionally, TRPC channels interact with other signalling pathways, such as the calcineurin/NFAT pathway, which further modulates pathological hypertrophy or heart failure (Seth M. et al., 2009).

Several studies have demonstrated that Angiotensin II activates phospholipase C (PLC), resulting in the hydrolysis of phosphatidylinositol 4,5-bisphosphate to produce

diacylglycerol (DAG) and inositol 1,4,5-trisphosphate (IP3). DAG subsequently activates protein kinase C (PKC), which promotes hypertrophic effects, leading to cardiac growth. This hypertrophic response to Angiotensin II triggers the activation of mitogen-activated protein kinases (MAPKs), including extracellular signal-regulated kinases (ERKs), c-Jun N-terminal kinases (JNKs), and p38-MAPKs. These MAPKs enhance the signal transducer and activator of transcription (STAT) pathway and other intracellular kinases, including both receptor and non-receptor tyrosine kinases. Additionally, Angiotensin II stimulates several downstream signalling pathways, such as MAPK/ERK and Ras/Rho, and causes MAPKs to translocate into the nucleus. It is also observed that various signalling pathways connect the AT1 receptor to the Gq-independent activation of phospho-extracellular signal-regulated kinase (p-ERK) 1/2 by Angiotensin II, promoting cell growth. Furthermore, cardiac hypertrophy is associated with increased intracellular Ca^{2+} levels due to the activation of the AT1 receptor (AT1R). Specifically, the coupling of AT1R with Gq/11-PLCβ generates IP3, which binds to its receptor and releases Ca^{2+} from the sarcoplasmic reticulum. Additionally, the activation of sarcolemmal Ca^{2+} channels by AT1R raises cytosolic Ca^{2+} concentrations. There is a significant correlation between sustained Ca^{2+} release and cell growth, suggesting these processes are closely linked, and indeed, Ca^{2+} is essential for Angiotensin II-induced cardiac hypertrophy (Bhullar SK et al., 2022). However, Angiotensin II can induce an increase in the production of reactive oxygen species (ROS) in cardiomyocytes, contributing to the hypertrophic response. Initially, the transient increase in Angiotensin II levels activates redox-sensitive mechanisms that facilitate adaptive cardiac hypertrophy. However, prolonged exposure to elevated levels of Angiotensin II leads to an imbalance between pro and antioxidants, resulting in excessive ROS production in the hypertrophic myocardium (Shah AK. et al., 2021). This imbalance is associated with a significant depression of cardiac function and the progression towards heart failure.

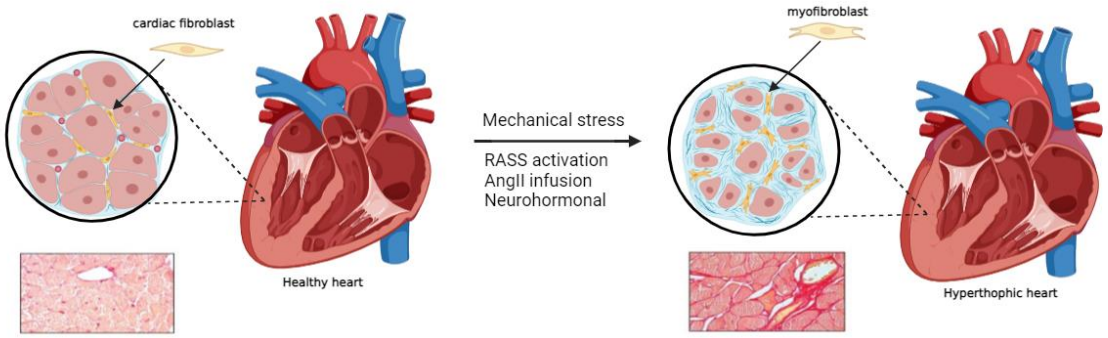

Figure 2: *The image illustrates how cardiac tissue remodelling can be induced by various factors, including the activation of Angiotensin II, which stimulates the production of reactive oxygen species (ROS) in cardiomyocytes.*

Pathological cardiac hypertrophy results from a complex interplay of mechanical, neurohormonal, molecular, and genetic factors. Understanding the mechanisms underlying this condition is crucial for developing effective therapeutic strategies. Continued research into these pathways will provide deeper insights into the prevention and treatment of pathological hypertrophy, ultimately improving patient outcomes.

1.4 Cardiac hypertrophy is a result of different tissue components

The heart is composed of cardiomyocytes (muscle cells), non-myocytes cells (e.g. fibroblasts, endothelial cells, mast cells, vascular smooth muscle cells), and the surrounding extracellular matrix (Nag AC., 1980). Cardiomyocytes account for 70-80% of the cardiac population so represent the main actors in case of disease; the presence of genetic mutation or alteration in their metabolism and excitation-contraction coupling lead to impaired cardiac function. At the same time, modifications in the extracellular matrix or in the non-myocytes population could also represent the trigger for cardiac dysfunction; also, the proximity among these components facilitates the signalling and they easily influence each other. The multicellular composition of the heart tissue and the strong cooperation between cellular and structural elements, makes hard to identify a unique responsible for cardiac disease. In the development of cardiac hypertrophy, many components are involved, and it is important to take them all in consideration when we try to find a proper treatment to limit or reverse the condition.

1.4.1 Hypertrophy at cardiomyocyte level

After birth, most cardiac myocytes lose their ability to proliferate, so growth of the heart occurs mainly through an increase in size. Myocytes are composed of bundles of myofibrils; the myofibrils contain myofilaments, which consist of sarcomeres, the basic contractile units of the cardiac muscle. Myocytes are arranged in a circumferential and spiral orientation around the left ventricle and need to contract simultaneously to ensure the heart pumps with a normal rhythm (Bernardo BC. et al., 2010). The intercalated discs are crucial for maintaining cell-cell adhesion and allowing the transmission of contractile force between adjacent cardiac myocytes. The growth of cardiac myocytes, as already mentioned, depends on several events such as the activation of signalling pathways, alterations in gene expression, increased rate of protein synthesis and organisation of contractile proteins into sarcomeric units. Cardiomyocytes possess an intrinsic mechanosensitive mechanism. Stretch-sensitive ion channels in the plasma membrane of cardiac myocytes, together with structural proteins such as integrins, contribute to linking the extracellular matrix, cytoskeleton, sarcomere, Ca^{2+} handling proteins and nucleus (Hoshijima M., 2006).

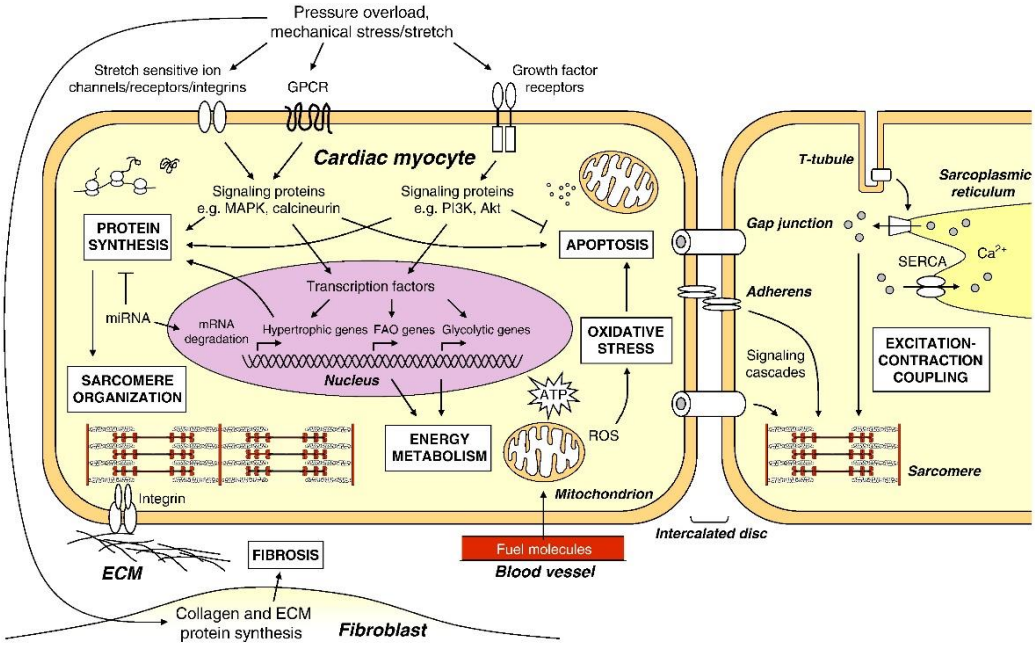

Figure 3: *Cellular processes involved in the development of cardiac hypertrophy (Bernardo Bianca C., et al., 2010).*

1.4.1.1 Ca^{2+} handling

Cardiac contraction is regulated by intracellular Ca^{2+} concentration within cardiomyocytes. During the excitation-contraction coupling process, the action potential, once membrane has

been depolarized, induces the opening of L-type Ca^{2+} channels located in the T-tubules. This event allows Ca^{2+} influx into the cardiomyocyte cytoplasm, initiating a cascade of events that ultimately leads to muscle contraction. Binding of Ca^{2+} to type 2 ryanodine receptors (RyR2) on sarcoplasmic reticulum (SR) membranes lead to Ca^{2+} release from the SR, a process known as Ca^{2+}-induced Ca^{2+} release (Bers DM., 2014). An increase in the intracellular concentration of Ca^{2+} ($[Ca^{2+}]_i$) promotes the binding of Ca^{2+} to troponin C, which is the motor on the thin filaments of sarcomeres, the contractile units of the heart. This promotes the formation of cross bridges between the thick and thin filaments and results in contraction. Muscle relaxation is mediated by the reduction of cytosolic Ca^{2+} levels through two primary mechanisms: the pumping of Ca^{2+} into the sarcoplasmic reticulum via the sarcoplasmic reticulum Ca^{2+}-ATPase pump, known as SERCA2a, and the extrusion of Ca^{2+} from the cell through the Na^{+}/Ca^{2+} exchanger (NCX). The activity of SERCA2a is regulated by phospholamban (PLN), a protein that exerts an inhibitory effect on the pump when in its dephosphorylated state. This inhibitory effect is attenuated when PLN is phosphorylated by protein kinases such as protein kinase A (PKA) or Ca^{2+}/calmodulin-dependent protein kinase II (CaMKII). Phosphorylation of PLN reduces its ability to inhibit SERCA2a, thereby facilitating the return of Ca^{2+} to the SR and promoting muscle relaxation (Kranias EG. et al., 2012). In the failing heart, Ca^{2+}-handling abnormalities contribute to contractile dysfunction (Feldman MD. et al., 1987). We observe Ca^{2+} accumulation in the cytosol in response to altered SERCA function resulting from reduced channel expression or reduced PLN phosphorylation, which prevents relaxation and reduces the Ca^{2+} pool available for release from the SR during systole. Downregulation of SERCA2a is consistently observed in experimental models of heart failure (Kawase Y. et al., 2008).

The leakage of Ca^{2+} from the SR due to RyR2 dysfunction can contribute to contractile dysfunction through several mechanisms. Firstly, such dysfunction can deplete the SR Ca^{2+} reserves, thereby progressively reducing Ca^{2+} availability for muscle contraction. Additionally, the increase in intracellular Ca^{2+} concentration ($[Ca^{2+}]_i$) can elevate the susceptibility to cardiac arrhythmias. This excess of intracellular Ca^{2+} can also increase the cell energy demand, as greater amounts of ATP is required to manage Ca^{2+} balance and maintain cellular homeostasis. Hyperphosphorylation of RyR2 has been observed in the failing human heart (Marx SO. et al., 2000). In addition, T-tubule dysregulation contributes to contractile dysfunction in heart failure, and it is associated with a reduction in the density of RyR2 clusters as well as reduced colocalization between RyR2 and L-type Ca^{2+} channels.

1.4.2 Inflammation and pro-inflammatory cytokines

A wide range of cytokines, including TNF-α, TGF-β, and interleukins such as IL-1, IL-4, IL-6, IL-8, and IL-18, are implicated in the pathogenic processes of various inflammatory cardiac conditions, such as ischemic heart diseases, myocardial infarction, heart failure, and genetic cardiomyopathies. Specifically, in ischemia-related conditions, the release of these cytokines into the bloodstream serves as biomarkers of inflammation, reflecting immune system activation and disease progression (Bartekova M. et al., 2018). All cytokines exert their biological effects by binding to their cell surface receptors. These transmembrane receptors are divided into six types according to their structure (Arimont M. et al., 2017) and include type I and type II cytokine receptors, the immunoglobin superfamily of receptors, the TNF receptor family, chemokine receptors and TGF-β receptors.

Following tissue injury, the heart activates a series of tissue repair mechanisms through the engagement of the innate immune system. The elevation of pro-inflammatory cytokines plays a crucial role in promoting cardiac remodelling. It is hypothesized that this acute pro-inflammatory phase is subsequently followed by a distinct anti-inflammatory response. This phase is essential for the resolution of the injury and the restoration of tissue homeostasis (Ionita MG. et al., 2010). However, because cardiac stress manifests in a different forms and intensities, the pro-inflammatory response in the heart can become prolonged. If this sustained inflammatory activity is not adequately counteracted by anti-inflammatory mechanisms, it may progress into chronic inflammation. This persistent inflammatory state can have detrimental effects, potentially leading to further cardiac dysfunction and contributing to long-term adverse outcomes (Oldfield CJ. et al., 2020).

The TGF- β family of cytokines regulate several different cellular processes, these cytokines are able to participate in the progression of pathological cardiac remodelling, cardiac fibrosis, and pathological cardiac hypertrophy. In patients with HCM, elevated TGF-β levels were found to be significantly associated with several adverse clinical features. Specifically, high TGF-β levels correlated with increased concentrations of brain natriuretic peptide, enlargement of the left atrium, thickening of the intraventricular septum, and a greater frequency of negative clinical outcomes. These associations suggest that elevated TGF-β may play a critical role in the progression and severity of HCM. In addition, several studies have shown increased TGF-β in diabetic cardiomyopathy, a condition characterized by cardiac remodelling (Yue Y. et al., 2017). In a mouse model of pressure overload-induced pathological cardiac hypertrophy, the knockdown of the type II TGF-β2 receptor was shown

to markedly reduce the progression of cardiac fibrosis (Oldfield CJ. et al., 2020), suggesting the involvement of TGF-β2 in triggering and sustain the remodelling subsequent to cardiac hypertrophy, both primary and secondary.

In conclusion, inflammation plays a critical role in the development and progression of cardiac hypertrophy. The chronic activation of pro-inflammatory cytokines significantly contributes to the pathological remodelling of the heart. Elevated levels of these cytokines not only exacerbate the hypertrophic response but also promote fibrotic changes, leading to deteriorating cardiac function and increased susceptibility to adverse outcomes. Understanding the intricate mechanisms of inflammatory signalling and its impact on cytokine production in cardiac hypertrophy is essential for developing targeted therapeutic strategies aimed at mitigating inflammation and improving cardiac health.

1.5 Extracellular matrix and fibrosis

The inflammatory process in the hypertrophic heart is closely related to the modification of the extracellular matrix (ECM), as pro-inflammatory cytokines released during inflammation stimulate the production and accumulation of extracellular components, thus contributing to remodelling and fibrosis of cardiac tissue. Excessive ECM contributes to reduced systolic and diastolic function, and it impairs electrical conduction, predisposing the heart to arrythmias (Rockey DC. et al., 2015). The components of the cardiac extracellular matrix form a highly complex three-dimensional network that provides structural support for different types of cells and integrates extracellular signals with cellular responses. This matrix not only stabilizes the tissue structure but also regulates cellular interactions and responses to environmental signals, thereby influencing the processes of remodelling and fibrosis in the context of cardiac hypertrophy.

The ECM primarily consists of fibrillar collagens, including types I and III, with smaller contributions from collagen types IV, V and VI (Mewton N. et al., 2011). Fibrillar collagens, specifically types I and III, serve as the primary structural proteins forming the extracellular matrix. Collagen type I constitutes approximately 85% of the total collagen content in the myocardium and is integral in forming robust fibres that confer tensile strength to the cardiac tissue. Collagen type III, which represents 11% of the total collagen content in the normal heart, assembles into fine fibres and is in charge of the elasticity of the matrix network (Borg TK. et al., 1996). Collagen type V, which compose a smaller population of fibrillar collagens,

interacts whit collagen type I to form heterotypic fibrils and modulates the fibrillogenic of collagen type I (Moravsky G. et al., 2013). Collagen type IV, the major constituent of basement membrane (BM), associates with laminin, nidogen and perlecan, and assembles into a mesh-like structure that provides mechanical stability to the BM and maintains endothelial cell function. Collagen type VI forms a microfilament network that organizes fibrillar collagens and anchors them to the BM. Fibronectin organizes into a fibrillar network on the cell surface and binds to different ECM components, such as collagen and fibrin, thereby modulating the structural and mechanical properties of the matrix and influencing the behaviour of adherent cells. The cardiac ECM also includes non-structural glycoproteins, proteoglycans, and glycosaminoglycans, which play essential roles in matrix function. Alterations in these components following injury are involved in the pathogenesis of cardiac fibrosis and ventricular dysfunction (Fox PR., 2004; Chu PY. et al., 2010).

The balance between extracellular matrix synthesis and degradation is crucial for maintaining the structural integrity of the heart. Metalloproteases (MMPs) represent the main enzymes responsible for the degradation of ECM components, with MMP-2, -9 and -13 emerging as the predominant subtypes in cardiac tissue (Frangogiannis NG., 2021).

The proteolytic activity of matrix metalloproteinases (MMPs) is regulated by tissue inhibitors of metalloproteinases (TIMPs), with TIMP-2, -3, and -4 being expressed in the normal heart. Cardiac fibrosis, characterized by excessive extracellular matrix deposition, is a common feature observed in various myocardial diseases, including hypertrophic, dilated, restrictive, inflammatory cardiomyopathies and pathophysiological conditions such as myocardial infarction, pressure overload, and aging. Fibrosis significantly contributes to cardiac dysfunction, highlighting the critical role of the balance between MMPs and TIMPs in regulating tissue remodelling and disease progression (Barker TH. et al., 2017; Mukherjee D. and Sens S, 1993). We observe different classifications of fibrotic. Histopathological analysis has classified fibrotic lesions into three distinct forms: replacement fibrosis, interstitial fibrosis, and perivascular fibrosis. Following myocardial infarction, necrotic cardiomyocytes are replaced by collagen deposition, forming scars that result in "replacement fibrosis," which serves to repair tissue after ischemic injury and is associated with systolic dysfunction. In contrast, "interstitial fibrosis" is characterized by the accumulation of extracellular matrix proteins in the absence of significant cardiomyocyte loss. The term "perivascular fibrosis" refers to the expansion of the microvascular adventitia. Both interstitial and perivascular fibrosis are closely associated with left ventricular

dysfunction, primarily by impairing diastolic function, with a less pronounced effect on systolic function (Frangogiannis NG., 2021). Although the initial factors and mechanisms leading to cardiac fibrosis differ across various heart diseases, the trans-differentiation of myofibroblasts is a critical event, triggered by fibrogenic mediators, and plays a central role in the fibrotic process.

1.5.1 Fibroblast

Cardiac fibroblasts are the primary actors in maintaining cardiac homeostasis, with the function of producing collagen and other ECM components. When activated in response to cardiac injury, fibroblasts are responsible for cardiac fibrosis by upregulating collagen production, a common feature of many cardiovascular diseases. The severity of fibrosis correlates with the progression of heart failure.

A fibroblast is defined as a cell capable of producing type I collagen and residing in the connective tissue or interstitial space of an organ. In the heart, different subtypes of cardiac fibroblasts are located in specific anatomical sites: adventitia (ventricular and septal), interstitium (ventricular and septal), atrium, fibrous ring, and valves (Tallquist MD., 2020).

Interstitial fibroblasts are located within the interstitial space between cardiomyocytes and the vascular structures of the heart. Interstitial fibrosis is characterized by an excessive accumulation of ECM proteins in this interstitial space, occurring without substantial loss of cardiomyocytes (Camelliti P. et al., 2005). This pathological accumulation disrupts the mechanical properties of the myocardium and can adversely affect cardiac function, particularly diastolic function. Abnormal activation of interstitial fibroblasts and their transformation into myofibroblasts are implicated in the pathogenesis of different cardiac diseases, including HCM and heart failure. Interstitial fibrosis is associated with impaired cardiac function and progression of heart disease. The fibroblast population most characteristic of the heart is located in the adventitial layer. These fibroblasts envelop the layer of the coronary arteries and are responsible for depositing a dense collagen matrix that provides structural support to the artery. Adventitia fibroblasts play an important role in the pathogenesis of several vascular diseases, including atherosclerosis and hypertension (Stenmark KR. et al., 2012). Perivascular fibrosis associated with activation of these fibroblasts may contribute to vessel narrowing and impaired perfusion. The activity of adventitia fibroblasts is crucial for vascular remodelling, which can be a normal aspect of the response to damage but can also become pathological if excessive. Other fibroblast

populations are situated in distinct anatomical locations, including those forming the fibrous rings that separate the atria from the ventricles, known as the annulus fibrosus. The atrioventricular conduction system crosses through the annulus fibrosus, and it is hypothesized that this dense fibrous matrix plays a key role in electrically isolating the atria from the ventricles, thereby facilitating normal electrical conduction (Tallquist MD., 2020).

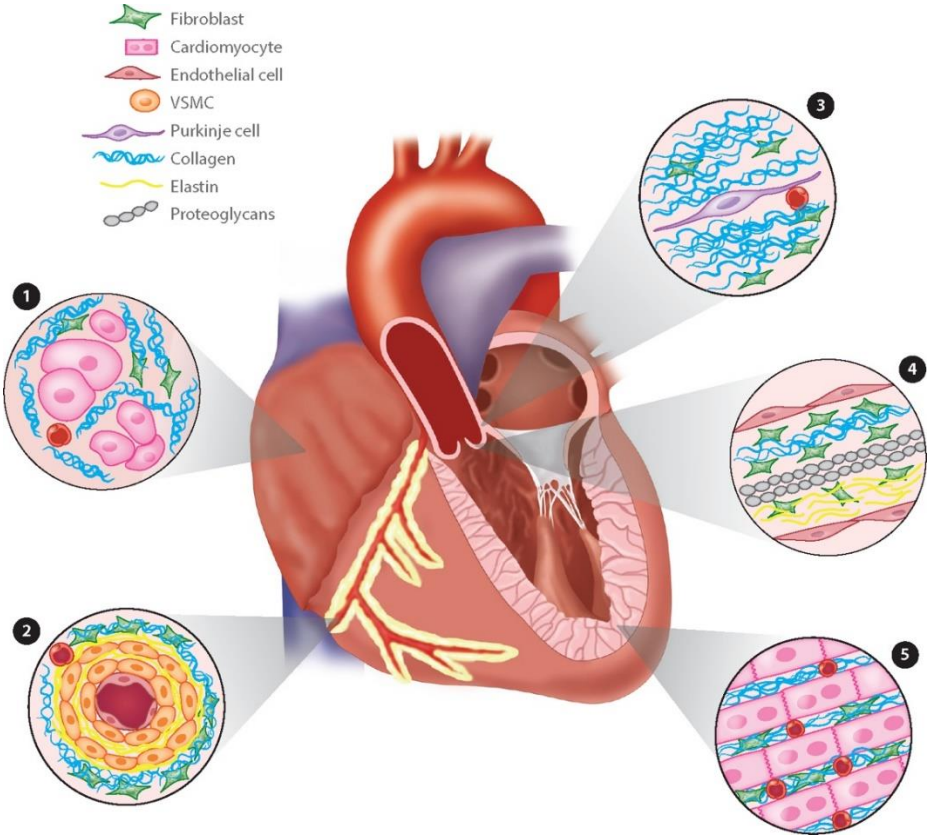

Figure 4: *Anatomic location of cardiac fibroblasts. Fibroblasts reside in distinct anatomic locations in the heart, and each population of fibroblasts is likely to express a different transcriptional profile.* ***1*** *Atrium-transverse section of atria where cardiomyocyte fibres are thinner and less dense compared to the ventricles.* ***2*** *Adventitia-transverse section through a coronary artery. The number of vascular smooth muscle cells (VSMCs) can vary depending on vessel diameter. Cell types other than fibroblasts have also been noted in the dense collagen surrounding the vessel.* ***3*** *The annulus fibrosus is a collagen-rich area surrounding the conduction system. Fibroblasts are present in these regions.* ***4*** *Valves: Fibroblasts reside in three layers (fibrosa, spongiosa, and ventricularis). These are composed of collagen, proteoglycans, and elastin, respectively.* ***5*** *Interstitium: This longitudinal section of myocardium would be found in the ventricles or ventricular septum (Tallquist MD., 2020).*

In response to cardiac stress, such as pressure overload or myocardial infarction, a series of cellular events leads to a process known as cardiac remodelling. Cardiomyocytes release stress signals that trigger inflammatory cell infiltration and fibroblast activation. The term "activation" in relation to cardiac fibroblasts involve a wide range of changes, including increased proliferation, matrix deposition, expression of contractile proteins, and secretion of cytokines and growth factors (Tallquist MD., 2020).

After cardiac injury, fibroblast start to express α-SMA (smooth α-actin) protein, an important molecule that allow contraction to fibroblast and determine its activation to myofibroblast (myoFBs). Higher expression of α-SMA affects directly matrix deposition, increasing collagen secretion and contribute to the increase stiffness of ECM, impairing cardiac function.

The presence of α-SMA is frequently used as a marker to identify myofibroblasts in tissues, as not all fibroblasts express these proteins. Expression of α-SMA indicates a state of activation of fibroblasts and their active involvement in repair and fibrosis processes.

1.5.2 Myofibroblast

During cardiac injury, functional cardiac fibroblasts (CFs) differentiate into myoFBs that are typical cells secreting contractile proteins. Cardiac myofibroblasts respond to proinflammatory cytokines (e.g. TNF-α, IL-1, IL-6, TGF-β), vasoactive peptides (e.g. angiotensin II, endothelin-1, natriuretic peptides) and hormones (e.g. noradrenaline), the levels of which, are increased in the remodelling heart. MyoFBs function is also modulated by mechanical stretch and changes in oxygen availability, as in ischemia-reperfusion (Porter KE. et al., 2009). As previously mentioned, α-SMA is a well-known differentiation marker but can also be expressed in other cell types, such as endothelial cells, mesenchymal cells, and smooth muscle cells (SMCs). Notably, fibroblast activation protein (FAP) is specifically expressed on the surface of differentiated myofibroblasts and is currently being investigated as a potential marker. Furthermore, recent studies suggest that the cardiac extracellular matrix in a deteriorating heart may activate cardiac fibrosis through hyperactivated YAP signalling (Liu M. et al., 2021).

Myofibroblast participate in the remodelling of the interstitium by releasing ECM-degrading metalloproteinases (MMPs), thereby facilitating collagen turnover. Nevertheless, they are

characterized by sustained proliferative activity, which amplifies pro-inflammatory signalling, promotes accumulation of collagen in the tissue and produce TGF-β, α-SMA and activates Angiotensin type 1 receptor (AT1R). Cardiac fibrosis, a pathological scarring process within the cardiac muscle, is a hallmark of nearly all forms of heart disease. This fibrotic response is commonly observed in conditions such as myocardial infarction (MI), hypertrophic cardiomyopathy, dilated cardiomyopathy, diabetic cardiomyopathy, and aortic stenosis. The development of fibrosis in these disorders contributes to the disruption of normal cardiac architecture and function, leading to progressive cardiac dysfunction and heart failure. By altering the extracellular matrix composition and increasing stiffness in the myocardium, cardiac fibrosis exacerbates the clinical outcomes of these heart diseases, making it a critical target for therapeutic intervention (Weber KT. et al., 2013).

Cardiac injury is closely related to necrosis of cardiomyocytes. Catecholamines modulate intracellular Ca^{2+} levels, with particular impact on intra-mitochondrial Ca^{2+}. The overloading of Ca^{2+} leads to oxidative stress and impaired ATP synthesis. The accumulation of reactive oxygen species induces the opening of the transition pore of the inner mitochondrial membrane, facilitating the passive entry of solutes and resulting in osmotic swelling of the mitochondria (Weber KT. et al., 2013).

The elevation of proteins such as creatine kinase, lactate dehydrogenase, myoglobin, and specific titin isoforms, both in serum and at the site of necrotic cardiomyocytes, can function as danger-associated molecular patterns (DAMPs), activating the innate immune system. Following necrosis due to ischemic or non-ischemic causes, inflammatory cells are attracted to the injured tissue by chemokine concentration gradients. These cells accumulate at the damage site within the first few days and initiate a complex wound-healing process aimed at tissue repair. Their function is to degrade and remove dead cells by proteolysis and phagocytosis. The inflammatory cells and myofibroblasts contribute to the generation of a 'secretome' at the site of cardiomyocyte necrosis, which plays a pivotal role in modulating extracellular matrix turnover. This secretome consists of a variety of signalling molecules, including cytokines, growth factors, and proteases, that coordinate the degradation and synthesis of matrix components, thereby influencing the tissue remodelling process. As previously described, myofibroblasts are activated following cardiomyocyte necrosis. As part of the wound healing response and in response to TGF-β1 (Bondi CD. et al., 2009), these myofibroblasts produce fibronectin, creating a temporary scaffold that facilitates the

subsequent deposition of type I and III fibrillar collagen. This process is mediated by TGF-β1 through the Smad signalling pathway and mitogen-activated protein kinases.

Scar tissue formation following injury involves the production and assembly of collagen fibres. Studies have shown that myofibroblasts can remain active for months or even years within the infarct scar (Cleutjens J. et al., 1995). Additionally, molecular signals generated at the site of the infarct can diffuse through the interstitial space and affect distant areas, stimulating interstitial and adventitial fibroblasts to produce collagen. This mechanism contributes to the progressive fibrosis of the myocardium. The formation of fibrous tissue in the myocardium has several negative effects. Firstly, fibrosis is a "crucial determinant" of the heterogeneity of myocardial tissue in pathological conditions. While the size of myocytes is normally variable, this variability is exacerbated in diseased hearts due to fibrosis. The fibrillar collagen accumulated in the scar tissue restricts the mobility and functionality of the surrounding cardiomyocytes, compromising their workload. This phenomenon can lead to cardiomyocyte atrophy and negatively impact overall cardiac function (Fidziańska A. et al., 2009). Moreover, myofibroblasts are interconnected via gap junctions, which are anchored to the fibrillar collagen matrix through adhesion molecules known as "fibronectins." These connections promote the formation of a contractile fibrous tissue. The tonic contraction of this tissue in response to local peptides, such as Angiotensin II, may explain changes in tissue stiffness. Chronic activation of the myocardial renin-angiotensin system leads to increased local expression of Angiotensin II, which contributes to cardiac hypertrophy. Specifically, it has been observed that Angiotensin II stimulates myofibroblasts to secrete exosomes containing miR-21 and miR-423. These microRNAs, induce the overexpression of AT1R and AT2R receptors in cardiomyocytes through the activation of mitogen-activated protein kinases (MAPK) (Lyu L. et al., 2015). The accumulation of matrix proteins during cardiac fibrosis, combined with the presence of myofibroblasts, contributes to electrical remodelling and a heightened risk of arrhythmias.

1.6 Primary hypertrophy and Secondary hypertrophy

Cardiac hypertrophy has distinct pathophysiological mechanisms and implications; on the base of the triggering factor that can be genetic or non-genetic, it is classified as primary or secondary. If hypertrophy is determined by genetic causes, as in case of HCM, it is primary; if it occurs as an adaptation to an increased workload, as in the case of aortic stenosis, it is classified as secondary hypertrophy.

Primary hypertrophy includes forms of cardiac hypertrophy that develop independently from other systemic pathologies. A significant example of primary hypertrophy, extensively covered in this thesis, is HCM. This disease is characterised by genetic mutations affecting genes involved in the mechanism of contraction of cardiomyocytes. The cellular alterations, in this case, are not directly associated with external factors or systemic diseases.

Secondary cardiac hypertrophy results from external stressors or underlying conditions that impose an increased workload on the heart. Common causes include hypertension, aortic stenosis, and other conditions that lead to pressure or volume overload. This type of hypertrophy develops as an adaptive response to the heightened hemodynamic demands placed on the heart, with the aim of maintaining cardiac function and compensating for the elevated stress.

Both conditions will be examined in detail below to allow a clear understanding of available drug treatments. The ultimate objective is to assess how such interventions can contribute to improving the quality of life of patients with both primary and secondary cardiac hypertrophy.

1.6.1 Primary hypertrophy:

1.6.1.1 Hypertrophic Cardiomyopathy

Hypertrophic cardiomyopathy is an autosomal dominant hereditary disease, which means there is a 50% chance it will be passed on to offspring. HCM has an incidence of 1 in 500 in the general population and is the most common hereditary heart disease, as well as the leading cause of sudden death in young people, including trained athletes (Maron BJ., 2003). This condition is a hereditary monogenic disorder that may result from over 1500 mutations in 11 or more genes that encode cardiac sarcomere proteins. HCM can be divided into two types: an obstructive form, characterized by dynamic obstruction of the left ventricle, and a non-obstructive form. Moreover, this pathological condition exhibits extreme variability and complexity, reflecting the different mutations and genes that may be involved in its

pathogenesis, which in turn is reflected in the marked heterogeneity of clinical manifestations.

The main evidence of HCM is the abnormal thickening of the ventricular walls of myocardium, leading to a decrease in the size of the internal chambers and compromising the heart's contractile function. Specifically, HCM is characterized by increased thickness of the left ventricular (LV) wall; in adults, this is defined as >15 mm in one or more LV myocardial segments and cannot be attributed exclusively to abnormal loading conditions, such as valve diseases or severe hypertension. This ventricular thickening can further be classified as mild (13-15 mm) or extreme (> or = 30 mm) (Nistri S. et al., 2006; Olivotto I. et al., 2003). This condition typically impacts the left ventricle, with the right ventricle being affected only in rare instances (Teekakirikul P. et al., 2019). The hypertrophy can occur in different regions, including the interventricular septum, apex, or mid-cavity of the myocardium. The diagnosis of HCM is primarily made using echocardiography (ECHO) or cardiac magnetic resonance (CMR).

The distinctive features of the pathology manifest around puberty or in the early adult phase and are:

1. *Asymmetric hypertrophy of the left ventricle, usually confined to the interventricular septum but can expand to the right ventricle;*
2. *Diastolic dysfunction;*
3. *Microcirculatory ischemia;*
4. *Myocardial fibrosis;*
5. *Altered sympathetic innervation;*
6. *Arrhythmic phenomena;*
7. *Alteration of the energetic profile of cardiomyocytes.*

HCM, as previously stated, is a disease associated with genetic abnormalities present from birth. The disease enormously variable genotype means that even within the same family, the onset of the disease can occur at different ages and with different clinical courses. Therefore, the disease is associated not only with sarcomeric mutations but also with multifactorial conditions such as environmental factors.

HCM is a principal etiological factor for sudden cardiac death, which predominantly occurs in both adults and children, with a reduced risk for individuals over the age of 60, suggesting that the incidence of ventricular arrhythmias may decrease with age. Sudden cardiac death in most cases is linked to mild exertional or sedentary activities; however, evidence indicates that it can also occur in young competitive athletes, which suggests that intense physical exertion may precipitate such events, potentially through mechanisms such as tachycardia and ventricular fibrillation. The electrophysiological instability associated with ventricular tachyarrhythmias likely base from specific histopathological and pathophysiological alterations inherent to the condition. For example, cardiac remodelling is associated with disorganization of cardiomyocytes, which exhibit a perpendicular orientation in certain areas (Maron BJ. et al., 1979). Additionally, silent microvascular ischemia leads to cell death, with the muscle tissue subsequently being gradually replaced by fibrotic tissue. The increase in fibrotic connective tissue contributes to the development of arrhythmic mechanisms. Moreover, patients affected by HCM can present highly variable clinical manifestation that include exertional chest pain and breathlessness, palpitations, dyspnoea, asymptomatic murmur, syncope, culminating in sudden cardiac death (SCD) (Hensley N. et al., 2015).

In addition, hypertrophic cardiomyopathy, as mentioned previously, can be divided into two main subtypes:

- *Obstructive hypertrophic cardiomyopathy*, that involves a severe impediment to blood leakage from the left ventricle;
- *Non-obstructive hypertrophic cardiomyopathy*, where blood flow from the left ventricle is only moderately reduced.

In patients with HCM, the severity of hypertrophy can lead to different complications, including diastolic dysfunction, myocardial ischemia, and mitral regurgitation. Approximately 70-75% of individuals with HCM will experience left ventricular outflow tract obstruction (LVOTO). The presence of significant thickening extending to the interventricular septum plays a critical role in determining whether the HCM presents in an obstructive or non-obstructive form. This condition is marked by partial obstruction in the left ventricular outflow, resulting in hemodynamic disturbances and acute heart failure symptoms, which are often worsened by physical exertion (Ommen S.R. et al., 2020).

HCM has been defined primarily as a “disease of the sarcomere” (Maron BJ. et al., 2012). The R403Q missense mutation was one of the first to be identified and is present at the level

of the gene encoding for the β myosin heavy chain (β-MyH7) (Tanjore R. et al., 2010). The mutation of this protein, together with Myosin Binding Protein C, is found in approximately 70% of patients; in about 5% of patients, mutations occur in the genes for Troponin T (TNNT2), Cardiac Troponin I (TNNI3), or α-Tropomyosin (TPM1). Unfortunately, in 40-55% of HCM patients, the genes involved in the pathogenesis of this disease remain unidentified (Marian AJ et al., 2017).

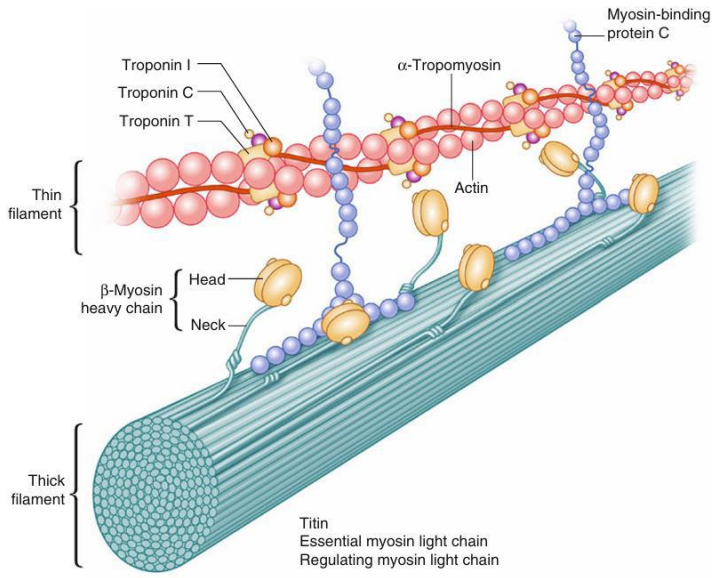

Figure 5: *Graphical representation of the sarcomere and all its components (Ingles J., et al, 2019).*

As an autosomal dominant disorder, HCM involves the inheritance of mutations that contribute to the condition. However, these mutations are not the only determinants of the pathological phenotype, given the substantial variability observed in the disease. Current research suggests that additional factors may influence the development of HCM, beyond the known genetic mutations. Studies on patients who have experienced sudden cardiac death highlight that sarcomere mutations associated with HCM play a significant role in myocardial structural remodelling. This remodelling leads to disruptions in the microcirculation, increasing the risk of ischemia and promoting the development of interstitial fibrosis within the affected myocardium. While these structural changes are critical in the broader context of HCM, they do not always directly correlate with the underlying pathogenic mechanisms of the disease.

Specific genetic mutations in genes such as α-myosin heavy chain (MYH6), titin (TNT), muscle LIM protein (CSRP3), telethonin (TCAP), vinculin (VLC), and junctophilin 2 (JPH2) have been identified as contributors to HCM. These mutations affect the structural and functional integrity of the heart muscle, leading to the complex remodelling processes observed in the disease. This functional alteration may promote the occurrence of ischemia and the onset of interstitial fibrosis in HCM myocardium which ultimately increase the risk of sudden cardiac death (Maron MS., 2009). However, the expression and impact of these mutations can be modulated by other genetic, environmental, and possibly epigenetic factors, contributing to the heterogeneity of the disease phenotype.

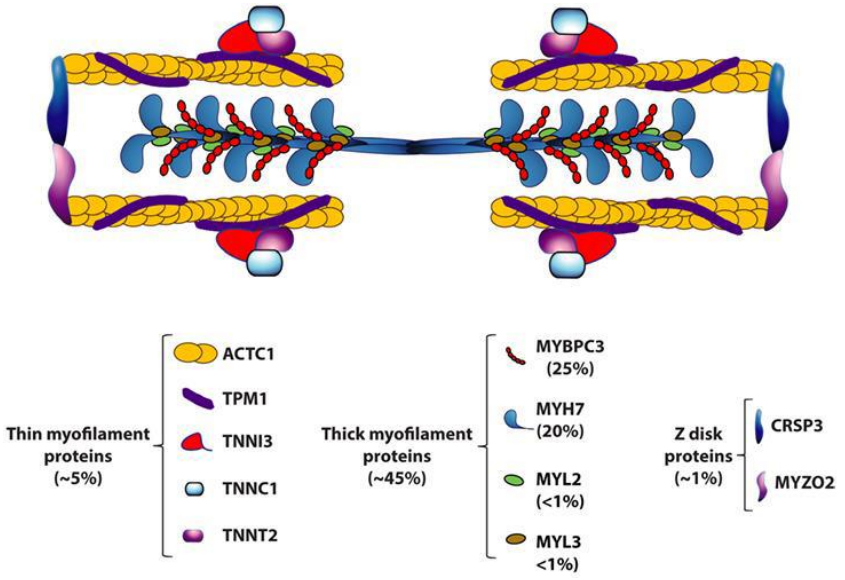

***Figure 6**: Localization of the cardiac sarcomere where genes affected by mutations are found in individuals with HCM (Marian A J., Brauwald E., 2017).*

At the molecular level, the overproduction of actin-myosin cross-bridges in the sarcomere during systole can result in heightened energy consumption by cardiomyocytes, which leads to the development of hypertrophy and myocardial dysfunction.

Diastolic dysfunction is associated with impaired left ventricular function. Diastolic dysfunction refers to the impaired ability of the left ventricle to relax and, consequently, its reduced capacity to fill with incoming blood. To better understand the key characteristics of diastolic dysfunction, it is essential to focus on one of the most important echocardiographic parameters, Tissue Doppler Imaging (TDI). TDI, along with other echocardiographic analyses, not only provides a detailed characterization of the pathophysiology at the pre-

clinical stage but also measures the velocity of blood flow in the myocardium during systole, atrial contraction, and early diastole. A reduction in the velocity during early diastole reflects the diastolic function, with decreased velocity indicating a significant alteration in relaxation (Nagueh SF. and Zoghbi WA., 1996).

Electrical abnormalities in the heart are associated with a prolonged duration of the action potential (AP), which results in an increased frequency of early afterdepolarizations (EADs) (Maron B. J. et al., 2006), which can lead to ventricular tachyarrhythmias (Yan GX. et al., 2001). In cardiomyocytes affected by HCM, there is an increase in the late sodium current (INa_L) and in the L-type Ca^{2+} current (ICa_L), along with a reduction in repolarizing potassium currents, such as the inward rectifier current (IK_r) and the transient outward current (Ito) (Coppini R. et al., 2013). These pathological changes enhance the probability of EADs, which are spontaneous depolarizations occurring during the plateau phase of AP. EADs are associated with the reopening of Na^+ and Ca^{2+} channels before repolarization is complete. Moreover, cardiomyocytes in HCM exhibit changes in diastolic Ca^{2+} levels, including delayed Ca^{2+} transient kinetics and elevated intracellular ion concentrations. These findings indicate that HCM can significantly impact the mechanisms of excitation-contraction coupling (Coppini et al. 2013).

The abnormalities in Ca^{2+} kinetics and its high diastolic concentration is mediated by several events:

- **Reduced density of T-tubules:** cardiomyocytes affected by HCM are characterized by a reduction in T-tubules, which leads to prolonged Ca^{2+} transients and asynchronous, incomplete Ca^{2+} release from the sarcoplasmic reticulum.
- **Ca^{2+} overload in the sarcoplasmic reticulum:** Ca^{2+} overload may lead to the release of Ca^{2+} during diastole. This could affect the diastolic Ca^{2+} concentration and result in post-potentials.
- **Altered function of the NCX exchanger:** the expression of genes encoding NCX is increased in the myocardium affected by HCM, leading to elevated intracellular Na^+ concentrations and enhanced "forward" mode of operation of the NCX exchanger.
- **Reduced activity of the Ca^{2+}-ATPase pump (SERCA):** in cardiomyocytes with HCM there is a decrease in the expression of genes encoding the Ca^{2+}-ATPase pump and phospholamban, which contributes to the slowing of Ca^{2+} transient kinetics.

These changes lead to the increase of intracellular Ca^{2+} concentration. In addition, the increase in INa_L promotes the action of the NCX exchanger in the "reverse" rather than "forward" mode, further increasing the intracellular Ca^{2+} concentration and promoting CaMKII activity. High levels of CaMKII autophosphorylation result in increased activity of the enzyme. Increased CaMKII activity results in higher phosphorylation of L-type Ca^{2+} channels, ryanodine receptor type 2, and phospholamban. This phosphorylation may have negative feedback on cellular function, including slowed inactivation of ICa_L current and increased susceptibility to arrhythmias. In addition, phospholamban phosphorylation helps to balance the effects of alterations in the sarcoplasmic reticulum caused by reduced SERCA2a expression and Ca^{2+} accumulation. The CaMKII-dependent signalling pathway plays a primary role in the remodelling process of HCM-affected cardiomyocytes (Hudmon and Schulman, 2002). Increased CaMKII activity, stimulated by increased intracellular Ca^{2+} concentration, contributes to limiting inactivation of the ICa_L current and increasing the amplitude of INa_L, prolonging the AP and promoting arrhythmogenesis (Coppini R. et al., 2013). CaMKII also contributes to alteration of Ca^{2+} transient kinetics and to increase of diastolic Ca^{2+} concentration, thereby influencing the excitation-contraction coupling.

Further studies have suggested that increased CaMKII activity might activate a gene expression program responsible for cellular hypertrophy (Backs J. et al., 2006). Indeed, CaMKII appears to be involved in the typical structural changes observed in cardiomyocytes affected by HCM, i.e. cellular hypertrophy, and in the development of intramyocardial fibrosis and cellular (Coppini et al, 2013).

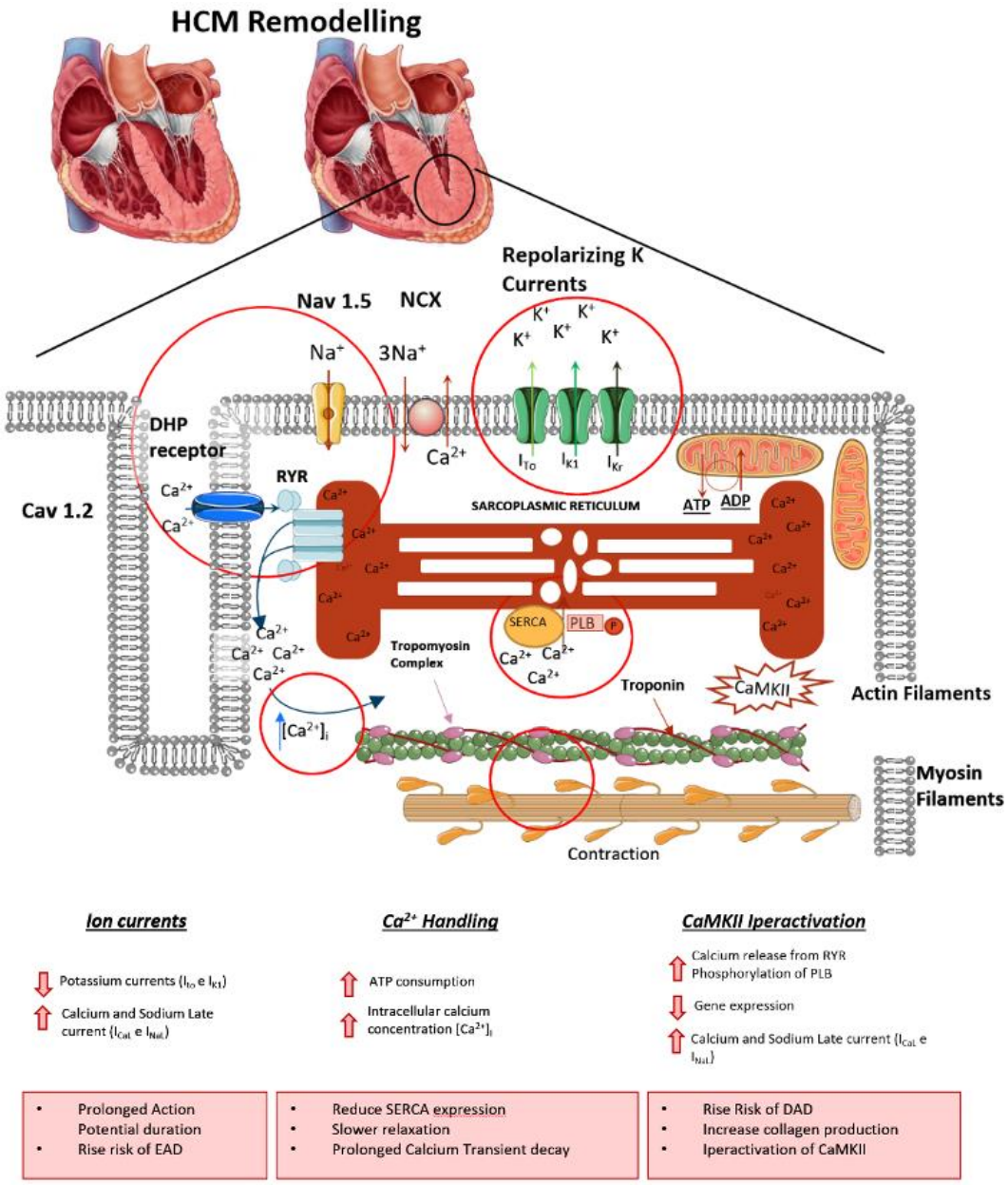

Figure 7: *The image illustrates the anatomical alterations characteristic HCM, characterized by the thickening of the interventricular septum. It also describes several alternating mechanisms, including high intracellular concentrations of Ca^{2+} and sodium, which are associated with the activation of the reverse mode of the sodium-Ca^{2+} exchanger (NCX). This leads to hypercontractility of the myofilaments and increased consumption of ATP. In addition, there is hyperactivation of CaMKII, which subsequently causes the downregulation of repolarizing currents. Downstream targets of CaMKII include ryanodine receptors, Ca^{2+} channels, potassium channels and sodium channels. All these pathological changes are linked to altered gene expression, which leads to reduced expression of SERCA, crucial for Ca^{2+} reuptake, and potassium channels, essential for cellular repolarization (Palandri C., PhD thesis, 2019).*

1.6.1.2 Fibrosis in HCM

Fibrosis is a key pathological feature of HCM that significantly contributes to disease progression and adverse outcomes. Myocardial fibrosis is characterized by the excessive accumulation of extracellular matrix components, such as collagen, within cardiac tissue, and it arises from chronic mechanical stress, inflammatory processes, and altered cellular signalling pathways such as TGF-β, angiotensin II, and endothelin-1. These factors activate fibroblasts and myofibroblasts to deposit collagen. Additionally, oxidative stress exacerbates fibrosis by damaging cardiomyocytes and activating fibrotic signalling pathways, while chronic inflammation further aggravates the process through the release of cytokines and growth factors that promote collagen deposition and myocardial fibrosis (Liu M. et al, 2021). Understanding fibrosis in HCM is crucial for comprehending its impact on cardiac function and for developing effective treatment strategies. Fibrosis in HCM can be categorized into two types: interstitial and replacement fibrosis. Interstitial fibrosis involves the deposition of collagen in the spaces between cardiomyocytes, disrupting normal myocardial architecture, increasing stiffness, and impairing diastolic function. It is often associated with the activation of fibrotic pathways involving transforming TGF-β and MMPs. Replacement fibrosis, conversely, results from cardiomyocyte death and is characterized by the substitution of dead or damaged myocytes with fibrous tissue. This form of fibrosis typically occurs in more advanced stages of HCM, contributing to disturbances in electrical conduction and an increased risk of arrhythmias. Replacement fibrosis is also the predominant form of myocardial fibrosis in HCM. Late gadolinium enhancement (LGE) on cardiac MRI, recognized as the gold standard for non-invasive assessment of myocardial fibrosis, is particularly effective in detecting replacement fibrosis. Furthermore, the presence of replacement fibrosis serves as a robust independent predictor of adverse clinical outcomes, likely because it contributes to the development of pathological condition that heightens susceptibility to cardiac disfunction and arrhythmias (Pagourelias ED. et al., 2021).

1.6.1.3 Diagnosis

In the diagnostic approach to HCM, the primary parameter considered is the thickness of the left ventricular wall. According to the 2023 guidelines, in adults, left ventricular wall thickening of 15 mm or greater is diagnostic of HCM. However, if the thickness is between 13 and 14 mm, further evaluation is required, including genetic testing, analysis of irregularities or abnormalities in the ECG, and a thorough assessment of family history to

identify any relatives with HCM. In paediatric patients, the diagnosis of HCM is based on left ventricular thickness that exceeds 2 standard deviations above the expected mean for the child age and sex, as the condition can develop at any age (Arbelo E. et al., 2023).

In patients with HCM, auscultation often reveals the presence of an acute, mid-systolic murmur. This murmur varies in correlation with the systolic output of the heart; thus, when the patient changes from a supine to an upright position or performs the Valsalva manoeuvre, the intensity of the murmur tends to increase, making it more audible (Marian AJ. and Braunwald E., 2017).

The diagnosis of HCM is established through the use of four essential and complementary diagnostic methods: echocardiography, electrocardiography, cardiac magnetic resonance imaging, and genetic testing. These tools provide a comprehensive diagnostic assessment, allowing for an accurate and integrated evaluation of the condition.

Echocardiography: Echocardiography is the most frequently employed diagnostic modality for HCM because of its accuracy and extensive accessibility; it serves as the foundational tool for diagnosing, screening, risk of sudden death, and monitoring patients with HCM.

In cases of confirmed or suspected HCM, echocardiography is indispensable as it provides comprehensive information about left ventricular (LV) systolic function and diastolic dynamics. It is particularly valuable for assessing the presence and mechanism of LVOTO, and for evaluating the size and functional status of the left atrium (Malik R. et al., 2014). By offering comprehensive information on these parameters, echocardiography facilitates a thorough evaluation of the structural and functional aspects of the heart, guiding clinical decision-making and management strategies (Mandeş L. et al., 2020).

Electrocardiogram: In many patients with HCM, the electrocardiogram can reveal abnormalities that are not limited to those with LVOTO but may also be present in cases with mild or no obstruction. Common electrocardiographic abnormalities include ST segment depression, T wave inversions, and pathological Q waves (Finocchiaro G. et al., 2020).

Cardiac Magnetic Resonance (CMR): Currently, cardiac magnetic resonance imaging is used in combination with echocardiography to identify areas of hypertrophy that may not be detectable by the echocardiographic examination. CMR also provides more accurate

measurements of wall thickness and helps to assess the potential risk of developing HCM. This enhanced imaging capability is critical to accurately measuring left ventricular wall thickness and identifying hypertrophy in areas that are difficult to visualize with other techniques (Marian AJ. and Braunwald E., 2017). One of the CMR notable strengths is its ability to detect myocardial fibrosis using late gadolinium (LGE). Fibrosis, a significant feature in HCM, affects prognosis and treatment planning. CMR helps to identify and quantify scar tissue, providing crucial data for therapeutic treatment (Gupta S. et al., 2021).

In addition, CMR provides valuable information on the size and function of the left atrium, an important aspect as left atrial enlargement is associated with adverse outcomes in HCM. This detailed assessment helps to assess the patient overall risk profile (Geske JB. et al., 2018). However, recent guidelines recommend that nuclear imaging should not be used for the prognostic assessment of HCM because of the risks related to radiation exposure. Nevertheless, nuclear imaging might be deemed appropriate in cases where the diagnostic benefits significantly exceed the associated risks, thereby necessitating a tailored assessment of the risk-benefit ratio.

1.6.2 Secondary hypertrophy:

Secondary cardiac hypertrophy is a consequence of hemodynamic stress, in which the heart can progress to heart failure. Major causes include aortic stenosis and hypertension.

Aortic Stenosis

Aortic stenosis (AoS) is a condition characterized by the calcification of a congenitally bicuspid or normal aortic valve. This calcification leads to a progressive reduction in the aortic valve orifice, impeding the normal unidirectional flow of blood from the left ventricle to the arterial system. The resulting outflow obstruction causes hypertrophic changes in the left ventricle. Valve calcification may present as a gradual thickening, leading to aortic sclerosis, or as severe calcification that impairs the movement of the flaps, causing aortic stenosis (Freeman RV. et al., 2005). AoS is one of the most common valvular heart diseases in the Western world, predominantly affecting individuals over the age of 65, many of whom require surgical intervention for valve replacement (Kanwar A. et al., 2018).

Several data show that AoS occurs in 20% of people between 65 and 75 years old, 35% of those between 75 and 85 years old and 48% of patients over 85 years old. In these same age groups, 1.3%, 2.4% and 4% of AoS cases evolve into a lethal form (Carabello BA. et al.,

2009). These data clearly show that the incidence of AoS increases progressively with age. As life expectancy continues to rise, it is likely that AoS will become more common in the elderly population.

From an anatomical perspective, the aortic valve, under normal physiological conditions, consists of three cusps, making it a tricuspid valve. The valve cusps are characterized by three specific layers: ventricular, spongiosa, and fibrosa, each playing an essential role.

- The ventricular layer, facing the ventricle, is composed of elastin-rich fibres aligned radially, perpendicular to the edge of the cusp. This orientation is effective for the opening and closing mechanism of the valve, as it facilitates changes in shape.
- The spongiosa is a layer of loose connective tissue located at the base of the cusp, between the fibrosa and the ventricular layer. It consists of fibroblasts, mesenchymal cells, and a matrix rich in mucopolysaccharides. This layer works together with the other layers to provide tensile strength and flexibility, protecting the valve from mechanical forces over decades of repetitive movement.
- The fibrosa, found on the aortic side of the cusp, is primarily composed of fibroblasts and circumferentially oriented collagen fibres, parallel to the cusp's edge. This arrangement generates the necessary force for the valve to function effectively (Stella JA. and Sacks MS., 2007; Freeman RV. et al., 2005).

In a healthy heart, the aortic valve has an area of approximately 3-4 cm^2. When the aortic valve area decreases below these values, an increase in pressure gradient can be observed using echocardiography. The rise in pressure gradient triggers compensatory mechanisms that lead to significant left ventricular hypertrophy, impairing diastolic function and increasing resistance to ventricular filling (Grimard BH. and Larson JM., 2008). Based on this measurement, aortic stenosis can be classified into three categories according to the European Society of Cardiology (ESC) 2012 guidelines.

- **Mild Aortic Stenosis:** Valve area greater than 1.5 cm^2, with a mean gradient of 40 mmHg or less and a maximum velocity less than 4 m/s.
- **Moderate Aortic Stenosis:** Valve area between 1.0 and 1.5 cm^2, with a mean gradient between 25 and 40 mmHg and a maximum velocity between 3 and 4 m/s.
- **Severe Aortic Stenosis:** Valve area less than 1.0 cm^2, with a mean gradient greater than 40 mmHg and a maximum velocity greater than 4 m/s.

The progressive reduction in aortic valve size exacerbates the severity of the stenosis, leading to chronic pressure overload in the left ventricle. This results in increased afterload, which impairs the ejection fraction and induces compensatory concentric left ventricular hypertrophy. This hypertrophy helps the heart maintain adequate cardiac output, allowing patients with AS to remain asymptomatic, at least in the early stages of the disease (Carabello BA. et al., 2009). When the progression of left ventricular hypertrophy becomes harmful, leading to symptoms such as angina, syncope and finally heart failure, surgery to remove the outflow obstruction appears today as the best solution for these patients.

A prominent feature of AoS, as mentioned above, is valve calcification, which appears to be induced by injury and mechanical stress. This condition can be divided into two distinct phases. The early stage, defined as initiation phase, is characterized by the deposition of lipids in the valve, followed by lesions and inflammation, with significant similarities to the atherosclerotic process. Subsequently, in the progression phase, pro-calcific and pro-osteogenic factors prevail, determining the further evolution of the pathology and leading to its advanced clinical manifestation (New SE. and Aikawa E., 2011).

During the initiation phase of AoS, endothelial damage triggers the release of oxidized lipids, including oxidized low-density lipoprotein (LDL) cholesterol, and inflammatory cells into the valve tissue. In the subsequent progression phase, these proinflammatory factors stimulate the valvular interstitial cells to undergo osteogenic differentiation. This process is mediated through various mechanisms, one of which involves the binding of receptor activator of nuclear factor-kappa B ligand (RANKL) to its receptor, RANK (Pawade TA. et al., 2015).

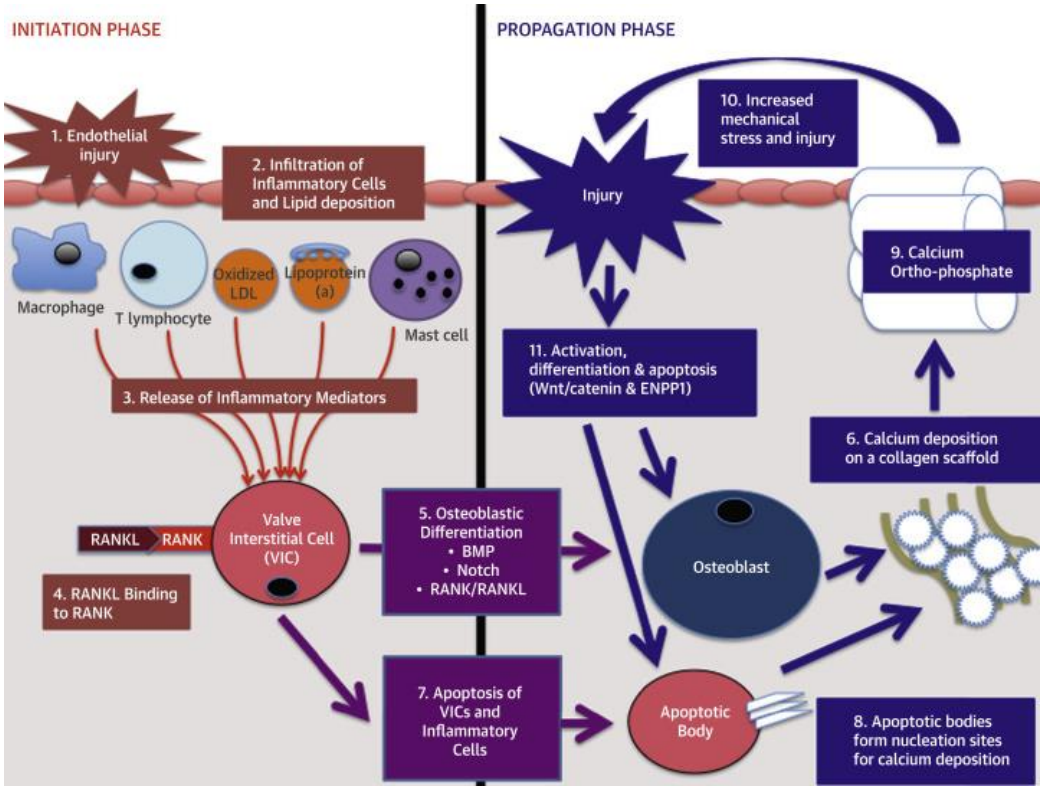

Figure 8: *The Pathophysiology of AS: Initiation Phase: Endothelial injury promotes the infiltration of oxidized lipids and inflammatory cells into the valve, along with the release of proinflammatory mediators. Propagation Phase: The ongoing proinflammatory processes subsequently drive valvular interstitial cells (VICs) to undergo osteogenic differentiation through various mechanisms, including the interaction of RANKL with its receptor RANK. Differentiated cells within the aortic valve initially lay down a collagen matrix and other bone-related proteins, causing the valve to thicken and stiffen, and eventually leading to Ca2+ deposition (Pawade TA. et al., 2015).*

Skeletal bone formation in aortic stenosis is initially marked by the deposition of collagen matrix, which precedes and anticipates subsequent pro-calcific processes. This fibrotic remodelling within the valve may be partially mediated by decreased nitric oxide (NO) expression resulting from endothelial damage. However, the renin-angiotensin system (RAS) is also considered a key factor in this process. In aortic valve calcification, angiotensin-converting enzyme (ACE) is upregulated and likely transported to the valve by low-density lipoproteins (LDL), its natural carrier. Increased expression of RAS is therefore implicated in the development of valvular fibrosis. Additionally, systemic activation of RAS contributes to the development of hypertension, which frequently guide aortic stenosis and

may accelerate disease progression by increasing mechanical stress on the valve (Peltonen T. et al., 2011; Pawade TA. et al., 2015).

The result of this fibrotic process is a structural change in the valve, characterized by an increase in thickness and stiffening of the valve cusps. This alteration in valve architecture compromises the normal function of the cusps, exacerbating blood flow obstruction and contributing to the progression of AoS. Furthermore, fibrosis is closely linked to the transition from a predominantly inflammatory pathology to a calcific one, as Ca^{2+} deposition is often preceded by significant fibrotic remodelling.

The primary symptoms in patients with severe aortic stenosis include angina, congestive heart failure, and syncope. These symptoms derived from an imbalance between the increased pressure in the LV and the hemodynamic load imposed by the valvular obstruction on the one side, and the LV capacity to manage this increased load both at rest and during exercise on the other side. As a consequence, there is an increase in cardiac mass, that results from hypertrophy of the cardiomyocytes and interstitial fibrosis. Cardiomyocyte growth is characterized by the addition of new sarcomeres, the fundamental contractile units of muscle cells, which increases cells width and consequently thickens the ventricular wall. Interstitial fibrosis arises from heightened activation of myofibroblasts, leading to the deposition of ECM. Therefore, patients with severe aortic stenosis have an unfavourable prognosis if they do not undergo surgical valve replacement (Lindman BR. et al., 2016; Freeman RV. et al., 2005).

1.6.2.1 Diagnosis

The exercise stress test can be valuable in assessing exercise tolerance and identifying potential symptoms. However, it is crucial to promptly terminate the test if the patient exhibits significant symptoms or if there is a drop in blood pressure or only a minimal increase (less than 20 mm Hg). (Freeman RV. et al., 2005).

The physical examination in patients with aortic stenosis includes:

- **Palpation of the carotid pulse:** The palpation of the carotid pulse directly reflects the arterial pressure waves. In cases of severe aortic stenosis, the carotid pulse is typically characterized by a slow rise, delayed peak, and low amplitude (Braunwald E., 2016).

- **Auscultation of the systolic murmur:** In aortic stenosis, the systolic murmur typically exhibits a late peak and is primarily auscultated at the base of the heart, with radiation towards the carotid arteries. In patients with calcified aortic valves, the murmur is often more pronounced at the base of the heart, while the higher frequency components are predominantly transmitted towards the apex, where the murmur may be more noticeable. A systolic murmur that is more intense and has a delayed peak compared to normal strongly suggests a more advanced and severe aortic stenosis (Braunwald E., 2016).
- **Dynamic auscultation:** The intensity of the systolic murmur in aortic stenosis can vary from beat to beat depending on the duration of diastolic filling, as seen in conditions like atrial fibrillation or following an extrasystole. This variability helps differentiate the murmur of aortic stenosis from that of mitral hypertrophy, which typically remains consistent. The murmur associated with aortic valve stenosis is amplified when the patient is in a squatting position, as this increases stroke volume Conversely, the intensity of the murmur decreases during the Valsalva manoeuvre and when standing, both of which reduce transvalvular flow (Braunwald E., 2016).
- **Splitting of the second heart sound:** Analysing the splitting of the second heart sound can be valuable in assessing the severity of aortic stenosis. In obstructive aortic stenosis (AoS), the reduced mobility of the valve leaflets and the prolonged left ventricular ejection time due to the obstruction can affect the aortic component of the second heart sound (A2). Specifically, the intensity of A2 may be diminished or merged with the pulmonary component (P2), making it difficult to distinguish between the two components. This fusion or attenuation of the second heart sound is indicative of increased severity of aortic stenosis (Braunwald E., 2016).

Auscultation of heart sounds, while useful, is not a reliable diagnostic tool for aortic stenosis. Current European guidelines do not recommend auscultation as the primary method for diagnosing AoS, making the use of alternative diagnostic tools necessary (Klocko DJ. et al., 2019).

Transthoracic echocardiography is recommended as the initial diagnostic test for patients with suspected aortic stenosis. This examination provides a reliable identification of the number of valve cusps and allows for detailed assessment of valve movement, cusp calcification, and left ventricular function (Cowie B., 2015).

In conclusion, Doppler echocardiography remains the most reliable diagnostic tool for aortic stenosis. This method allows precise estimation of the aortic valve area, transvalvular gradients, and maximum aortic velocity. Assessment of these three parameters is crucial for accurate diagnosis of aortic stenosis, with the severity of the condition directly related to the reduction in the aortic orifice area (Grimard BH. and Larson JM., 2008).

Hypertension

Cardiac hypertension is a pathological condition characterized by a persistent increase in blood pressure in the arteries. This phenomenon is particularly significant for the heart, as it imposes a greater load on the heart muscle, leading to structural and functional adaptations that can result in significant cardiac complications. Hypertension is recognized as a primary risk factor for several cardiovascular diseases and is the main risk factor for stroke, myocardial infarction, and renal failure. Additionally, it is associated with heart valve diseases, such as aortic valve stenosis, and heart failure (Al Ghorani H. et al., 2021). These complex interactions between elevated blood pressure and the heart highlight the importance of effective hypertension control to prevent the onset of cardiac diseases and improve long-term clinical outcomes. Hypertension induces an increase in total peripheral resistance, compelling the heart to exert greater effort in propelling blood throughout the circulatory system. This heightened workload results in the thickening of the cardiac muscle, particularly within the left ventricle, a condition known as left ventricular hypertrophy (LVH). Initially, LVH serves as a compensatory adaptation aimed at preserving cardiac output despite elevated arterial pressures. However, prolonged and uncontrolled hypertension can transform this adaptive process into a maladaptive state, leading to myocardial stiffness and reduced ventricular compliance, which subsequently precipitate diastolic dysfunction. Over time, the sustained pressure overload and structural alterations may also impair systolic function, culminating in the development of heart failure. Consequently, the interaction between LVH, diastolic dysfunction, and systolic dysfunction progressively contributes to heart failure characterized by either preserved or reduced ejection fraction (Slivnick J. et al., 2019).

Heart failure

Heart failure, as stated above, is a chronic disorder marked by the heart decreased capacity to pump adequate blood during systole, a condition known as left ventricular systolic dysfunction. In Western populations, the prevalence of heart failure is estimated to be 1-2%, with an annual incidence rate of about 5-10 per 1,000 individuals. Echocardiography is the

primary tool used to evaluate left ventricular systolic function; an ejection fraction (EF) of 40% or less typically indicates significant impairment. Epidemiologically, we observe a higher incidence with advancing age, in the female sex and with comorbidities that contribute to myocardial stiffness (e.g., metabolic and inflammatory) or exacerbate the functional abnormality (e.g., atrial fibrillation and valvulopathy). The higher incidence in women is observed as they have a longer life expectancy and advancing age causes comorbidities to accumulate (Campbell P. et al., 2024). Heart failure classification is based on the ejection fraction; we can distinguish HFpEF and HFrEF.

HFpEF now accounts for about 50% of all heart failure cases, is characterized by diastolic dysfunction, where the heart fails to fill properly and is associated with elevated left ventricular filling pressures. The pathophysiology of HFpEF is complex and multifaceted, reflecting the heterogeneous nature of the syndrome. It is associated with diseases such as obesity, diabetes mellitus, hypertension and renal disfunction, which contribute to its development and progression. In addition, ageing is a significant risk factor that further complicates the clinical presentation. Patients with HFpEF have a range of classic symptoms associated with heart failure, including exercise intolerance, dyspnoea and accumulation of extravascular fluid in different compartments such as the lungs, subcutaneous tissues and abdominal cavities. In addition, individuals with HFpEF often experience episodes of cardiovascular decompensation that require urgent hospitalization for diuretic therapy (Shahim A. et al., 2021).

HFpEF is associated to concentric hypertrophy, characterized by volume chamber reduction as consequence of cardiomyocytes enlargement. Several studies have demonstrated that HFpEF cardiomyocytes exhibit more pronounced hypertrophy and increased myofibrillar density compared to those with HFrEF, in particular a swich from collagen type III to type I and an increase in crosslinker among collagens. In vitro, cardiomyocytes from HFpEF patients showed heightened sensitivity to Ca^{2+}. Titin, a sarcomeric protein, plays a key role in myocardial stiffness. Interactions between titin and actin account for approximately 40% of left ventricular viscosity, significantly influencing the delayed myocardial relaxation.

Experimental data from an aortic banding model have shown a reduction in the amplitude of Ca^{2+} transients and a slower decay of Ca^{2+} transient kinetics (Ca^{2+}) (Hamandani N. et al., 2009), which may contribute to impaired relaxation. Furthermore, the ratio of sarcoendoplasmic reticulum Ca^{2+}-ATPase (SERCA2a) to phospholamban (PLN) content has

been found to be reduced in HFpEF myocardium compared to that of HFrEF patients. Many myofilament proteins may undergo post-translational modifications, increasing diastolic stress in HFpEF and compromising cellular bioenergetics (Lourenço AP. et al., 2018).

Systemic inflammatory status is a key predictive factor for HFpEF, and elevated levels of IL-6 are observed in these patients, which stimulate endothelial production of ROS and TNF-α. The diastolic dysfunction observed in these patients is also correlated with an increase in type I collagen. Collagen overproduction is primarily regulated by growth factors such as TGF-β and Endothelin-1 (ET-1), which promote the trans-differentiation of fibroblasts into active myofibroblasts. These myofibroblasts migrate through the inflamed microvascular endothelium, contributing to fibrosis. Microvascular inflammation directly promotes myofibroblast proliferation leading to reduce NO availability, which stimulates the activation of angiotensin II and aldosterone. This mechanism perpetuates a state of low-grade chronic inflammation, creating a vicious cycle that contributes to disease progression (Paulus WJ. et al., 2013; Mesquita T. et al., 2021).

Impairment of cardiac systolic function is the result of different process: hypertrophy, perivascular or interstitial fibrosis and infiltration of inflammatory cytokines. As consequence, the strategy to prevent or treat it, has many common points to that of primary cardiomyopathy.

HFrEF is a condition characterized by a deficit in the systolic phase of the cardiac cycle, resulting in a decreased ability of the heart muscle to contract effectively. In HFrEF direct damages to the myocardium cause depletion of contractile tissue and its substitution with fibrotic tissue. On the other hand, the loss of cardiomyocytes leads to increment the size of those remnants, causing eccentric hypertrophy for volumetric compensation. This pathological remodelling is often a consequence of previous ischemic events, such as myocardial infarction, which result in the loss of contractile tissue and subsequent volumetric compensation (Alcaide P. et al., 2024). Furthermore, the loss of cardiomyocytes results in cell death mechanisms, such as excessive autophagy, apoptosis, or necrosis, all triggered by oxidative stress. The excessive stress on the ventricular wall induced by loss of cardiomyocyte disrupts the balance between collagen deposition and degradation in the extracellular matrix. These alterations in the extracellular matrix significantly contribute to left ventricular dilation and eccentric remodelling. Other etiological factors include chronic coronary artery disease, dilated cardiomyopathy, and uncontrolled hypertension, all of which

further exacerbate left ventricular dysfunction. In a biomolecular context, patients with HFrEF typically have elevated levels of biomarkers such as brain natriuretic peptide (BNP) and its N-terminal prohormone (NT-proBNP). These markers indicate volume overload and distension of the ventricular walls, reflecting increased intracardiac pressures and impaired cardiac function aimed to maintain adequate perfusion (Oikonomou E. et al., 2019).

Additionally, elevated plasma levels of TNF-α and IL-6 are observed, which exacerbate systemic endothelial dysfunction. Unlike HFpEF, in HFrEF, the elevated plasma levels of TNF-α and IL-6 are not attributed to pre-existing comorbidities but are a direct consequence of the pathological processes underlying the condition (Paulus WJ et al., 2013). However, the immune cells and activation mechanisms involved differ significantly between these two aetiologies. This difference may contribute to the distinct responses observed in patients with HFrEF and HFpEF to current heart failure therapies (Alcaide P. et al, 2024).

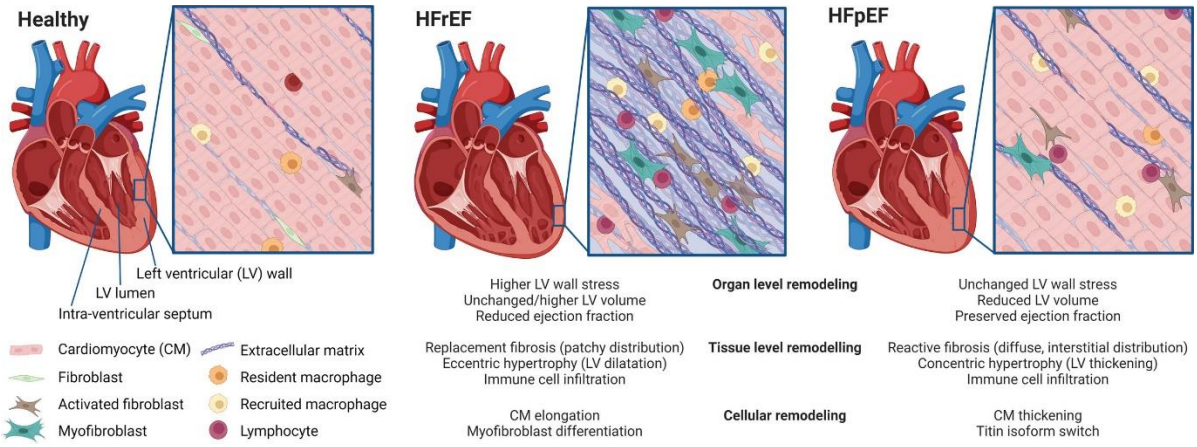

Figure 9: *Adverse myocardial remodelling at the organ, tissue, and cellular levels differs significantly between HFpEF and HFrEF. This illustration represents the overall remodelling processes at both cellular and tissue levels for both types of heart failure. HFpEF refers to heart failure with preserved ejection fraction, while HFrEF denotes heart failure with reduced ejection fraction (Alcaide P. et al,2024).*

The treatment of HFrEF focuses on reducing cardiac workload and improving ventricular contractility through several key strategies. ACE inhibitors are employed to reduce vasoconstriction and prevent ventricular remodelling, thereby enhancing cardiac function. β-blockers decrease myocardial oxygen consumption and improve survival by mitigating sympathetic overactivity. Diuretics relieve congestion by reducing plasma volume, while aldosterone receptor antagonists limit cardiac fibrosis and reduce mortality. Recently, SGLT2 inhibitors (SGLT2i), one of the topics of this thesis, have emerged as a new therapeutic option, offering significant benefits beyond glucose control, including improved cardiovascular outcomes. These benefits, which are not limited to diabetic patients and are not yet extensively studied in asymptomatic individuals, may be attributed to mechanisms such as enhanced natriuresis without tubular injury, improved cardiac metabolism and substrate utilization, reduced inflammation, and decreased oxidative stress (Krittanawong C. et al, 2023). SGLT2 inhibitors also have a modest impact on systolic blood pressure and can be safely initiated in patients with low-normal blood pressure, provided there are no other contraindications.

1.7 Pharmacological treatments:

1.7.1 Primary hypertrophy

Hypertrophic cardiomyopathy is a multifactorial disease, today there is still no specific treatment (Coppini et al., 2013). Patients suffering from the above-mentioned pathology often require drug treatments to control symptoms such as stress dyspnoea, palpitations and chest pain. A therapeutic strategy based on pharmacotherapy is the use of negative inotropes, β-blockers and Ca^{2+} antagonists such as Verapamil and Diltiazem; the latter two can be administered either to patients that are not able to take the drug or to patients not responsive to β-blockers.

β-blockers and Ca^{2+} antagonist should be gradually administer aiming to a resting heart rate not lower than or equal to a 60 bpm. These drugs are effective because their action involves the inhibition of cardiac stimulation caused by the sympathetic nervous system. (Antunes MO., and Scudeler TL., 2020; Marian AJ. and Braunwald E., 2017).

β-blockers

β-blockers are specifically used in patients who have LVOTO, as they act on the sympathetic modulation of heart rate, ventricular contractility, and myocardial stiffness during diastole. They help to make ventricular relaxation more effective, increase the time required for diastolic filling, and reduce excitability (Spirito et al., 1997; Marian AJ., 2009). The demonstrated efficacy of β-blockers in reducing both left LVOTO and myocardial ischemia has led current guidelines to recommend β-blockers as first-line drugs in symptomatic patients, both in the presence and absence of rest obstruction (Maron et al., 2003; Gersh et al., 2011).

Non-dihydropyridine Ca^{2+} channel blocker

Diltiazem and Verapamil are used in the patients without obstruction. The beneficial effects of treating patients with Ca^{2+} channel blockers are mediated by their negative chronotropic and inotropic action: the use of this class of drugs (Diltiazem, Verapamil) ensures a prolonged time for left ventricular filling and improves the redistribution of blood flow toward the sub-endocardial layer of the left ventricle (Spirito et al., 1997; Marian AJ., 2009; Choudhury et al., 1999). Among Ca^{2+} channel blockers, Verapamil has been the most extensively studied drug for the treatment of HCM. However, clinical trials conducted so far have not provided conclusive evidence on whether Verapamil definitively improves functional capacity in patients with HCM (Rosing et al., 1980; Gistri et al, 1994; Sherrid et al, 1998).

Disopyramide

Disopyramide is an antiarrhythmic drug (Class IA) exerting negative inotropic and dromotropic effects due to its anticholinergic activity that inhibits parasympathetic tone (January CT. et al., 2014). Moreover, this drug is able to avoid arrhythmic events in cells with an increase spontaneous activity, slowing the depolarization phase of action potential duration. Similar to other Class IA antiarrhythmic agents, Disopyramide also affects the delayed rectifier potassium current by inhibiting its rapid component. This action, combined with sodium channel blockade, results in QT interval prolongation. The potential for QT interval prolongation makes Disopyramide risky for conditions associated with prolonged QT, such as congenital or acquired long QT syndromes. In the context of myocardial infarction, its use must be carefully considered to avoid arrhythmic complications. Additionally, caution is advised when administering this drug to elderly patients due to their increased susceptibility to adverse effects. Furthermore, Disopyramide's negative inotropic

effect reduces left ventricular contractility and decreases the acceleration of blood flow through the outflow tract during diastole; however, its use is limited by its anticholinergic side effects.

Cibenzoline

Cibenzoline is a class IA antiarrhythmic drug, used in Japan and Korea, to manage obstructive hypertrophic cardiomyopathy (oHCM). Although it is not currently used in clinical practice in Europe and USA, this molecule is able to reduce the upstroke velocity of action potential, slightly prolongs the QT interval and does not affect heart rate.

This drug has a negative inotropic effect, for this reason it should be administered with caution. It has various advantages compared to Disopyramide as it has fewer anticholinergic side effects such as dry mouth, constipation and urinary hesitation (Palandri C. et al., 2022). Moreover, Cibenzoline acts on the sodium (Na^+) voltage-dependent channels, in particular it causes a decrease in the intracellular concentration of Na^+ ($[Na^+]_i$) in cardiomyocytes. As a response, the sodium-Ca^{2+} exchanger (Na^+/Ca^{2+}) is activated, promoting a rebalance of intracellular Na^+ levels, causing further reduction of intracellular Ca^{2+} concentration ($[Ca2^+]_i$), contributing to a negative inotropic effect, reducing the contraction force (Hamada M. et al., 2021).

Hamada and colleagues have conducted many studies comparing Cibenzoline with other class I antiarrhythmic drugs: they observed, after treatment, an improvement of diastolic LV dysfunction, a regression of LV hypertrophy and arrhythmic events in patients with oHCM (Hamada M. et al., 2014). This study validates the safety and tolerability of Cibenzoline, underlining its potential beneficial effects on symptoms of oHCM, additionally, the drug plays a role in preventing the progression of disease toward systolic heart failure and end-stage conditions (Palandri C. et al., 2022).

We must consider, as previously discussed, that treatments for the improvement of symptoms of HCM are focused on symptomatic relief with β-blockers, Ca^{2+} channel blockers non-dihydropyridine and Disopyramide. However, these treatments are not patient-specific and have several adverse effects; for this reason, patients very often undergo surgical septal reduction therapies, including surgical myectomy of the septum and alcohol ablation of the septum (Olivotto I. et al., 2020).

Mavacamten

As mentioned above, HCM is a disease characterized by alterations in the physiology of the cardiomyocyte. In particular, sarcomeric mutations are responsible for contraction abnormalities, with an increased amount of ATP producing the same strength. For this reason, a therapeutic strategy could be to act directly at the level of the contractile phase, in such a way that it can restore the physiological conditions underlying the mechanism of contraction. Green and collaborators identified a molecule, MYK-461, which is able to suppress the development of ventricular hypertrophy, cardiomyocyte disorder and myocardial fibrosis and attenuates hypertrophic and profibrotic gene expression in mice hosting human heterozygous mutations in the heavy myosine chain (Green EM. et al., 2016).

Mavacamten acts directly on the chemo-mechanical cycle of myosin: its main action is on the head of myosin; in particular, it inhibited by 50% the basal speed (only of myosin) of ADP release without affecting the rate of ADP release of cardiac myosin in a state associated with actin. This effect results in a substantial reduction of the heads of myosine available for interaction with actin (Palandri C. et al., 2022). The effect of Mavacamten on strength generation has also been confirmed in human ventricular myofibrils from frozen LV samples from human donors expressing mainly MYH7 (Reiser PJ. et al., 2001).

Moreover, its effect is also evident at the histological level, promoting a reduction of fibrosis after a treatment of 20-26 weeks. However, this effect has been observed only in the early stages of the disease onset (Palandri C. et al, 2022).

The EXPLORER-HCM study is a phase III, multicenter, randomized, double blind, placebo-controlled study conducted in 68 cardiovascular clinical centres in 13 countries, with the aim of evaluating the efficacy and safety profile of Mavacamten. The 30% of patients treated with the drug showed a reduction in the LVOT gradient to less than 30 mmHg with a clear improvement in symptoms, in particular, the greatest benefit was observed in patients who were not taking β-blockers (Olivotto I. et al., 2020). The latter evidence suggests that Mavacamten may represent a novel drug revolutionizing the therapeutic approach of HCM.

1.7.2 Secondary hypertrophy

In severe cases of aortic stenosis, the primary treatment is aortic valve replacement. This surgery has many clinical benefits, including improvement of symptoms such as dyspnoea, significant enhancement of cardiac function, and prevention of complications such as heart

failure and cardiac sudden death. The surgery reduces the pressure on the heart and restores proper blood flow, improving patients' quality of life and long-term prognosis (Braunwald E. et al., 2016).

Patients who are not suitable for surgery, often suffering from heart failure associated with reduced ejection fraction, require targeted pharmacological treatment. In these cases, therapy involves the use of Angiotensin-converting enzyme inhibitors (ACE) that are able to improve symptoms and reduce the mortality (Garg R. et al., 1995).

A promising family of drugs reducing heart failure are the gliflozins, which are the subject of this thesis. These drugs are already exploited for the condition of HFrEF and HFpEF, but numerous studies are underway to understand their mechanism of action and the potential use for other cardiac diseases.

Pharmacological treatments indicated in patients with (NYHA class II–IV) heart failure with reduced ejection fraction (LVEF ≤40%)

Recommendations	Class[a]	Level[b]
An ACE-I is recommended for patients with HFrEF to reduce the risk of HF hospitalization and death.[110–113]	I	A
A beta-blocker is recommended for patients with stable HFrEF to reduce the risk of HF hospitalization and death.[114–120]	I	A
An MRA is recommended for patients with HFrEF to reduce the risk of HF hospitalization and death.[121,122]	I	A
Dapagliflozin or empagliflozin are recommended for patients with HFrEF to reduce the risk of HF hospitalization and death.[108,109]	I	A
Sacubitril/valsartan is recommended as a replacement for an ACE-I in patients with HFrEF to reduce the risk of HF hospitalization and death.[105]	I	B

© ESC 2021

ACE-I = angiotensin-converting enzyme inhibitor; HF = heart failure; HFrEF = heart failure with reduced ejection fraction; LVEF = left ventricular ejection fraction; MRA = mineralocorticoid receptor antagonist; NYHA = New York Heart Association.
[a]Class of recommendation.
[b]Level of evidence.

Figure10: *Table 1. European Society of Cardiology (ESC) guidelines, 2021.*

Gliflozins

Recent studies have shown that Sodium-glucose cotransporter 2 (SGLT2) inhibitors, called gliflozins, constitute a novel class of oral pharmacological treatments exerting beneficial effects on type 2 diabetes mellitus and heart failure. Among the gliflozins, most effective agents are: Empagliflozin, Canagliflozin and Dapagliflozin. The latter has been specifically studied in present research thesis.

Between 2012 and 2017, the Food and Drug Administration (FDA) and the European Medicines Agency (EMA) approved the use of Canagliflozin and Empagliflozin as medications to reduce hyperglycemia in patients with type 2 diabetes.

These inhibitors are recognized for their efficacy to enhance glycemic control, as well as to induce reductions of body weight and arterial blood pressure. The function of SGLTs is intrinsically linked to the accessory protein MAP17, which is indispensable for the facilitation of glucose transport. The genes encoding SGLTs are classified within the SLC5A gene family (Braunwald E., 2022) and comprise two members, the sodium/glucose cotransporters SGLT1 and SGLT2, which are predominantly expressed in the kidneys and intestines, where regulate glucose absorption of glucose.

The kidney each day is able to filter 180L of plasma and 180g of glucose; SGLT-2 transporter is responsible for approximately 90% of renal glucose reabsorption at the level of the first segment of the proximal tubule. Instead, SGLT-1 transporter is responsible for 10% of the most distal reabsorption of the proximal tubule. At the luminal surface of tubular epithelial cells, glucose is reabsorbed via an active transport mechanism mediated by SGLT2 receptors, against its concentration gradient. This process is coupled with Na^+ reabsorption, utilizing energy generated by the Na^+/K^+-ATPase enzyme system. Interestingly, the SGLT-1 receptors are expressed in the intestine and heart, while the SGLT-2 receptor is mainly located in the kidneys and partially expressed in the pancreas (Verdecchia P. et al., 2023).

Importantly, in addition to their hypoglycemic effects, SGLT2 inhibitors prevent renal damage and cardiovascular events, in particular heart failure with both reduced and preserved ejection fraction, reducing also the occurrence of hospitalization (Salvatore T. et al., 2022).

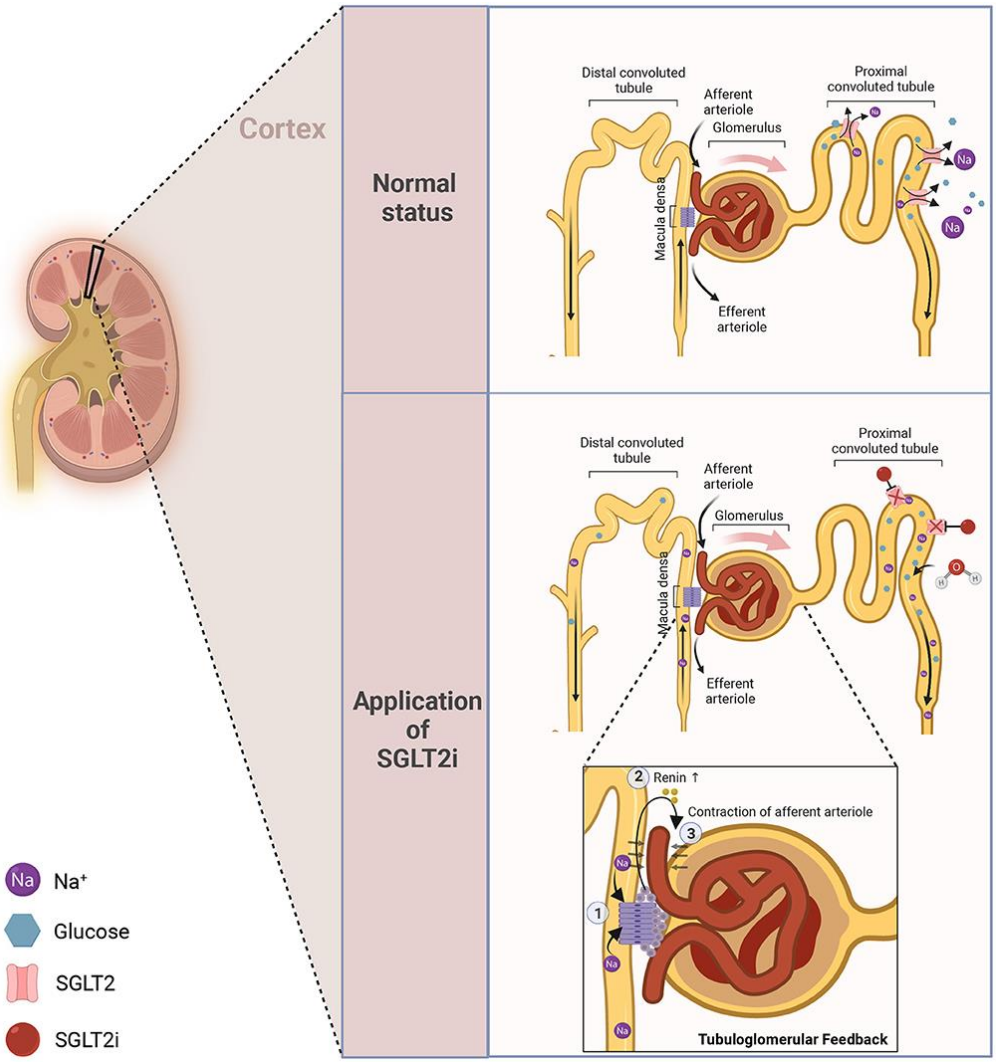

Figure11: *The mechanism by which SGLT2 inhibitors (SGLT2i) lower blood glucose involves blocking glucose reabsorption in the proximal convoluted tubule, where glucose and sodium are normally efficiently reabsorbed to maintain glucose balance. Following SGLT2i administration, this reabsorption is inhibited, resulting in increased glucose excretion in the urine, as well as diuresis and natriuresis (Li J. et al., 2022).*

Several studies have shown that after with 2 weeks of Dapagliflozin treatment, there is a consistent reduction of plasma glucose concentration and weight loss in patients with type 2 diabetes, thus improving the consequences of glucotoxicity (Merovci A. et al., 2014). Similarly, gliflozin administered to normoglycemic non-diabetic patients induces similar but not significant results (Salvatore T. et al., 2022).

It is now known that diabetic patients have an increased risk of cardiovascular disease, which leads to ischemic events and sudden death (Roger VL. et al., 2011). For this reason, a deeper

understanding of the pharmacological actions of this drug is important; in particular, in a randomized trial, placebo-controlled, EMPA-REG-OUTCOME, the SGLT2 inhibitor empagliflozin has shown marked cardiovascular benefits and improved survival. In another clinical trial, the primary objective was to assess the safety of Dapagliflozin at a dose of 10 mg. Secondary objectives included kidney function, glomerular filtration rate, and reduction of mortality risk from any cause. The results showed a reduction in mortality due to cardiovascular events and hospitalizations related to heart failure. However, adverse effects such as diabetic ketoacidosis and genital infections have been reported which led to discontinuation of treatment due to their severity (Wiviott SD. et al., 2019).

Subsequently, focused studies were conducted on heart failure patients regardless of the presence or absence of diabetes. In the international, multicentre, parallel group, randomized, double-blind, placebo-controlled study DAPA-HF, Dapagliflozin was tested on patients with HFrEF; treated patients showed a reduction of the risk of cardiovascular death and worsening heart failure (McMurray JJV. et al., 2019). Based on these outcomes, the guidelines of the American Heart Association recommend the use of gliflozin for the treatment of chronic heart failure with reduced fraction, moderately reduced or preserved. Currently, these molecules have been approved for the basic therapy of heart failure in the EU and the US.

Dapagliflozin in patients with HFrEF and HFpEF

According to the guidelines, pharmacotherapy indicated for patients affected by HFrEF, with a left ventricular ejection fraction equal or less than 40%, involves the inhibition of the renin-angiotensin-aldosterone, of the neprilysin and of the sympathetic systems.

In particular, main drug class indicated for these patients are angiotensin converting enzyme inhibitors (ACE), angiotensin receptor blockers II (ARB), angiotensin receptor neprilysin inhibitors (ARNI), β-blockers and mineral corticosteroid receptor antagonists (Gupta M. et al., 2021).

In the placebo-controlled randomized DAPA-HF study patients with ejection fraction of 40% or less were treated with Dapagliflozin in combination with other therapies recommended by the guidelines. Outcomes demonstrated a reduction of the risk of mortality and hospitalization for HF and improved symptoms. Moreover, Dapagliflozin proved able to have beneficial effects in the 55% of patients without type 2 diabetes as in those with

diabetes. These data suggest that treatments with Dapagliflozin is independent of glucose reduction, providing a basis for indications in different pathological conditions (McMurray JJV. et al., 2019). In patients with HFpEF, where cardiac compensation is directly influenced by cardio-metabolic abnormalities, improvements in symptoms have been observed following treatment with SGLT2 inhibitors, both in the presence and absence of diabetes. These inhibitors have been shown to rapidly lower pulmonary arterial pressure, which helps reduce congestion and leads to improvements in both symptoms and exercise activity (Nassif ME. et al., 2021). Furthermore, they could improve myocardium homeostasis, ameliorate microvascular dysfunction and systemic endothelial function, reduce systemic inflammation and oxidative stress. Finally, evidence suggest an improvement of insulin sensitivity and activate fatty acid oxidation in skeletal muscle (Verma S. et al., 2018; Juni RP. et al., 2019; Shah SJ. et al., 2018; Nambu H. et al., 2020). Altogether these functions make gliflozins very promising drugs for the treatment of different cardiac diseases.

2.AIM

To date, HCM and AoS remain orphaned of a specific pharmacological therapy, with drug treatments mainly limited to addressing symptoms such as dyspnoea, palpitations, heart failure, and the prevention of arrhythmogenic events, which can culminate in sudden cardiac death (SCD). Classical pharmacological approaches, involving the administration of Ca^{2+} antagonists, antiarrhythmic agents, ACE inhibitors, and β-blockers, can minimize the main pathological manifestations associated with these cardiac diseases. In recent years, there has been a growing shift toward personalized therapies, driven by the recognition that individual patients may exhibit varying responses to medications. Personalized approaches aim to reduce the risk of hospitalization, heart transplantation, or the implantation of cardiac defibrillators by addressing the unique pathophysiological mechanisms underlying each patient's condition (Peled Y., 2024).

HCM and AoS are characterized by pathological alterations, in terms of electrophysiological and functional abnormalities leading to an increased risk of occurrence of arrhythmic events, culminating in sudden death. In particular, HCM is associated with significant asymmetric hypertrophy of the left ventricle, myocardial fibrosis and alterations in the energetic profile of the cardiomyocytes. Instead, the principal symptoms of AoS involve aortic valve calcification, which leads to an impediment to the normal blood flow in the myocardium. In this thesis, we investigated the alterations in electrophysiological features associated with these two different pathological conditions, testing specific pharmacological compounds in acute administration.

Cibenzoline. Despite Cibenzoline is currently used in Asia for the treatment of some cardiac disorders, including HCM, in Europe is not in clinical use due to the limited availability of data derived from clinical trials. For this reason, we decided to test this antiarrhythmic drug in cardiomyocytes derived from patients with obstruction of left ventricle. In HCM, to evaluate the effect of Cibenzoline, ventricular cardiomyocytes isolated from human surgical samples are subjected to an acute treatment at different concentrations: 1 μM, to validate the pharmacological effects observed in Asian patients and 10 μM, to assess the onset of cardiotoxicity.

Dapagliflozin. In addition, several clinical trials highlighted the potential cardioprotective effects of a new class of drugs, Gliflozins, currently in use for the treatments of the type 2 diabetes. Moreover, a member of this class of drugs, Dapagliflozin, has been shown to reduce

the risk of hospitalisation and heart failure occurrence, ameliorating the quality of life in the patients. Although molecular mechanisms of these beneficial effects are still not clear, probably the effects on the cardiac cells are mediated by different molecular target. On base of this evidence, we perform patch clamp experiments to evaluate the acute treatment on cardiomyocytes isolated from human surgical biopsies derived from HCM and AoS patients. We used two different concentration (1 and 10 μM), to investigate the electrophysiological effects on action potential duration and Na^+ current density, in terms of late and peak Na^+ current.

Moreover, we evaluated the functional role of Ca^{2+} channels in fibroblasts; derived from HCM patients and commercial control line. Fibroblasts play a critical role in maintaining tissue homeostasis. The identification of disease-specific alterations in fibroblasts is a key step in understanding the molecular pathways underlying pathological changes (Wei K. et al, 2021). They are involved in various pathologies, as they are responsible for collagen deposition, contributing to scar formation and tissue remodelling. This process is one of the main factors driving the development of cardiac hypertrophy. For this reason, we performed functional assessment on intracellular Ca^{2+} regulation, analysing the activation of L-type and TRP Ca^{2+} channels. The aim was to investigate how the increase in cytosolic Ca^{2+} can modulate, both directly and indirectly, the transition of fibroblasts into myofibroblasts, thereby promoting pathological fibrosis. To assess the concentration of Ca^{2+} entering the cells through specific channels, we performed an acute treatment with two drugs: SKF and Lacidipine. The drugs were selected based on their ability to modulate the activity of Ca^{2+} channels. Following the treatment, we measured intracellular Ca^{2+} levels using fluorescent probes. The results were analysed to determine the efficacy of the drugs in modifying Ca^{2+} entry into the cells.

3.MATERIALS AND METHODS

3.1 Cardiomyocytes isolation from human surgical samples

In this thesis I will describe the methods to obtain vital cardiomyocytes. In particular, cardiomyocytes are derived from patients who have undergone, at the Careggi hospital, a surgical myectomy to remove a portion of the interventricular septum due to severe LVOTO, linked to primary hypertrophy (HCM) or secondary hypertrophy (AoS). Vital cardiomyocytes are obtained through a combination of enzymatic and mechanical digestion (Coppini et al., Circulation, 2013). Specifically, the heart tissue was cut into small pieces (~1mm^3) in a cardioplegic solution containing (in mM) KH2PO4 50, MgSO4 8, HEPES 10, adenosine 5, glucose 140, mannitol 100 and taurine 10. All fibrous and adipose tissue, as well as any clots present, were removed. This produces a sample composed exclusively of muscle tissue; moreover, a part was frozen in liquid nitrogen for cryopreservation. After cutting, the tissue was rinsed with dissociation buffer without Ca^{2+} (HEPES 10 mM, glucose 10 mM, taurine 20 mM, pyruvate 5 mM, NaCl 120 mM, KH2PO4 1.2 mM, KCl 10 mM, $MgCl_2$ 1.2 mM, pH 7.2). Enzymatic digestion was carried out using collagenase type V and protease type XXIV (Sigma) at 0.4 mg/ml and 0.2 mg/ml, respectively, for the degradation of the extracellular matrix in association with mechanical digestion, using a custom-made apparatus, called “tritur”. This device generates a continuous circular motion, enabling the mechanical digestion of the sample; the tritur is placed in a bath maintained at a constant temperature of 37°C. The tissue undergoes further enzymatic digestion cycles using collagenases to promote dissociation and release of individual cardiomyocytes. During digestion, the buffer containing cardiomyocytes was collected at the end of each cycle, and the enzyme action was stopped with an equal volume of KB solution at room temperature. KB solution contained: glucose 20 mM, creatine 5 mM, taurine 5 mM, EGTA 0.5 mM, succinic acid 5 mM, K2-ATP 2mM, pyruvic acid 5 mM, β-hydroxybutyric acid 5 mM, KCl 85 mM, and K2HPO4-7H2O 5mM.

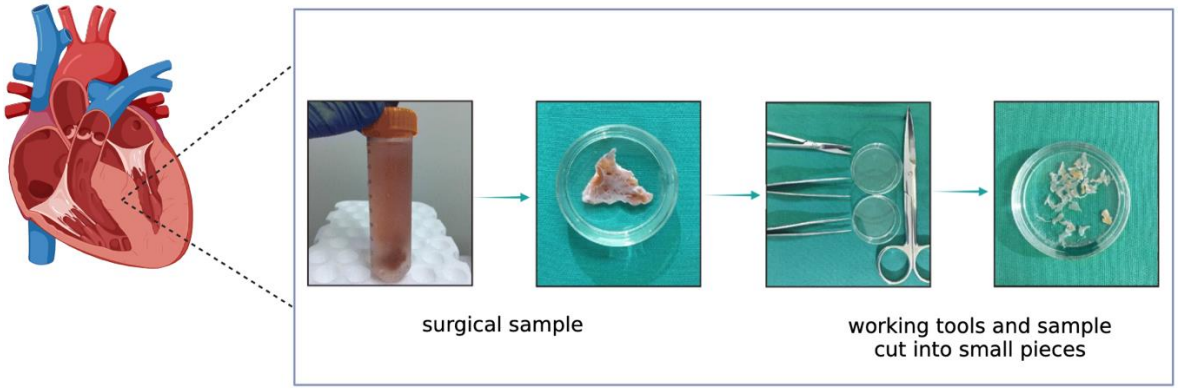

Figure 12: *Viable cardiomyocytes isolation from human surgical samples. Cardiac tissue is divided into small pieces and fibrotic and fat tissues were removed.*

A small portion of the cell suspension was subsequently examined under a microscope to assess the quantity and morphology of the isolated cardiomyocytes. The cell suspension derived from all digestion cycles was centrifuged at 700 x g for 5 minutes, and the pellet was resuspended in a Ca^{2+}-free Tyrode solution containing (in mM): $MgSO_4 \cdot 7H_2O$ 1.2, KCl 3.7, NaCl 138, KH_2PO_4 1.2, HEPES 10, glucose 5, supplemented with 1 mg/ml albumin and 0.1 mM $CaCl_2$. In conclusion, the cardiomyocytes were gradually adapted to a physiological calcium concentration by incrementally adding $CaCl_2$ until a final concentration of 0.6 mM was reached. After this stage, the cardiomyocytes were ready for functional measurements, including patch-clamp experiments and Ca^{2+}-fluorescence recordings. In any case, the selected cells must meet specific requirements for experiments: rod-shaped, presence of visible striations, well-defined cellular borders, absence of visible vacuolization or inclusions, and absence of spontaneous beating.

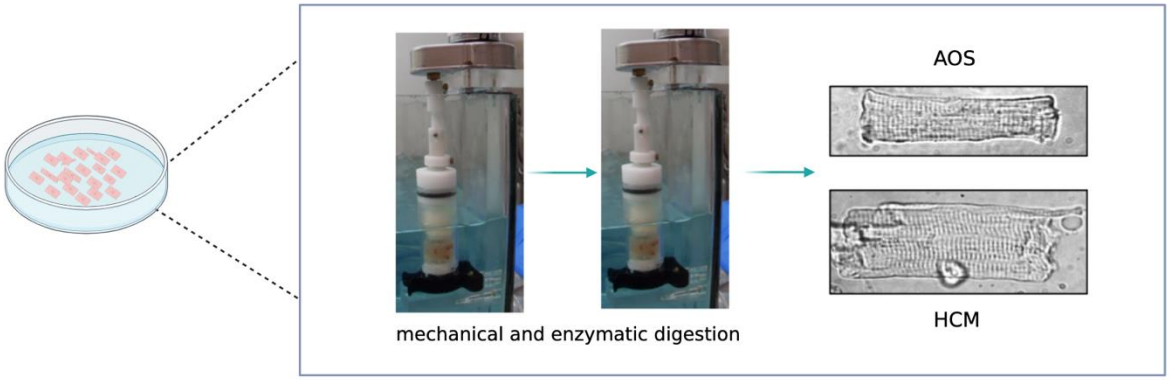

Figure 13: *Enzymatic and mechanical digestion to obtain viable cardiomyocytes. Cardiomyocytes were obtained using a custom-made tritur with a solution of collagenase and protease.*

3.1.1 Electrophysiological evaluation using patch clamp measurements

Cardiomyocytes obtain from human surgical samples of patients affect to HCM and AOS were used to perform patch-clamp experiments; the main goals are to characterize and evaluate electrophysiological changes in the presence or absence of drug treatments. Using a custom-made six-way perfusion system, we tested the acute effects of various molecules at different concentrations on the same cardiomyocytes. Regarding electrophysiological measurements, isolated cells were placed in a chamber at a temperature of 35±2 °C to perform current-clamp and voltage-clamp recordings aimed at evaluating the duration characteristics of action potentials and Na^+ currents. In all Na^+ current protocols, a holding potential of -120 mV and a cycle time of 5 s were used. The currents were filtered at 5 kHz and digitized at 20 kHz. For the sodium current recordings, the bath solution contained: NaCl 140 mM, CsCl 10 mM, $CaCl_2$ 2 mM, $MgCl_2$ 1 mM, glucose 5 mM, HEPES 10 mM, pH 7.4 adjusted with NaOH. The pipette solution contained: CsF 110 mM, CsCl 10 mM, NaF 10 mM, $MgCl_2$ 1 mM, $CaCl_2$ 1 mM, Na_2ATP 2 mM, EGTA 11 mM, HEPES 10 mM, pH 7.2 adjusted with CsOH. For perforated patch-clamp experiments, amphotericin was used. For action potential recordings, the pipette solution contained (in mM): 115 KMES (potassium methanesulfonate), 25 KCl, 10 HEPES, 3 $MgCl_2$. The standard Tyrode bath solution contained (in mmol/L): 136 NaCl, 5.4 KCl, 0.33 Na_2PO_4, 1.8 $CaCl_2$, 1 $MgCl_2$, 10 dextrose, and 10 HEPES-NaOH; the pH was adjusted to 7.35 with NaOH. Membrane potential and action potentials were measured after short stimuli of 3 ms at different stimulation frequencies (0.2 Hz, 0.5 Hz, and 1 Hz). Subsequently, the data were analysed using Clampfit software.

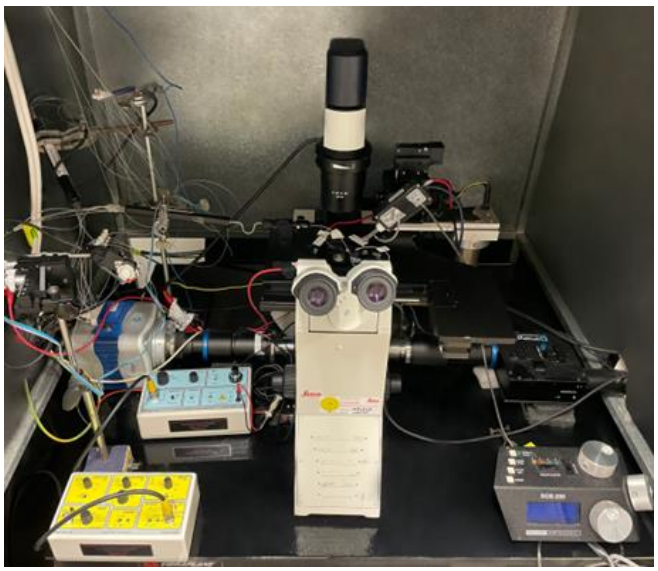

Figure 14: *inverted microscope (Leica DMi8), a fast acquisition camera (Photometrics Cascade 128+, Photometrics Evolve Delta) and a LED monochrome lamp.*

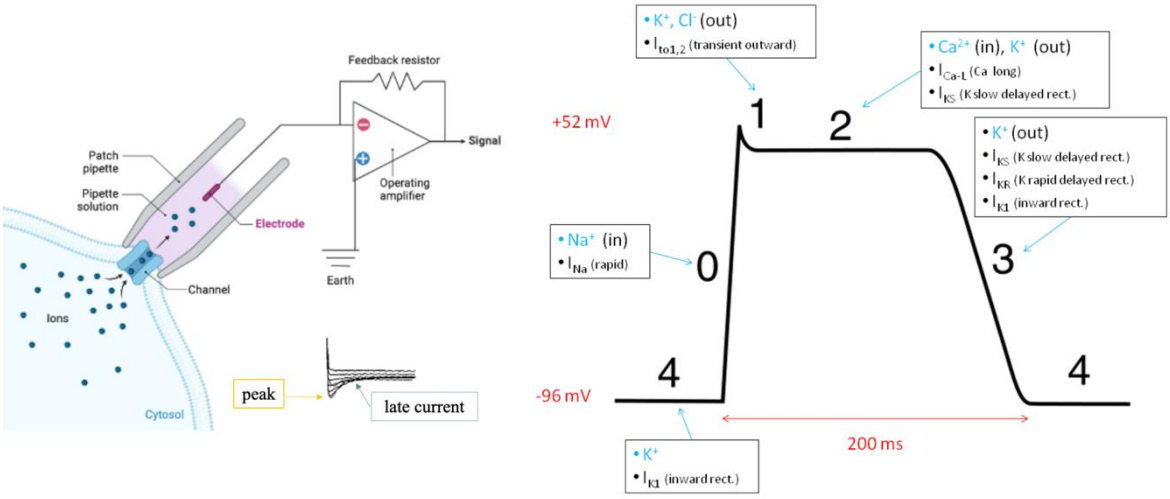

Figure 15: *Schematic representation the patch-clamp measurements; cardiac action potential and sodium current.*

3.1.2 Ca^{2+} handling evaluation using fluorescence dyes

The evaluation of Ca^{2+} concentration and fluxes between the cytosol and sarcoplasmic reticulum, in cardiomyocytes derived from patients selected for surgery, is performed by using fluorescent probes. These fluorescent molecules are able to pass through the cell membrane, binding Ca^{2+}; therefore, when excited to a specific wavelength, they are able to emit light at a different wavelength that will be captured by a camera. We associated an inverted microscope to a LED source of light and high-speed cameras (high-speed high-sensitivity EMCCD Camera, model Evolve Delta by Photometrics, USA Photometrics Cascade 128+, Photometrics Evolve Delta). Isolated cardiomyocytes were loaded by incubating cells for 30 minutes in Tyrode bath solution containing 10 μmol/L of dye, Cal520 (Quest Bioscience), together with Pluronic buffer to promote probe entrance into the cells; when incubation time ends, cells were placed to settle for 5 minutes, after we removed the supernatant and resuspended with TYR with Ca^{2+} [1.8mM]. A small drop whit the cardiomyocytes suspension is put in the microscope chamber where temperature is checked and set at 35±5 °C and the field stimulation is possible thanks to two platinum electrodes on the sides of the chamber. After waiting 5 min to let cells adhere to the glass bottom of the chamber, we started the perfusion system that helps us to have a constant perfusion (0,3 ml/min) in the chamber and finally it also allows us to change the chamber solution with those containing the drugs or different molecules we want to test. The perfusion solution is kept at controlled temperature around 38±5 °C thanks to a heating system (Warner). Cardiomyocytes suspension washed with Tyrode solution, is used for 30 minutes after incubation with the dye. The emission and excitation wavelengths of the Ca^{2+} probe (CAL520) is 490nm (EX)/520nm (EM). We recorded the fluorescence emitted at 520nm wavelength by the Ca^{2+} probes after excitation at 490nm with a LED monochrome light source, thanks to a fast acquisition camera (Photometrics Cascade 128+, Photometrics Evolve Delta). To obtain Ca^{2+} transients, cell suspension is stimulated at different frequencies (0.5Hz and 1Hz) with pulses of less than 3 msec. We evaluated the incident of premature Ca^{2+} waves, Ca^{2+} transients and the kinetics of Ca^{2+} transients, focusing the experimental evaluation on specific parameters as rising and decay phase (50-90%), amplitude. These experiments performed in presence or absence, in human cardiomyocytes, of Cibenzoline.

3.2 Long-term culture and characterization of human cardiac fibroblasts

As mentioned above, fibrosis in the heart is a factor that helps to remodel the cardiac tissue mediated by fibroblasts, representing the main responsible for this pathological process, hence our interest in the study.

We used human-cardiac fibroblasts that were expanded and maintained in culture in IMDM with L-Glutamin, Penicillin/Streptomycin, HyClone™ -Fetal Bovine Serum (Hy-FBS), basic fibroblast growth factor (bFGF), without any coating in the dish. The cells were thawed in a bath at 37° and then plated in dish 60mm and kept in culture for several days, the medium was changed every two days.

Once the cells reached 70-80% confluence, they were detached with TrypLe and plated in ibidi® plate (35 mm imaging dish with a polymer coverslip bottom for high-end microscopy and cell-based assays); the latter is a particular dish that can be used for the high resolution in microscopy. The day before the experiment, cells were starved and incubated at 37°C and 5 %CO_2. The next day, cells were loaded with a fluorescent probe, Cal520 (Quest Bioscience), which binds calcium ions, as mentioned previously. Then, we applied a protocol to identify the calcium channels responsible for calcium entry in fibroblast cytoplasm.

In particular, we focused on TRPC channels that can be activated by different stimuli. More in detail, functional measurements were performed through chemical stimulation by using different molecules carried via a custom-made six-way perfusion system in Tyrode solution with and without calcium [1.8mM]. During the experiment, cardiac fibroblasts were subsequently perfused with the following compounds:

- **Thapsigargin**, a non-competitive inhibitor of SERCA pump;
- **Lacidipine**, a L-type calcium channel antagonist; or **SKF**, an inhibitor of pre-activated transient receptor potential canonical (TRPC) channels and Ca^{2+} influx;
- **Ionomycin**, a compound that increases Ca^{2+} influx leading apoptosis;

Cardiac fibroblasts were maintained in a basal Tyrode solution without Ca^{2+}; only thapsigargin was added to deplete sarcoplasmic reticulum Ca^{2+} stores. After 3 min of recording in basal condition, we added 1.8mM Ca^{2+} to evaluate the increment of intracellular calcium concentration, when no Ca^{2+} channel blockers are present. After a wash out of the calcium, we moved to solution without Ca^{2+} but with drugs (SKF or LACI). Finally, we

switched to the same solution added of 1.8mM Ca^{2+} to evaluate the Ca^{2+} entrance and we measured the Ca^{2+} transient generated by the solution switch. At the end, we passed Tyrode solution with 1.8mM Ca^{2+} and ionomycin, that induces the maximum calcium entry flux in the cells, causing apoptosis.

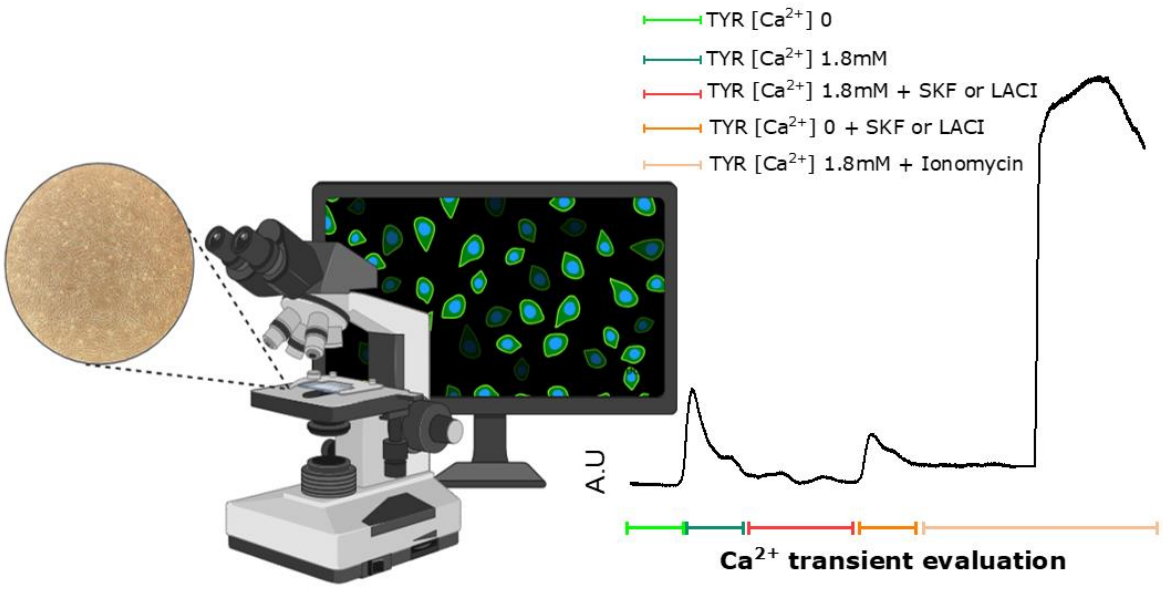

Figure16: *Schematic representation of human cardiac fibroblasts and the protocol to measure plasmalemmal* Ca^{2+} *entry in response to drugs and molecules acting on different channels and transporters. TyR= Tyrode solution; TyR [*Ca^{2+}*] = Tyrode plus [*Ca^{2+}*] 1.8mM; SKF is a drug to inhibit TRPC channels; LACI is a drug to inhibit L-type* Ca^{2+} *channel; Ionomycin is a molecule to increase membrane* Ca^{2+} *permeability.*

3.3 Fibroblasts differentiation protocol from pluripotent stem cells

In the context of processes such as fibrosis, the study of fibroblasts and the analysis of potential drug treatments are important. However, the limited availability of human samples often makes difficult to obtain enough cells. For this reason, the use of induced pluripotent stem cells (iPSCs) provides a useful tool, as it allows a higher number of cells to be generated for study, overcoming the limitations associated with a scarce availability of human samples. Thanks to the research group of Dr Albano Meli in Montpellier, starting from iPSCs, a cardiac fibroblast differentiation protocol was developed; in particular, this protocol was modified from Zhang et colleagues (Zhang et al., 2019, Nature).

Initially, the iPSCs were expanded and maintained in culture in Stemflex (Gibco) with antibiotic (Normocin) on a Corning® Matrigel hESC-Qualified Matrix (StemCell Technologies), at 37°C with 5% CO_2. After reaching 80-90% of confluence, cardiac fibroblast differentiation is promoted by the addition of medium RMPI + B27 without insulin, supplemented by Normocin and CHIR (12microM). At day 1, medium was replaced with RMPI + B27 without insulin to remove CHIR. At day 2, the medium was changed with high glucose [4,5 g/L] DMEM medium supplemented by antibiotic, glutamax [7,5mM] and all components to induce the differentiation. In particular, among these components we can find human serum albumin [500µg/ml], linoleic acid [0,6 µM], lecithin [0,6 µg/mL], ascorbic acid [50 µg/mL], hydrocortisone hemisuccinate [1,0 µg/mL], bFGF [75 ng/mL] and human recombinant insulin [5 µg/mL]; the acronym is CFBM. After 20 days in culture, we obtained fully differentiated cardiac fibroblasts. To validate the efficiency of differentiation protocol and to adjust density, increasing the number of differentiated cells obtained, immunofluorescent evaluation will be performed.

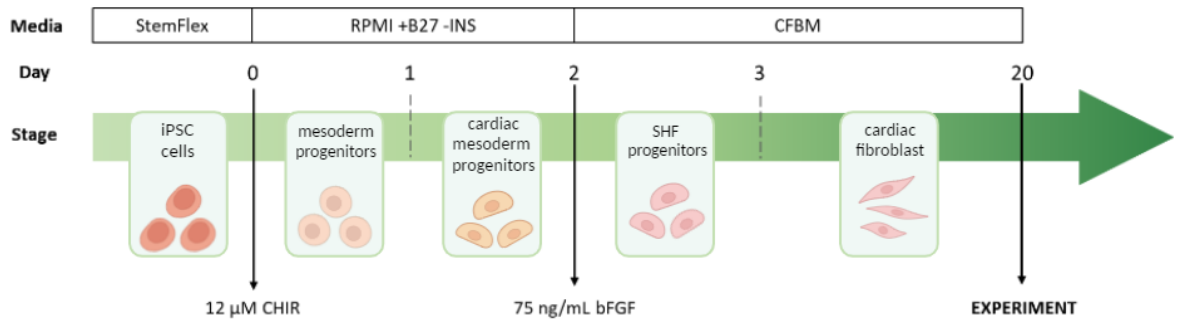

Figure 17: *Schematic timeline differentiation in cardiac fibroblast derived from iPSc.*

4. RESULTS

4.1 Electrophysiological evaluation of human ventricular cardiomyocytes from patient whit primary and secondary hypertrophy

Hypertrophy is a condition that can be physiological and pathological, which occurs in the heart and usually happen as a response to the increased perfusion requirement by peripheral organs. As mentioned in the introduction, based on the condition that causes it we have different types of hypertrophy. In particular, pathological hypertrophy represents a maladaptive response of the heart to chronic stressful conditions. HCM (Hypertrophic Cardiomyopathy), a form of primary hypertrophy, commonly associated with genetically determined sarcomere dysfunction. The main feature of HCM is the abnormal thickening of the ventricular walls; in particular, the left ventricle hypertrophy is characterized by an asymmetric distribution across the different regions of the LV (Nistri S. et al., 2006; Iacopo Olivotto et al., 2003). In addition, in HCM activated fibroblasts induce fibrosis, which contributes to the increased risk of arrhythmias and to the abnormal electrical condition.

The secondary hypertrophy is a consequence of external factors or systemic diseases that induce hemodynamic stress. Aortic Stenosis (AoS) may cause hypertrophy of the LV wall, which might also lead to obstruction of the left ventricular outflow, resulting in a large remodelling of the cardiac tissue.

We conducted a translational evaluation of these two pathological conditions, highlighting similarities and differences. The patients included in the study are the following: 132 patients with hypertrophic cardiomyopathy (HCM), 42 patients with aortic stenosis and severe LVH (AoS-LVH) and 12 non-failing non-hypertrophic patients with valve disease (NF-NH, used here as controls), who underwent surgical myectomy at the Careggi University Hospital of Florence.

Specifically, *figures 18 and 19)* display the clinical history, the clinical/instrumental features and the pre-surgical pharmacological therapy of the patients belonging to the 3 cohorts. All clinical information refers to the last visit before surgery.

Patients	***HCM***	***AoS-LVH***	***NF-NH***
Number	132	42	12
Female sex, n (%)	68 (52%)	21 (50%)	6 (50%)
Age at first visit, yrs, median [IQ range]	45 [30-59]	68 [61-74]	45 [30-59]
Age at operation, yrs, median [IQ range]	54 [39-65]	74 [69-80]	57 [45-66]
Clinical history and status			
Family History of HCM, n (%)	33 (25%)	0 (0%)	0 (0%)
Family History of SCD, n (%)	18 (14%)	3 (7%)	0 (0%)
Syncope, n (%)	26 (19%)	8 (21%)	0 (0%)
History of Atrial Fibrillation	36 (28%)	14 (33%)	0 (0%)
Exercise limitation (NYHA class ≥II)	94 (71%)	33 (78%)	0 (0%)
Therapy before surgical myectomy			
β-blockers, n (%)	109 (82%)	27 (64%)	6 (50%)
Verapamil/diltiazem, n (%)	15 (11%)	0	0 (0%)
Disopyramide, n (%)	50 (38%)	0	0
Amiodarone, n (%)	28 (21%)	4 (10%)	0
Ranolazine, n (%)	12 (9%)	0	0
ACE-I, sartans, diuretics, n (%)	42 (32%)	29 (68%)	3 (25%)

Figure 18: *clinical history and pharmacological treatment of patients with HCM, AOS-LVH or NF-NH.*

Patients	***HCM***	***AoS-LVH***	***NF-NH***
Number	132	42	12
Female sex, n (%)	68 (52%)	21 (50%)	6 (50%)
Age at first visit, yrs, median [IQ range]	45 [30-59]	68 [61-74]	45 [30-59]
Age at operation, yrs, median [IQ range]	54 [39-65]	74 [69-80]	57 [45-66]
Instrumental evaluation before surgical myectomy			
Heart rate, median [IQ range]	60 [55-66]	63 [57-70]	69 [62-77]
QTc interval, median [IQ range]	468 [438-480]	447 [413-464]	468 [438-480]
IVS, mm, median [IQ range]	21 [16-25]	17 [15-19]	12 [10-15]
LAD, mm, median [IQ range]	46 [41-50]	47 [40-52]	37 [33-43]
LVEF, %, median [IQ range]	68 [58-72]	62 [58-66]	61 [57-64]
Rest LVOT gradient >30mmHg, n(%)	132 (100%)	29 (71%)	0 (0%)
Bulging Septum	0	0	12
Aortic valve stenosis	0	42 (100%)	2
Severe Mitral regurgitation	0	0	3
Aortic valve insufficiency	0	0	7
Cardiac MRI, n (%)	78 (59%)	0	0
LGE (intramyocardial or transmural), n (%)	58 (75%)	0	0
Comorbidity: CAD	0	15 (36%)	0
Comorbidity: hypertension	13 (10%)	28 (68%)	1 (9%)
Comorbidity: diabetes	0	9 (21%)	0

Figure 19: *instrumental evaluation before surgical intervention in patients with HCM, AOS-LVH or NF-NH.*

Electrophysiological evaluations were performed on fresh ventricular human cardiomyocytes isolated from myectomy samples obtained from patients affected by primary and secondary hypertrophy, in comparison to NF-NH patients, used here as controls. Viable cardiomyocytes were obtained through the isolation protocol described in the materials and methods section and were then subjected to patch-clamp investigations.

In particular, patch-clamp measurements shown in *figure 20)* from cells display a significant prolongation of action potential duration at 90% in HCM and AoS-LVH cardiomyocytes, compared to control cardiomyocytes, at all stimulation frequencies tested (0.5Hz and 1Hz). This evidence highlights that pathological remodelling, in term of hypertrophy, observed in HCM and AoS result in abnormalities occurring in action potential kinetics. Furthermore, HCM cardiomyocytes show a more pronounced prolongation of action potential duration as compared with AoS, with respect to non-hypertrophic patients.

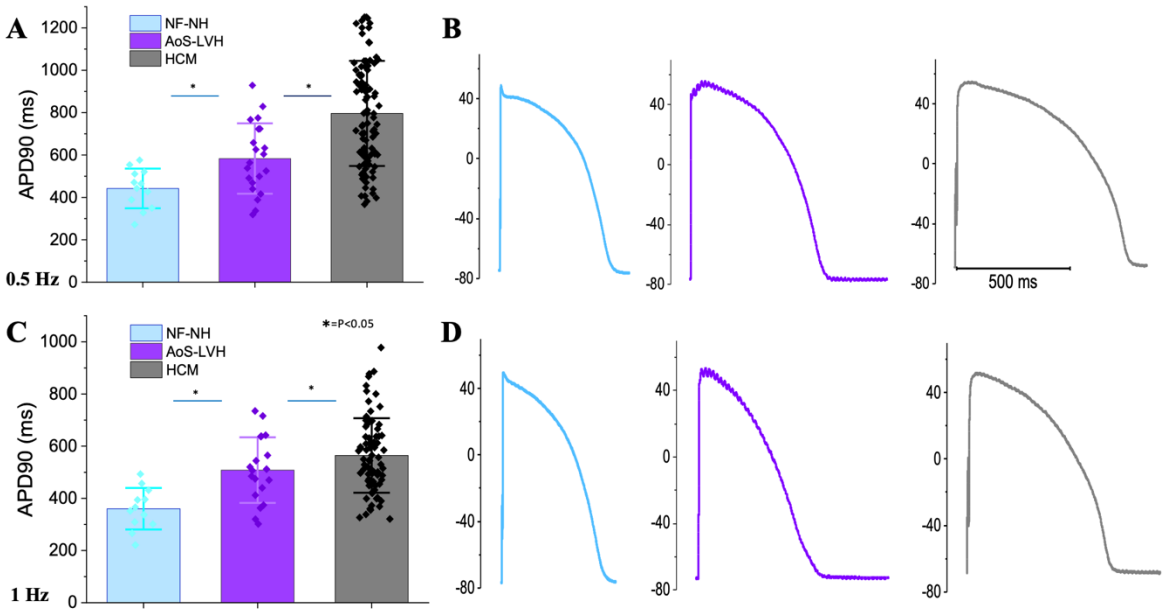

Figure 20: Electrophysiological characterization of ventricular cardiomyocytes isolated from control, aortic stenosis and hypertrophic cardiomyopathy surgical samples: current clamp configuration. A) *Action potential duration at 90% repolarization (APD90%) recorded during stimulation 0.5Hz in human ventricular cardiomyocytes isolated from CTRL (light blue), Aos-LVH (violet) and HCM (grey) surgical samples.* ***B)*** *Representative action potential traces recorded in human ventricular cardiomyocytes isolated from CTRL (light blue), Aos-LVH (violet) and HCM (grey) surgical samples recording at 0.5hz.* ***C)*** *Action potential duration at 90% repolarization (APD90%) recorded during stimulation 1Hz in human ventricular cardiomyocytes isolated from CTRL (light blue), Aos-LVH (violet) and HCM (grey) surgical samples.* ***D)*** *Representative action*

*potential traces recorded in human ventricular cardiomyocytes isolated from CTRL (light blue), Aos-LVH (violet) and HCM (grey) surgical samples during stimulation at 1hz. * = p<0.05 (each dot is a patient).*

In addition, to evaluate Ca^{2+} handling in hypertrophic cardiomyocytes, Ca^{2+} measurements were performed after loading the isolate cells with a Ca^{2+}-sensitive fluorescent dye (Cal520) to highlight the movements of Ca^{2+} ions inside the cytosol. Ca^{2+} imaging technique was carried out in ventricular cardiomyocytes isolated from AoS, HCM and CTRL and Ca^{2+} transient kinetics was evaluated during external pacing at 0.5 and 1Hz, as described in the material and methods. In particular, in *figure 21)*, our results suggest that the Ca^{2+} transient (50% decay) is significantly increased in HCM and AoS ventricular cardiomyocytes compared to control cells, at all frequencies tested (0.5Hz; 1Hz). Moreover, Ca^{2+}-transient prolongation is more pronounced in HCM vs. AoS-LVH cardiomyocytes.

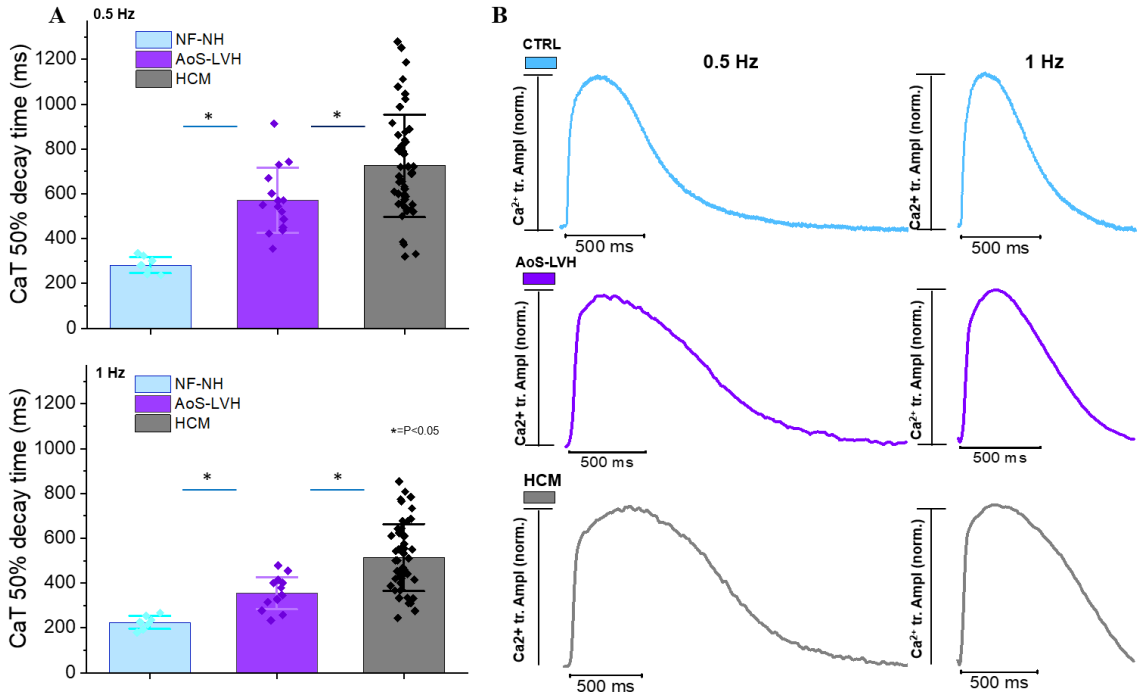

***Figure 21: Functional measurement of Ca^{2+}transient kinetics**. **A)** Evaluation of Ca^{2+} transient 50% decay (ms) at imposed stimuli of 0.5Hz and 1Hz in human ventricular cardiomyocytes isolated from CTRL (light blue), Aos-LVH (violet) and HCM (grey) surgical samples. **B)** Representative traces of Ca^{2+}transient recorded in human ventricular cardiomyocyte isolated from CTRL (light blue), Aos-LVH (violet) and HCM (grey) surgical samples during stimulation at 0.5hz and 1Hz, * = p<0.05 (each dot is a patient).*

Furthermore, as shown in *figure 22)*, Ca^{2+} transient time to peak is prolonged in HCM and in AoS cells, with regards to control myocytes. The evaluation of diastolic Ca^{2+} concentration in the 3 experimental groups (HCM, AoS, ctrl) revealed an increased accumulation of diastolic Ca^{2+} when stimulation rate is increased from 0.5Hz to 1Hz in diseased cells *(panels B and C)*. This marked increase of diastolic Ca^{2+}-concentration is observed in both HCM and AoS myocytes.

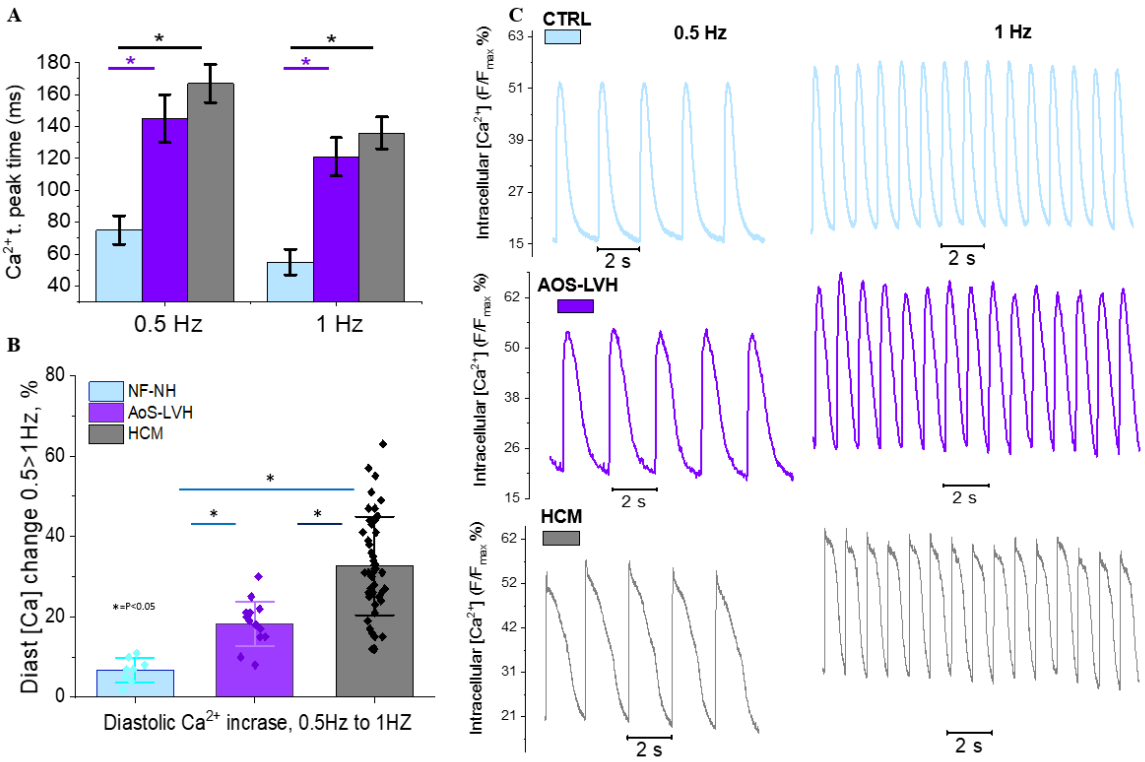

Figure 22: Functional measurement of Ca^{2+} transient kinetics. A) *Measurements of Ca^{2+} time to peak (ms) at imposed stimuli of 0.5Hz and 1Hz in human ventricular cardiomyocyte isolated from CTRL (light blue), Aos-LVH (violet) and HCM (grey) surgical samples.* ***B)*** *Evaluation of diastolic Ca^{2+} concentration (%) during the stimulation at 0.5Hz in comparison to 1Hz in human ventricular cardiomyocyte isolated from CTRL (light blue), Aos-LVH (violet) and HCM (grey) surgical samples.* ***C)*** *Representative traces of intracellular Ca^{2+} concentration in human ventricular cardiomyocyte isolated from CTRL (light blue), Aos-LVH (violet) and HCM (grey) surgical samples during stimulation at 0.5hz and 1Hz,* ***** *= $p<0.05$ (each dot is a patient).*

In addition, since HCM is characterized by electrophysiological alterations that occur at the level of ion currents, we performed specific voltage-clamp investigations. In particular, L-type Ca^{2+}current was increased in HCM and AoS compared to control. This effect is more evident in patients affected by HCM rather than in those with secondary hypertrophy.

Moreover, the kinetics of Ca^{2+}-current inactivation was slower in HCM and AoS cells as compared to control myocytes.

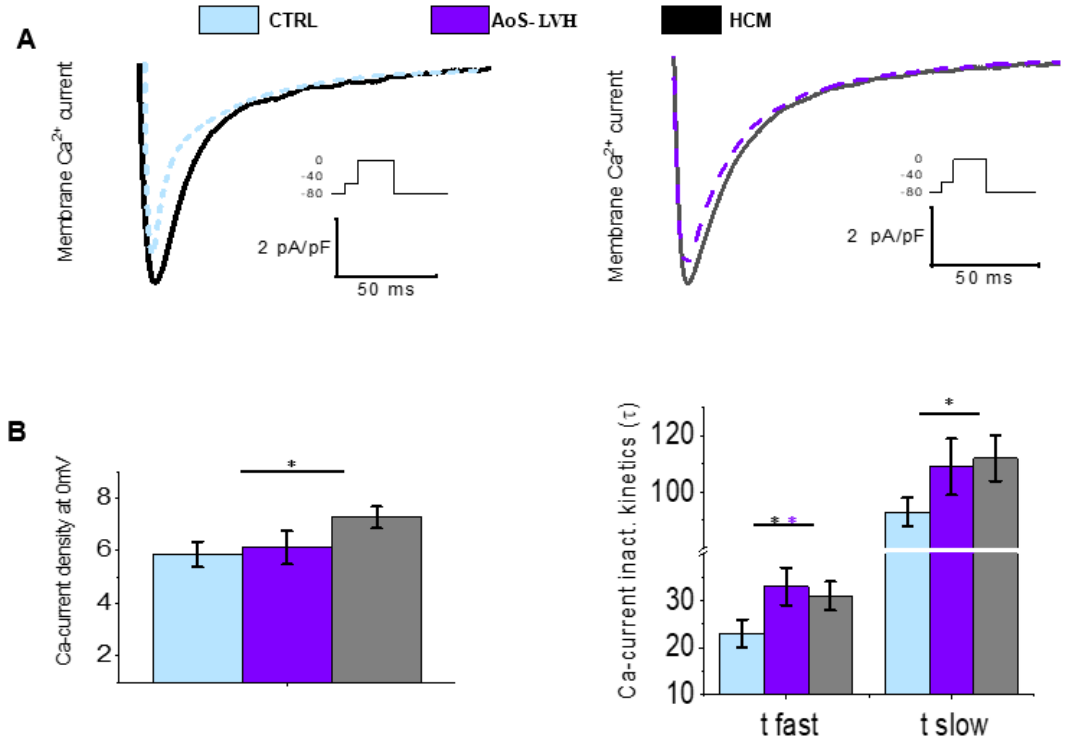

Figure 23: Functional measurement L-type Ca^{2+}-current. A) *Representative traces of Ca^{2+} current measured in voltage-clamp configuration in human ventricular cardiomyocyte isolated from CTRL (light blue), Aos-LVH (violet) and HCM (grey) surgical samples (depolarization step from -80 to 0 mV).* ***B)*** *LEFT: Representation of average L-type Ca^{2+}-current density in voltage-clamp configuration in human ventricular cardiomyocyte isolated from CTRL (light blue), Aos-LVH (violet) and HCM (grey) surgical samples the recording has been performed at 0.5H. RIGHT:L-type Ca current inactivation kinetics in the 3 cell group: a biphasic exponential was used to fit the decay curves and two time constants (tau values, fast and slow) were calculated,* ******* *= $p<0.05$.*

In addition, we measured late Na^+ current, i.e. the component of Na^+ current that does not inactivate rapidly and persists for over 50ms. The normalized inward of Na^+ inward current was calculated in each condition. The analysis revealed that late Na^+ current is markedly increased in both HCM and AoS myocytes as compared with controls, the increase being larger in HCM than in AoS cells.

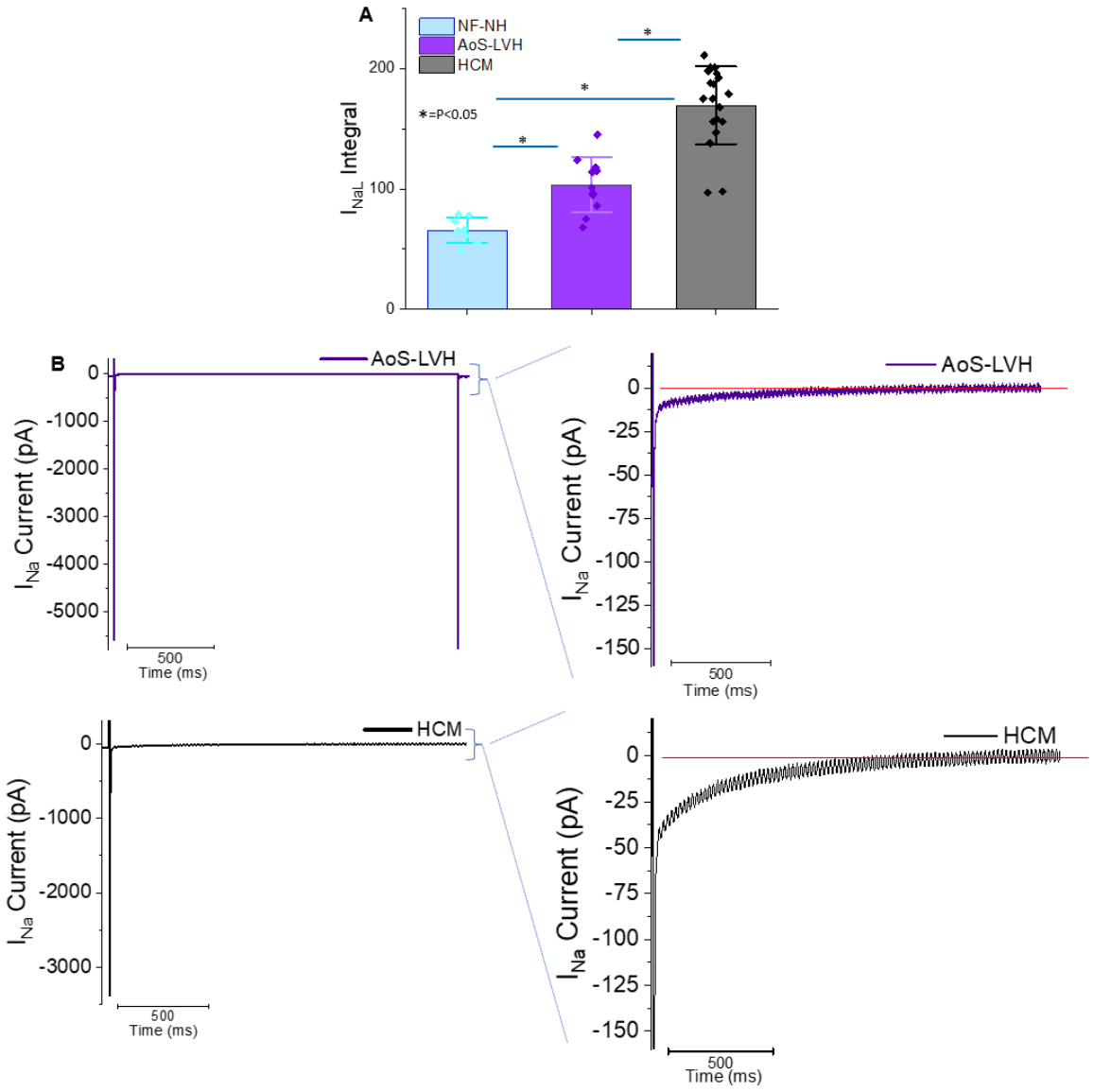

Figure 24: Functional measurement late Na^+ current. A) *Evaluation of Na^+ current in voltage-clamp configuration in human ventricular cardiomyocytes isolated from CTRL (light blue), Aos-LVH (violet) and HCM (grey) surgical samples; the recording has been performed at 0.5Hz,* ******* *= $p<0.05$ (each dot is a patient).* ***B)*** *Representative I_{Na} traces focused on the late current (depolarization step from -120 to -10mV) in human ventricular cardiomyocyte isolated from CTRL (light blue), Aos-LVH (violet) and HCM (grey) surgical samples.*

In conclusion, these results demonstrate that both HCM and AoS-LVH cardiomyocytes undergo significant pathological remodelling, characterized by a prolongation of action potential duration and impaired Ca^{2+} handling. However, the extent of electrophysiological abnormalities is greater in HCM, suggesting that primary hypertrophy is associated with more severe ion current dysregulation.

4.2 Evaluation of Cibenzoline in patients with HCM

In HCM myocardium, the alteration of ion channels and electrical currents can lead to a prolongation of action potential duration. This prolongation may disrupt the normal repolarization, increasing the susceptibility to arrhythmic events. In particular, the prolongation of action potential is driven by excessive Na^+ and Ca^{2+} influx, which leads to intracellular Ca^{2+} overload. In patients with obstructive hypertrophic cardiomyopathy (oHCM), Disopyramide is often employed due to its negative inotropic effects to reduce obstructive symptoms. Disopyramide, however has a number of sides effects and has limited efficacy and tolerability. There is a compelling need to introduce new drugs for obstructive HCM.

In this context, Cibenzoline is a promising drug for the treatment of oHCM. Like Disopyramide, it is a class I antiarrhythmic drug. Nevertheless, the drug has not yet evaluated in ventricular cardiomyocytes derived from patients with oHCM. Our previous studies demonstrated that Disopyramide, an antiarrhythmic drug, is able to shorten the action potentials, reduce late Na^+ current and normalize intracellular Ca^{2+} handling.

We evaluated the effects of two different preparations of Cibenzoline, CT-G20 (Cibenzoline L-stereoisomer) and CT-G11 (Cibenzoline racemate) on action potentials, Na^+ current and Ca^{2+} transients in oHCM cells.

Dose-dependent shortening of action potential duration exerted by CT-G20 in ventricular cardiomyocytes from oHCM patients

A total of 33 ventricular cardiomyocytes isolated from 11 surgical samples of oHCM patients were studied with the patch-clamp technique. Current clamp experiments showed that CT-G20 induced a dose-dependent shortening of action potential duration, at all the frequencies of stimulation tested (0.2Hz, 0.5Hz, 1Hz). In particular, in *figure 25)* we measured the average kinetics of action potential at APD20 (time from stimulus to 20% of repolarization), APD50 (time from stimulus to 50% repolarization) and APD90 (time from stimulus to 90% of repolarization). CT-G20 did not exert any significant shortening effect on action potential at the concentration of 0.4 μM. Instead, at 1 μM we observed a significant reduction of action potential duration, and the effect increased at 4 and 10 μM.

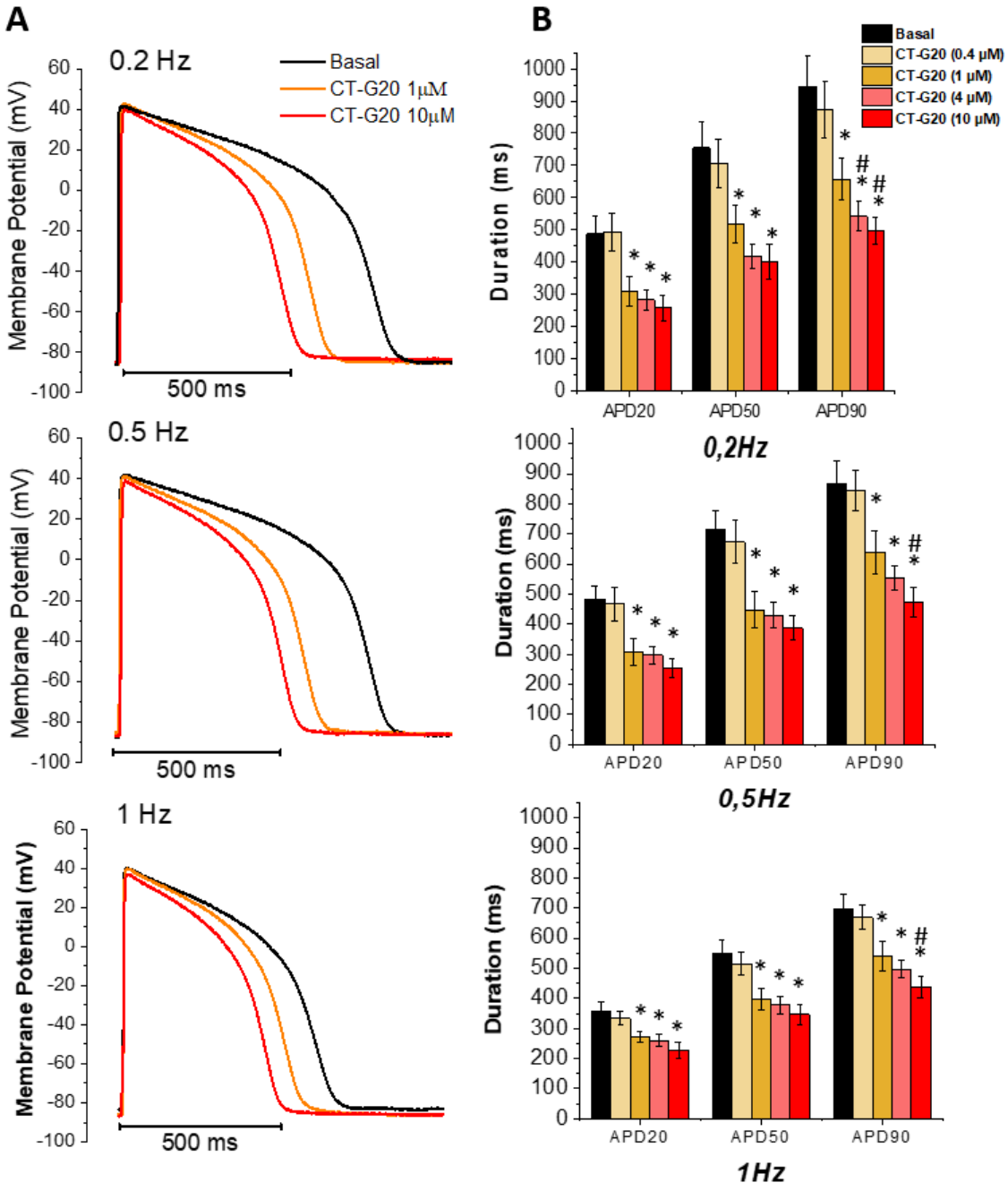

Figure 25: Evaluation of action potentials by CT-G20 in oHCM cardiomyocytes. A) *Representative traces of action potentials recorded during stimulation at 0.2 Hz, 0.5 Hz and 1Hz from oHCM cardiomyocytes, before drug exposure (black traces) and during exposure to different CT-G20 at the concentration of 1 µM (orange traces) and 10 µM (red traces).* ***B)*** *Average action potential duration at 20%, 50% and 90% of repolarization (APD20%, APD50%, APD90%) recorded in oHCM ventricular cardiomyocytes at 0.2 Hz, 0.5 Hz and 1Hz, before and after exposure to different CT-G20 concentrations (0.4 µM, 1 µM, 4 µM, 10 µM). Means± S.E.M. (Standard Error of Mean). *= P<0.05 at paired t-test versus basal and 0.4 µM concentration; #= P<0.05 at paired t-test versus 1 µM concentration.*

Moreover, we calculated the EC50 values for action potential shortening and the data show that the shortening was similar at all pacing rates and EC50 values were slightly below 1 µM.

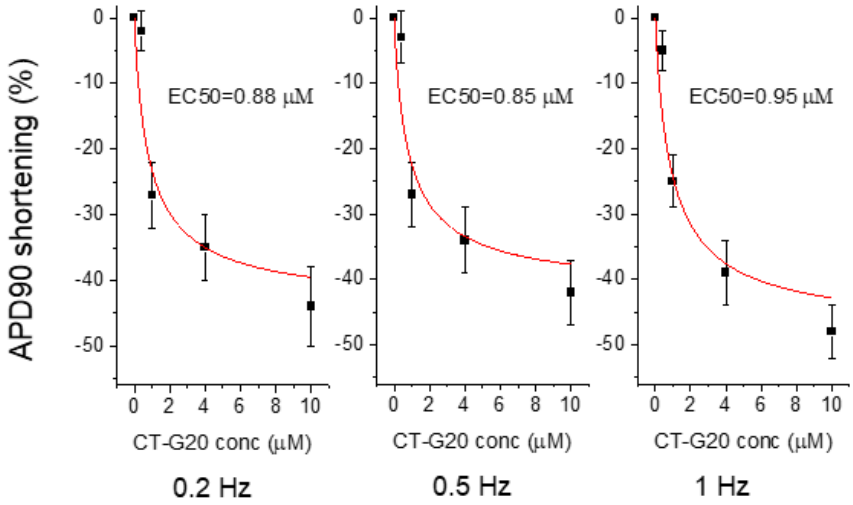

Figure 26: Evaluation of EC50. *Percentage variation of APD90 from baseline at the different CT-G20 concentrations (0.4 µM, 1 µM, 4 µM, 10 µM) in oHCM cardiomyocytes paced at different frequencies (0.2Hz, 0.5Hz and 1Hz). Concentration-effects curves were fitted with logistic equations (curves shown in red) to calculate EC50.*

Furthermore, we studied the effects of CT-G20 on action potential upstroke speed, the *figure 27)*, showing magnified action potential upstrokes with different concentrations of the drug, highlighting the slowing of upstroke with higher CT-G20 concentrations. The reduction of action potential upstroke slope was very slight at 1 µM: at this concentration, the difference was significant only at higher pacing rates. The upstroke speed reduction became more substantial at 4 µM and was even more pronounced when CT-G20 concentration was raised up to 10 µM. Calculated EC50 values for action potential upstroke speed reduction were moderately below 4 µM. Remarkably, the reduction of action potential upstroke speed was quantitatively larger at higher rates such as 1Hz, as compared with slower rates; in particular, upstroke slowing was maximal at the concentration 10 µM.

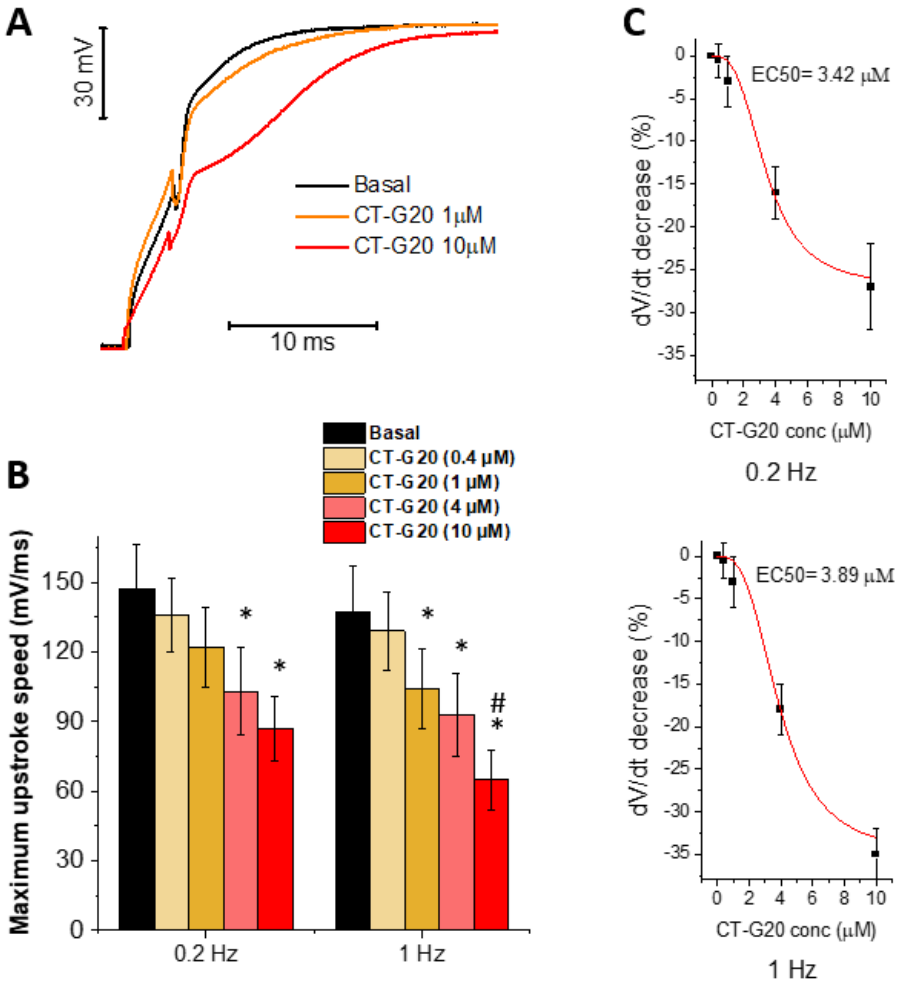

Figure 27: Action potential kinetics. A) *Magnification of the upstroke phase of the action potential recorded in oHCM cardiomyocytes, before and after exposure to different CT-G20 concentrations (1 µM and 10 µM.)* ***B)*** *Maximum upstroke speed of action potential recorded in ventricular cardiomyocytes from oHCM patients at 0.2 Hz and 1 Hz, before and after exposure to different CT-G20 concentrations (0.4 µM, 1 µM, 4 µM, 10 µM). Means± S.E.M. (Standard Error of Mean). *= P<0.05 at paired t-test versus basal and 0.4 µM concentration; #= P<0.05 at paired t-test versus 1 µM concentration.* ***C)*** *Percentage variation of action potential upstroke speed from baseline at the different CT-G20 concentrations (0.4 µM, 1 µM, 4 µM, 10 µM), in oHCM cardiomyocytes paced at different frequencies (0.2 and 1 Hz). Curves fitted with logistic equations to calculate EC50.*

Dose-dependent shortening of action potential duration exerted by CT-G11 in cardiomyocytes from oHCM patients

A total of 23 ventricular cardiomyocytes isolated from 7 surgical specimens of oHCM patient were investigated with the patch-clamp technique. In line with the effects of CT-G20, current clamp experiments revealed that CT-G11 induced a dose-dependent shortening of action potential duration, at all the frequencies of stimulation tested (0.2Hz, 0.5Hz, 1Hz). In particular, in *figure 28)* we observed the average kinetics of action potential at APD20 (time from stimulus to 20% of repolarization), APD50 (time from stimulus to 50% repolarization) and APD90 (time from stimulus to 90% of repolarization). A significant reduction on action potential duration was observed with 1 µM CT-G11 and the effect increased while raising the drug concentration to 4 µM and 10 µM.

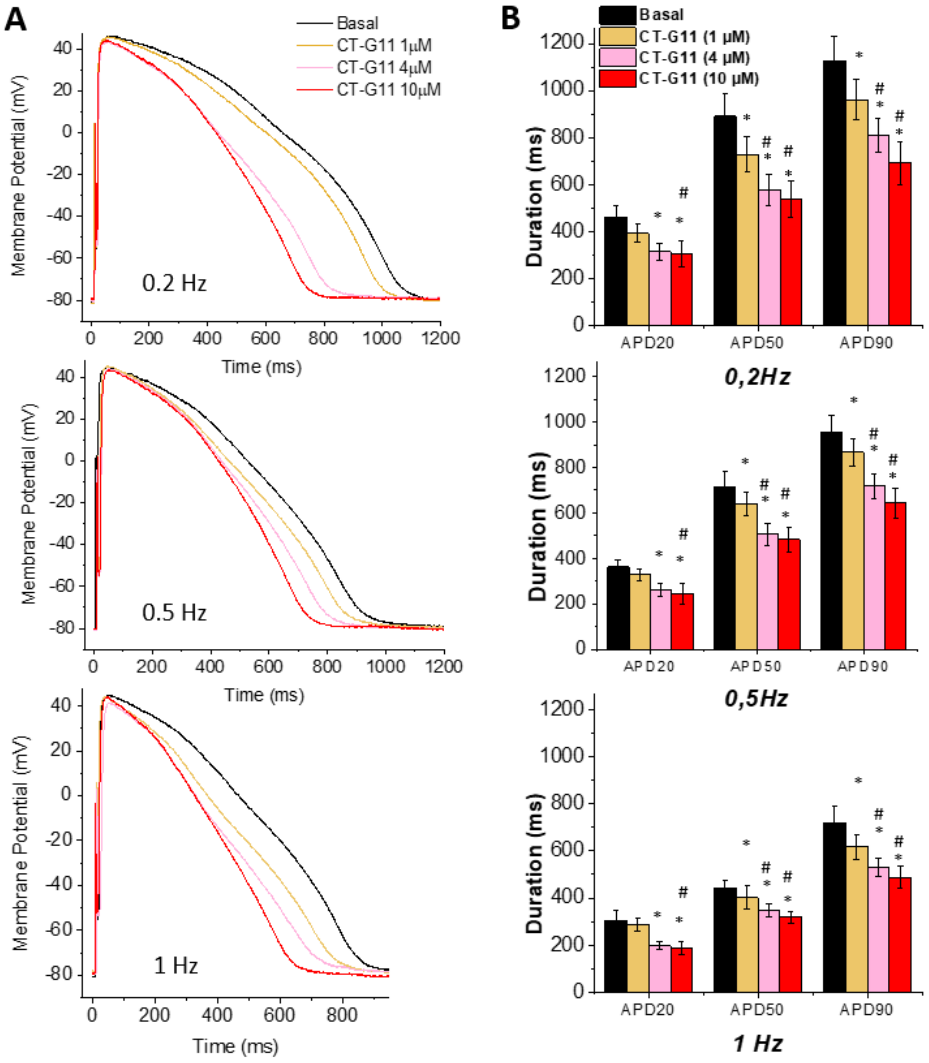

Figure 28: Evaluation of action potentials by CT-G11 in oHCM ventricular cardiomyocytes. A) *Representative traces of action potentials recorded during stimulation at 0.2 Hz, 0.5 Hz and 1Hz*

from oHCM cardiomyocytes, before drug exposure (black traces) and during exposure to different CT-G11 at the concentration of 1 µM (orange traces) 4 µM (pink traces) and 10 µM (red traces). ***B)*** *Average of action potential duration at 20%, 50% and 90% of repolarization (APD20%, APD50%, APD90%) recorded in oHCM ventricular cardiomyocytes at 0.2 Hz, 0.5 Hz and 1Hz, before and after exposure to different CT-G11 concentrations (1 µM, 4 µM and 10 µM).*

Moreover, we analysed the EC50 values for action potential shortening and the data show that values were similar at all pacing rates, that is, around 3 µM.

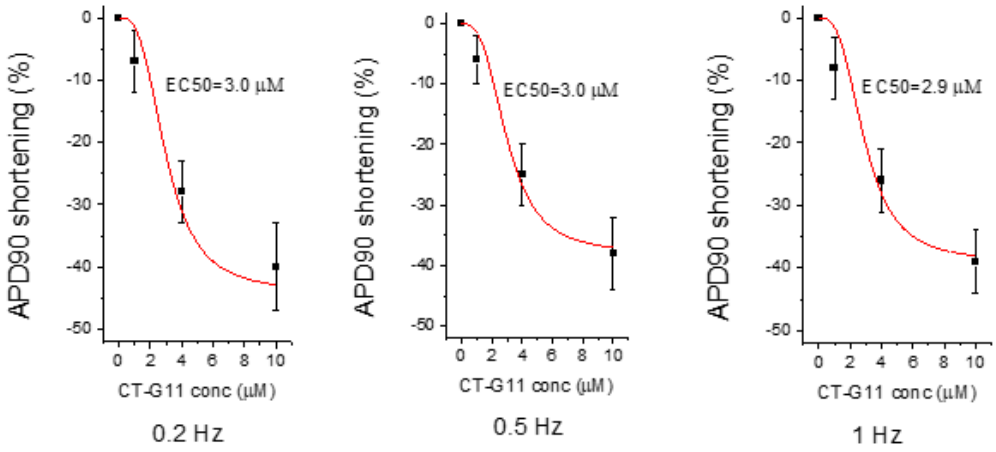

Figure 29: Evaluation of EC50. *Percentage variation of APD90 from baseline at the different CT-G11 concentrations (1 µM, 4 µM and 10 µM) in oHCM cardiomyocytes paced at different frequencies (0.2Hz, 0.5Hz and 1Hz). Concentration-effects curves were fitted with logistic equations (curves shown in red) to calculate EC50.*

Further, we studied the effects of CT-G11 on action potential upstroke speed, in *figure 30)*, showing that the drug determined a reduction of upstroke slope at all frequencies that we tested (0.2 Hz, 0.5Hz and 1Hz). Upstroke slowing was not present at 1 µM but only at higher CT-G11 concentration (4 µM and 10 µM). Calculated EC50 values for action potential upstroke speed reduction were about 3 µM and the reduction is larger at 0.5 Hz and 1 Hz, as compared with 0.2 Hz, underlining a frequency-dependent effect. The potency of CT-G11 in reducing the action potential duration and the upstroke speed is the same, at variance with CT-G20, which shows increased potency in reducing AP duration.

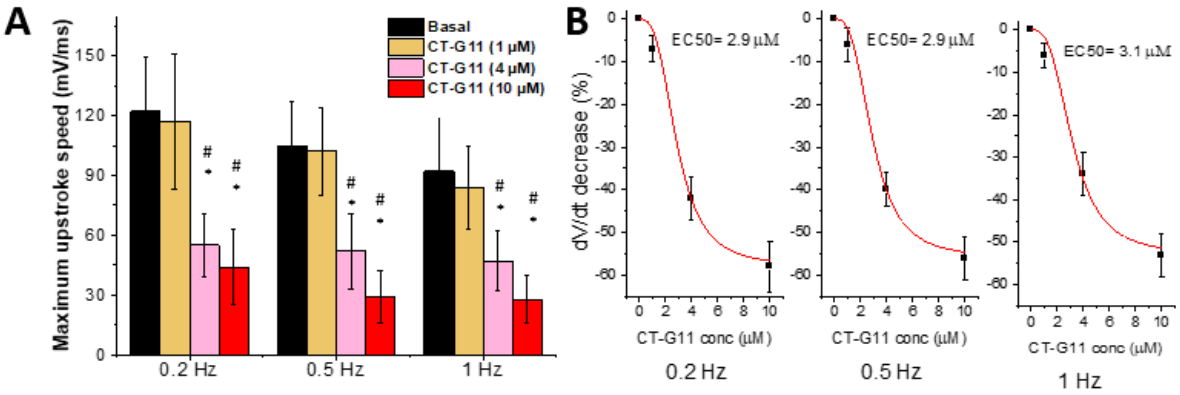

Figure 30: Evaluation of upstroke and EC50. A) *Maximum upstroke speed of action potential recorded in ventricular cardiomyocytes from oHCM patients at 0.2 Hz and 1 Hz, before and after exposure to different CT-G11 concentrations (1 µM, 4 µ and, 10 µM).* ***B)*** *Percentage variation of action potential upstroke speed from baseline at the different CT-G11 concentrations (1 µM, 4 µM and 10 µM), in oHCM cardiomyocytes paced at different frequencies (0.2Hz, 0.5Hz and 1 Hz). Curves fitted with logistic equations to calculate EC50.*

Evaluation the reduction of late and peak Na^+ currents exerted by CT-G20 in oHCM cardiomyocytes

We performed patch-clamp experiment in cardiomyocytes isolated from surgical sample of oHCM patients. We measured the effects of CT-20 on I_{NaL} elicited with long depolarization steps from -120mV to -10mV. In line with the observed shortening of AP duration, we have a significant reduction of Na^+ current at all concentrations except for 0.4 µM. Interestingly, our data show that the efficacy of CT-G20 for the inhibition of late and peak Na^+ current is different. Notably, the late Na^+ current was significantly reduced even at 1µM, while the peak Na^+ current showed only a slight reduction at 1µM. A more pronounced reduction in peak Na^+ current was observed only when the drug concentration was increased to 4 µM and 10 µM.

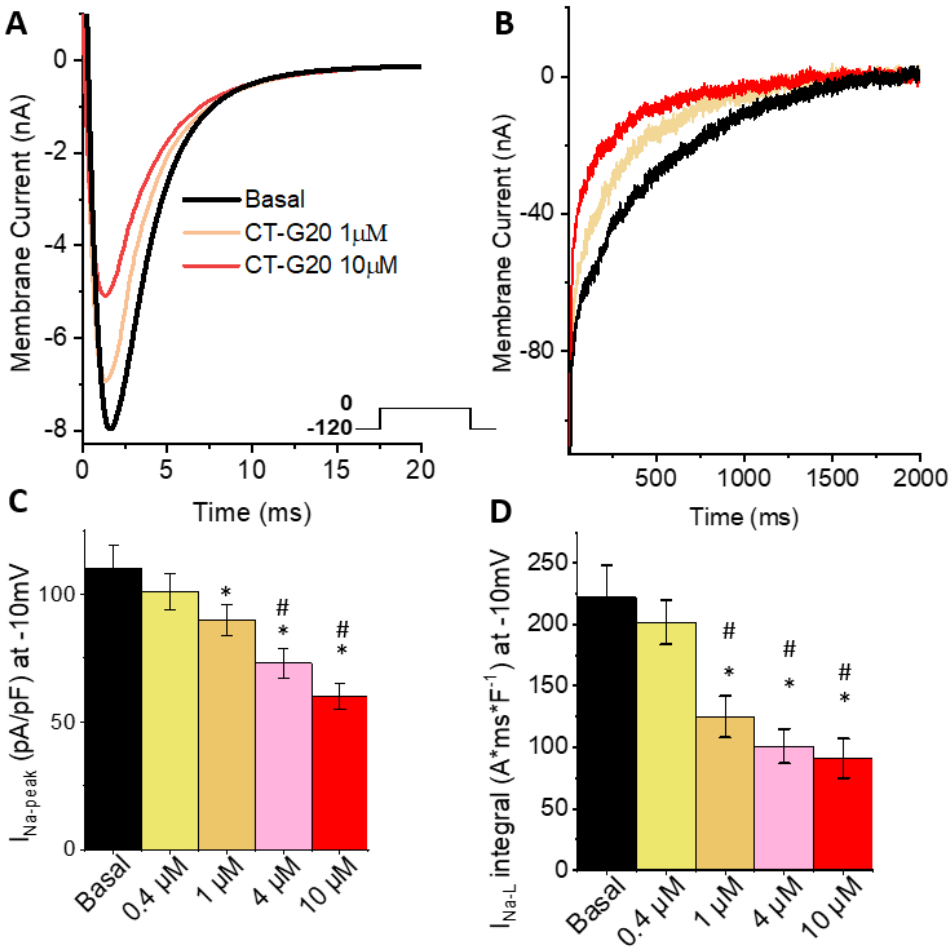

Figure 31: Evaluation late and peak Na^+ current with CT-G20 in oHCM cardiomyocyte. A) *Representative I_{Na} traces focused on the peak current (first 25 ms of the depolarization step from -120 to -10mV), recorded in oHCM cardiomyocytes, before and after exposure to different CT-G20 concentrations (1 µM, 10 µM).* ***B)*** *Representative I_{Na} traces focused on the late current, recorded in oHCM cardiomyocytes, before and after exposure to different CT-G20 concentrations (1 µM, 10 µM).* ***C)*** *Average $I_{Na\text{-}Peak}$ density in oHCM cardiomyocytes before and after exposure to different CT-G20 concentrations (0.4 µM, 1 µM, 4 µM, 10 µM). Means± S.E.M. (Standard Error of Mean) from 25 cardiomyocytes (12 patients).* ***D)*** *Average integrals of I_{NaL} calculated between 50 milliseconds from depolarization onset till the end of the depolarization step, while eliciting the current in oHCM cardiomyocytes, before and after exposure to different CT-G20 concentrations (0.4 µM, 1 µM, 4 µM, 10 µM). Means± S.E.M. (Standard Error of Mean) from 15 cardiomyocytes (8 patients). *= P<0.05 at paired t-test versus basal and 0.4 µM concentration; #= P<0.05 at paired t-test versus 1 µM concentration.*

Moreover, the calculated EC50 for late Na^+ was below 1 µM, instead the EC50 for peak current was approximately 3 µM, confirming the increased selectivity of CT-G20 for late over peak Na^+ current.

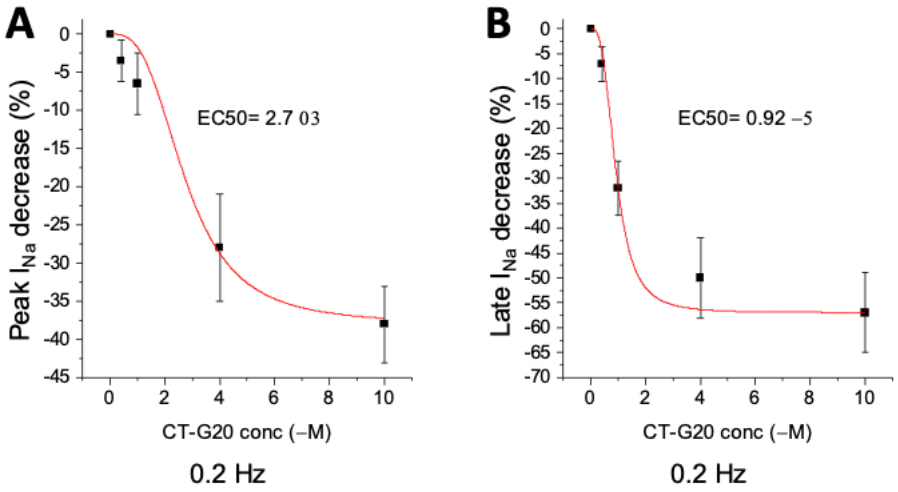

Figure 32: Evaluation of EC50. A) *Percentage variation of peak I_{Na} density from baseline at the different CT-G20 concentrations (0.4 µM, 1 µM, 4 µM, 10 µM), in oHCM myocytes where the current is elicited at 0.2 Hz. Curves fitted with logistic equations to calculate EC50.* ***B)*** *Percentage variation of late Na^+ current from baseline at the different CT-G20 concentrations (0.4 µM, 1 µM, 4 µM, 10 µM), in oHCM myocytes where the current is elicited at 0.2 Hz. Curves fitted with logistic equations to calculate EC50.*

Dose-dependent reduction of late and peak Na^+ currents exerted by CT-G11 in ventricular cardiomyocytes from oHCM patients

We performed patch-clamp experiment in cardiomyocytes isolated from surgical sample of oHCM patients. The effects of CT-G11 were dose-dependent reduction of late and peak Na^+ current. At variance with CT-G20, the action of CT-G11 for inhibition of late and peak Na^+ current is comparable. Both the late and peak Na^+ current was similarly reduced at a concentration of 1µM, while the drug showed comparable potency when the concentration was subsequently increased to 4 µM and 10 µM.

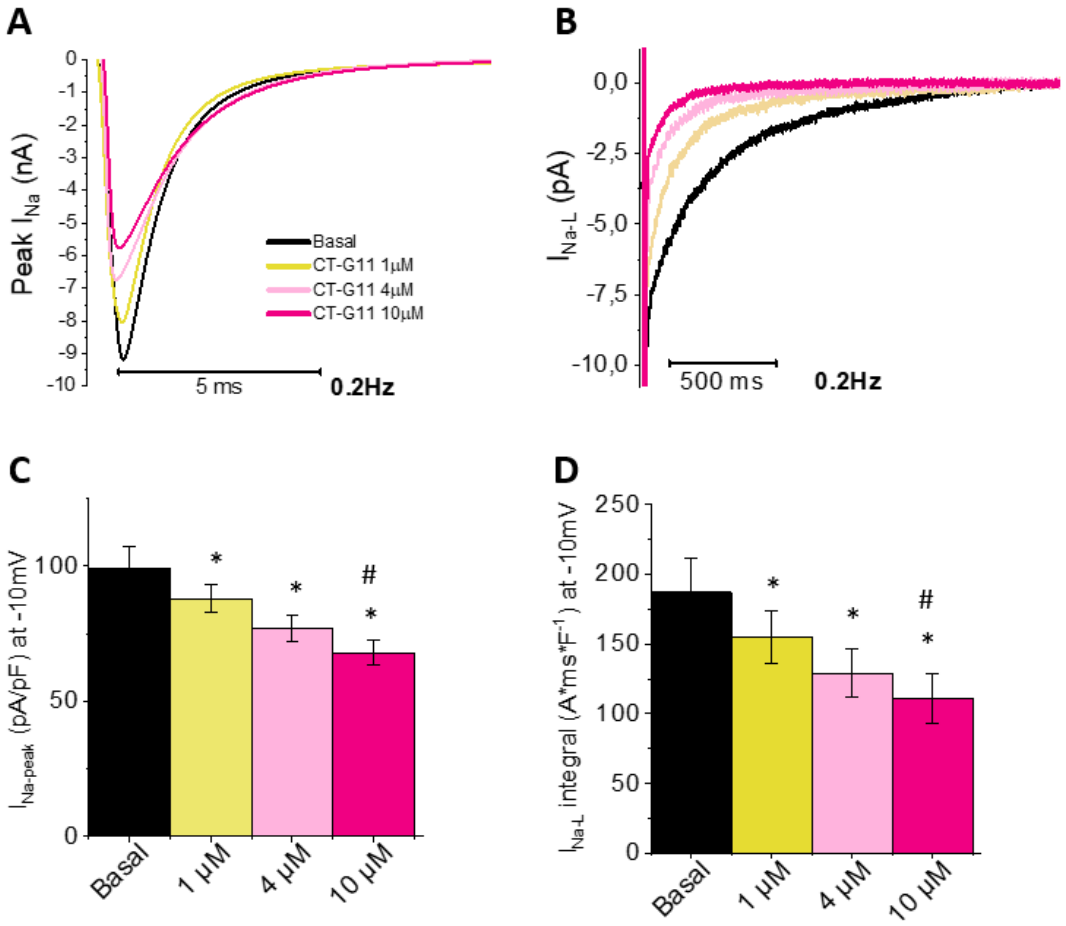

Figure 33: Evaluation of CT-G11 on Peak and Late Na^+ current A) *Representative I_{Na} traces focused on the peak and late current, recorded in oHCM cardiomyocytes, before and after exposure to different CT-G11 concentrations (1 µM,4 µM and 10 µM).* ***B)*** *Average $I_{Na-Peak}$ density and integrals of I_{NaL} in oHCM cardiomyocytes before and after exposure to different CT-G11 concentrations (1 µM, 4 µM, 10 µM). Means± S.E.M. (Standard Error of Mean) from 20 cardiomyocytes (10 patients) *= P<0.05 at paired t-test versus basal; #= P<0.05 at paired t-test versus 1 µM concentration.*

The calculated EC50 was slightly below 3 µM for both late and peak Na^+ current. We concluded that CT-G11 does not show any selectivity for late over peak Na^+ current.

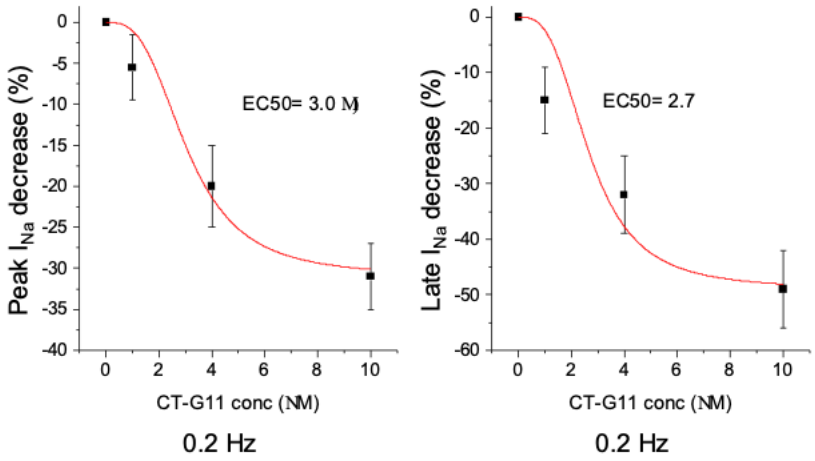

Figure 34: Evaluation of EC50 with CT-G11: *Percentage variation of peak I_{Na} density and I_{NaL} integrals from baseline at the different CT-G11 concentrations (1 µM, 4 µM, 10 µM), in oHCM myocytes where the current is elicited at 0.2 Hz. Curves fitted with logistic equations to calculate EC50.*

Evaluation the effects of CT-G20 on Ca^{2+} transient amplitude and kinetics in ventricular myocytes

Cardiomyocytes were loaded with Ca^{2+} sensitive fluorescent dye Cal520 as described in the materials and methods section, in order to investigate Ca^{2+} transient amplitude and diastolic Ca^{2+} during regular electrical pacing at different frequencies. Our data suggests that CT-G20 reduces Ca^{2+} transient amplitude at all frequencies (0.5 Hz and 1Hz), in line with the expected negative inotropic effect. We tested this effect while exposing cells to CT-G20 at 3 different concentrations (1 µM, 4 µM, 10 µM): we observed that the decrease of Ca^{2+} transient amplitude is dose-dependent. Then, we analysed the effects of the drug on diastolic Ca^{2+}, and found that the drug induces a significant reduction of diastolic [Ca^{2+}] at all frequencies (0.5 Hz and 1Hz). In *figure 35)*, we show that the lowest concentration (1 µM) exerted a small but significant reduction of diastolic [Ca^{2+}]. The effect was more pronounced at 4 µM and even more evident when10 µM CT-G20 was used.

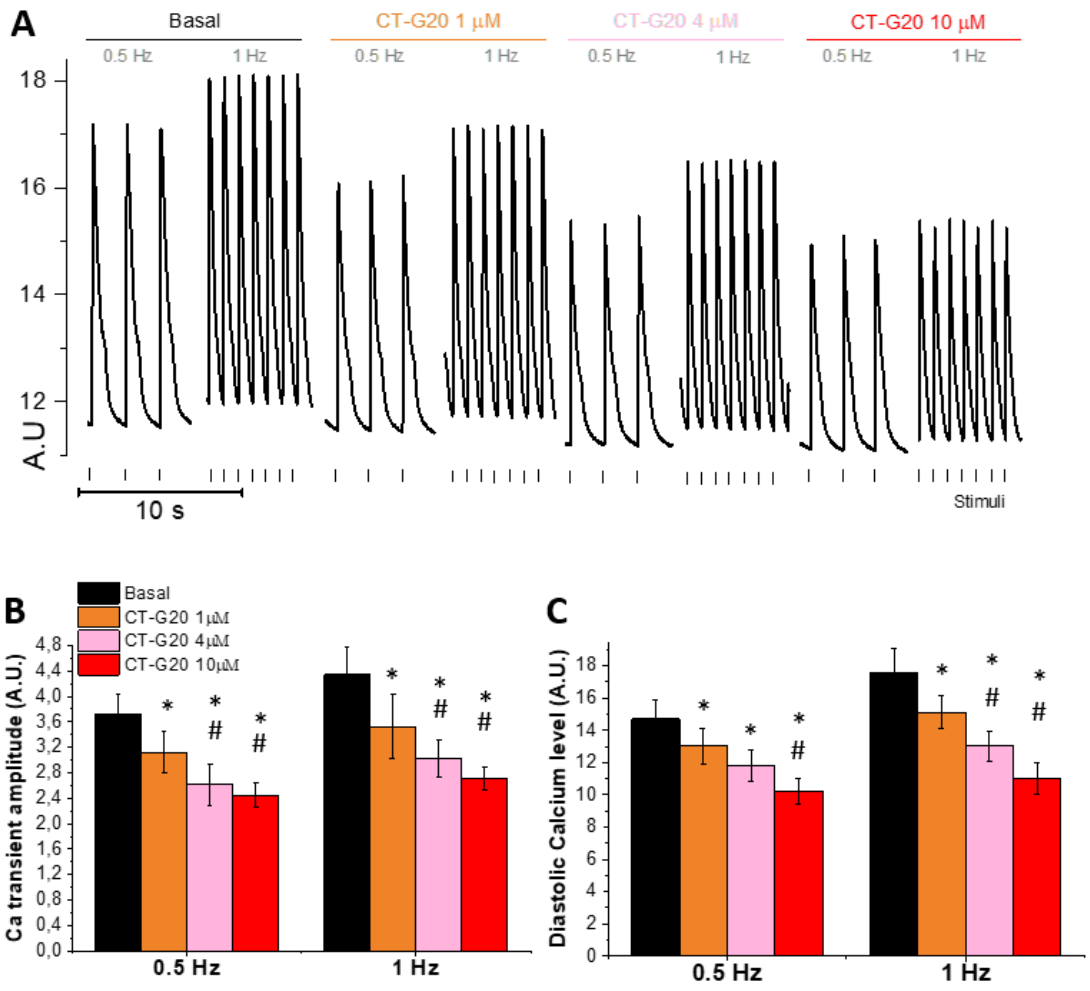

Figure 35: Effects of CT-G20 on Ca^{2+} transient amplitude and diastolic Ca^{2+} in oHCM cardiomyocytes. A) *Representative Ca^{2+} fluorescence traces obtained during field stimulation at 0.5 and 1Hz, before and after exposure to different CT-G20 concentrations (1µM,4µM and 10 µM).* ***B)*** *Average Ca^{2+} transient amplitude (elicited at 0.5 and 1Hz) before and after exposure to different CT-G20 concentrations (1 µM, 4 µM, 10 µM).* ***C)*** *Average diastolic Ca^{2+} level (during regular stimulation at 0.5 and 1Hz) before and after exposure to different CT-G20 concentrations (1 µM, 4 µM, 10 µM). Means± S.E.M. (Standard Error of Mean). *= P<0.05 at paired t-test versus basal; #= P<0.05 at paired t-test 1 µM concentration.*

In addition, we measured time from stimulus to peak (peak-time) and time from peak to 50% decay (50% decay). Our data showed that CT-G20 is able to significantly accelerate Ca^{2+} transient kinetics at both tested pacing frequencies (0.5 Hz and 1 Hz), but this effect was only observed at when the drug was employed at 4 µM or at 10 µM. On the other hand, the rising phase of Ca^{2+} transients is not significantly affected by the drug in any of the conditions we tested.

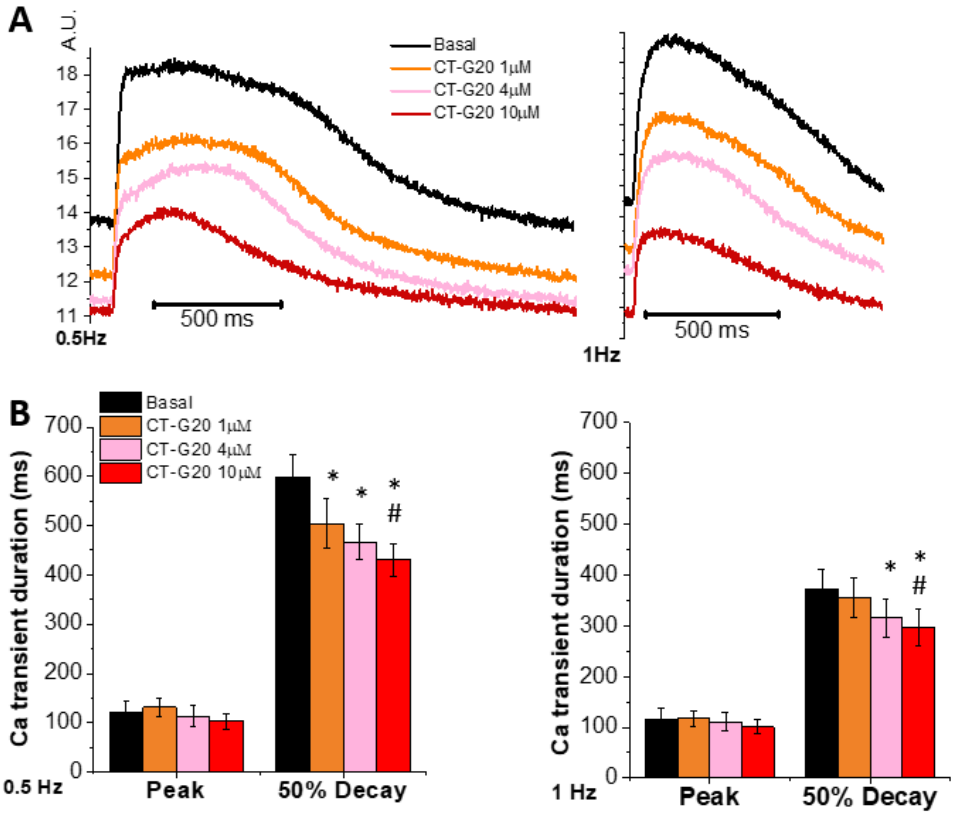

Figure 36: Effects of CT-G20 on Ca^{2+} transient kinetics in oHCM cardiomyocytes. A) *Representative magnified Ca^{2+} transients obtained during field stimulation at 0.5 and 1Hz, before and after exposure to different CT-G20 concentrations (1µM, 4µM and 10 µM).* ***B)*** *Average Ca^{2+} transient kinetics (time to peak and time from peak to 50% decay) and after exposure to different CT-G20 concentrations (1 µM, 4 µM, 10 µM), at 0.5Hz and 1Hz. Means± S.E.M. (Standard Error of Mean). *= P<0.05 at paired t-test versus basal; #= P<0.05 at paired t-test 1 µM concentration.*

Evaluation the effects of CT-G11 on Ca^{2+} transient amplitude and kinetics in ventricular myocytes

Cardiomyocytes were loaded with the Ca^{2+} sensitive fluorescent dye (Cal520). After the exposure to CT-G11, we observed a reduction of Ca^{2+} transient amplitude, in line with that observed with CT-G20. Moreover, the decrease in diastolic Ca^{2+} exerted by CT-G11 was similar to that observed with CT-G20.

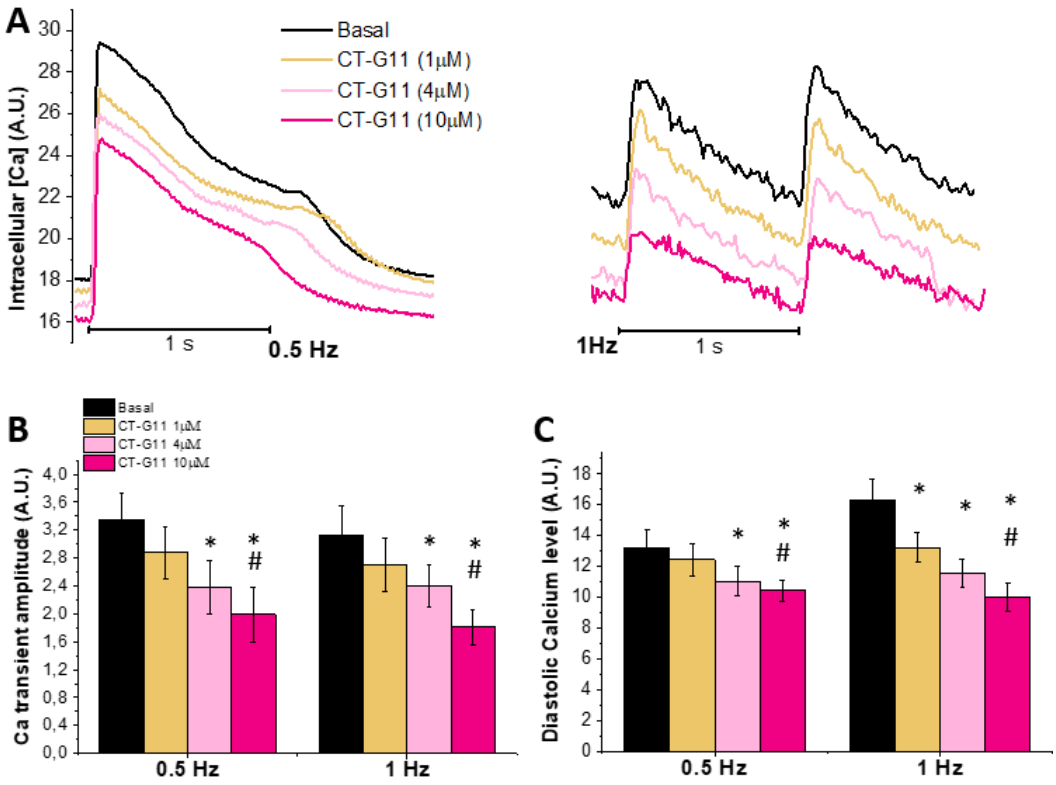

Figure 37: Effects of CT-G11 on Ca^{2+} transients in oHCM cardiomyocytes. A) *Representative magnified Ca^{2+} transients obtained during field stimulation at 0.5Hz and 1Hz, before and after exposure to different CT-G11 concentrations (1µM,4µM and 10 µM).* ***B)*** *Average Ca^{2+} transient amplitude (elicited at 0.5 and 1Hz) before and after exposure to different CT-G11 concentrations (1 µM, 4 µM, 10 µM).* ***C)*** *Average diastolic Ca^{2+} level (elicited at 0.5 and 1Hz) before and after exposure to different CT-G11 concentrations (1 µM, 4 µM, 10 µM). Means± S.E.M. (Standard Error of Mean). *= P<0.05 at paired t-test versus basal; #= P<0.05 at paired t-test versus 1 µM concentration.*

However, peak time and 50% decay of Ca^{2+}-transients were minimally modified by CT-G11. Our data suggests that CT-G11 decreases Ca^{2+}-transient amplitude but has minimal impact on Ca^{2+} transient kinetics, at variance with CT-G20.

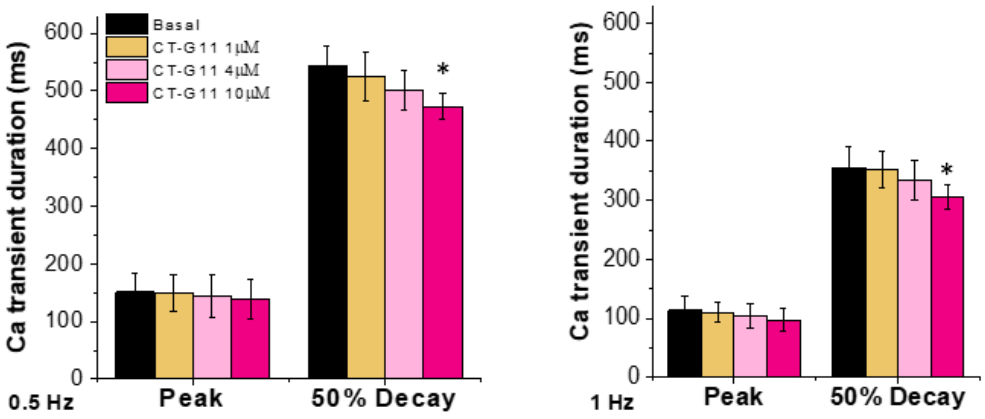

Figure 38: Effects of CT-G11 on Ca^{2+} transients in oHCM cardiomyocytes. *Average Ca^{2+} transient kinetics (time to peak and time from peak to 50% decay) in oHCM cardiomyocytes before and after exposure to different CT-G11 concentrations (1 µM, 4 µM, 10 µM), at 0.5Hz and 1Hz. Means± S.E.M. (Standard Error of Mean). *= P<0.05 at paired t-test versus basal; #= P<0.05 at paired t-test versus 1 µM concentration.*

In conclusion, CT-G20 is a potent blocker of both late and peak Na^+ currents, showing greater selectivity for late Na^+ current inhibition. Additionally, it is more effective at shortening action potential duration in oHCM cardiomyocytes compared to CT-G11. The latter exhibits lower inhibitory potency on both peak and late Na^+ currents, with no clear selectivity. In addition, the reduction of Ca^{2+} transients' kinetics is more pronounced with CT-20 than with CT-G11 at the same concentrations. This profile positions CT-G20 as a more effective therapeutic agent in modulating electrophysiological dysfunctions and contractile abnormalities associated with hypertrophic cardiomyopathy.

4.3 Evaluation of Dapagliflozin in patients with HCM and AoS

The main cause of death and hospitalization is cardiovascular diseases, despite the recent advancements in their diagnosis and therapy. Evaluation and testing of novel therapies is essential to improve patient management, ultimately preventing the life-threatening complications of these diseases.

Studies suggests that sodium-glucose cotransporter-2 inhibitors (SGLT2-i) provide marked benefits in patients with heart failure, in terms of reduction of morbidity and mortality. The molecular and cellular mechanisms underlying the cardioprotective effects of gliflozins are still under investigation, but a role of the activation of anti-inflammatory and anti-oxidative pathways has been proposed, in addition to the elimination of excess blood glucose through urine and to the improvement of the endothelial function (Tomasoni D. et al., 2019).

In particular, recent clinical trial highlighted that Dapagliflozin significantly reduced the risk of atrial fibrillation, while also reducing heart failure related mortality (HF) and the rate of hospitalizations, even in non-diabetic patients with HF (EMPEROR-Reduced trial).

Based on this evidence, we here studied the effects of Dapagliflozin in ventricular cardiomyocytes derived from patients undergoing myectomies with primary hypertrophy (HCM) and patients with secondary hypertrophy (aortic stenosis -AoS-LVH). The evaluation of the electrophysiological effects of Dapagliflozin in cardiomyocytes, obtained as previously described (Coppini et al, Circulation 2013), was performed by patch-clamp measurements. Cells from the two experimental groups were perfused with a physiological Tyrode solution at 37°C.The experiments were carried out in the presence and absence of Dapagliflozin at two different concentrations: 1 μM, which is close to the plasma levels derived from patients during clinical treatment, and 10μM, a very high concentration used here to assess the potential cardiotoxicity of this drug.

Evaluation of action potentials in HCM ventricular cardiomyocytes

Our result show that treatment with Dapagliflozin leads to modification in action potential kinetics, which is markedly prolonged in HCM cardiomyocytes.

In particular, 1 μM Dapagliflozin produces a significant reduction of action potential duration at 90%, compared to basal, at all stimulation frequencies tested (0.2-0.5-1 Hz). Moreover, at 10 μM, the AP shortening we observed was more pronounced, as compared with 1 μM, confirming the presence of a dose-dependent effect of the drug.

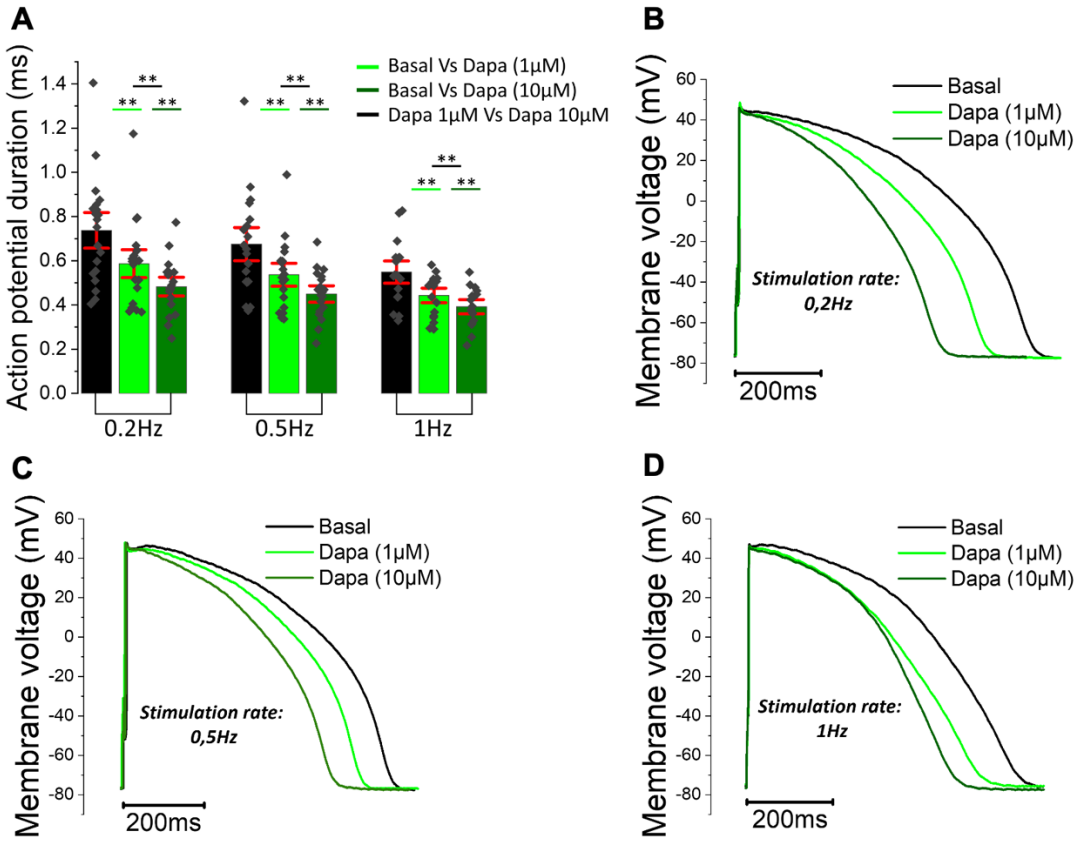

Figure 39: Effect of Dapagliflozin on action potential kinetics of ventricular cardiomyocyte derived from HCM surgical samples: current clamp configuration. A) *Action potential duration at 90% repolarization (APD90%) recorded during stimulation at 0.2Hz, 0.5Hz and 1Hz in human ventricular cardiomyocytes isolated from HCM patients.* ***B)*** *Representative action potential traces recorded at 0.2Hz in HCM cardiomyocytes, in basal condition (black traces) and during exposure to Dapagliflozin at the concentration of 1 µM (light green traces) and 10 µM (dark green traces).* ***C)*** *Representative action potential traces recorded at 0.5Hz in HCM cardiomyocytes, in basal condition (black traces) and during exposure to different Dapagliflozin at the concentration of 1 µM (light green traces) and 10 µM (dark green traces).* ***D)*** *Representative action potential traces recorded at 1Hz in HCM cardiomyocytes, in basal condition (black traces) and during exposure to Dapagliflozin at the concentration of 1 µM (light green traces) and 10 µM (dark green traces). Data from 20 cardiomyocytes obtained from 13 HCM patients.* ***** **= $p<0.01$*

Evaluation of Dapagliflozin effects on action potentials in AoS ventricular cardiomyocytes

The same experiment was performed in cardiomyocytes from patients with secondary hypertrophy due to AoS. In line with the effects observed in HCM, Dapagliflozin was able to reduce the action potential duration in ventricular cardiomyocyte from AoS patients. Patch clamp evaluation at concentration AoS cells showed a significant reduction of action potential duration at 90% when Dapagliflozin was added to the perfusion solution at 1 μM and 10 μM, at all stimulation frequencies tested (0.2-0.5-1 Hz). Again, we here observed a concentration-dependency of the AP shortening effect on Dapagliflozin.

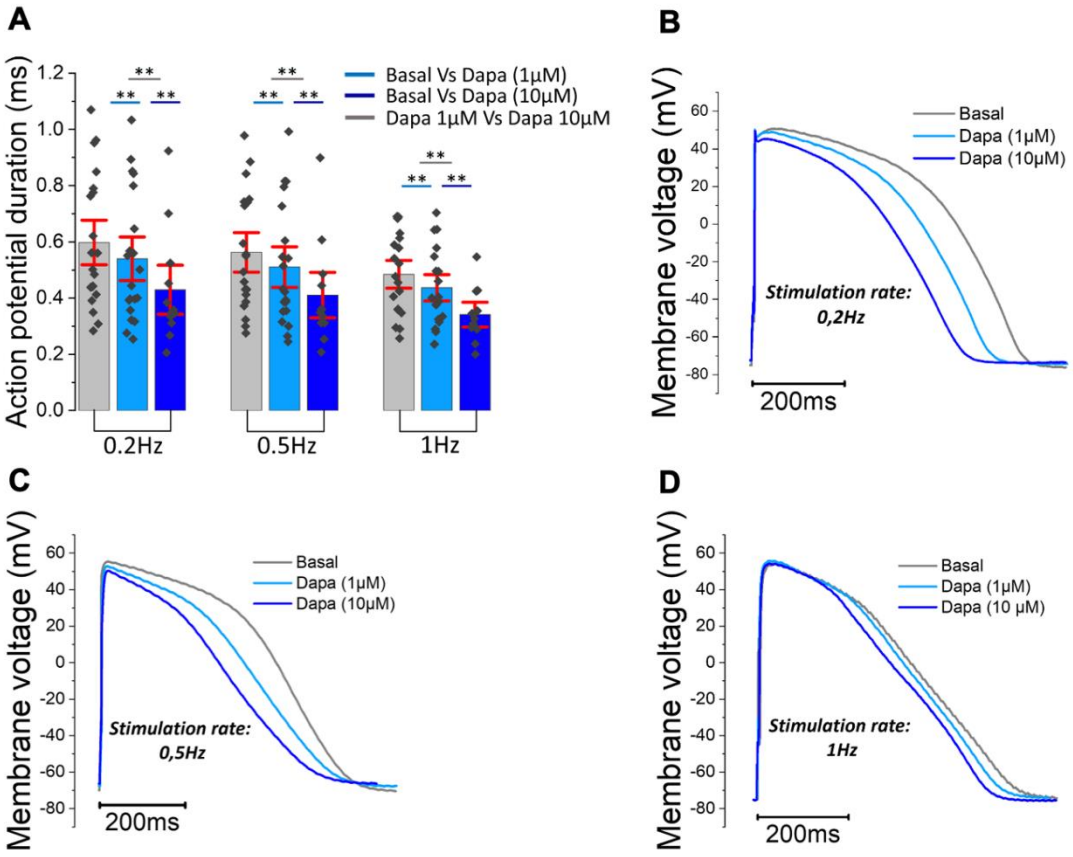

Figure 40: Effect of Dapagliflozin on action potential kinetics of ventricular cardiomyocyte derived from AoS surgical samples: current clamp configuration. A) *Action potential duration at 90% repolarization (APD90%) recorded during stimulation at 0.2Hz, 0.5Hz and 1Hz in human ventricular cardiomyocytes isolated from AoS patients.* ***B)*** *Representative action potential traces recorder at 0.2Hz in AoS cardiomyocytes, in basal condition (grey traces) and during exposure to different Dapagliflozin at the concentration of 1 μM (light blue traces) and 10 μM (dark blue traces).* ***C)*** *Representative action potential traces recorder at 0.5Hz in AoS cardiomyocytes, in basal condition (grey traces) and during exposure to different Dapagliflozin at the concentration of 1 μM*

(light blue traces) and 10 µM (dark blue traces). ***D)*** *Representative action potential traces recorder at 1Hz in AoS cardiomyocytes, in basal condition (grey traces) and during exposure to different Dapagliflozin at the concentration of 1 µM (light blue traces) and 10 µM (dark blue traces). Data from 19 cardiomyocytes from 9 different AoS patients.* ***** *= p<0.01*

Furthermore, treatment with Dapagliflozin did not show any significant effects on the maximum rise slope of action potential in both HCM and AoS cardiomyocytes in figure *41*.

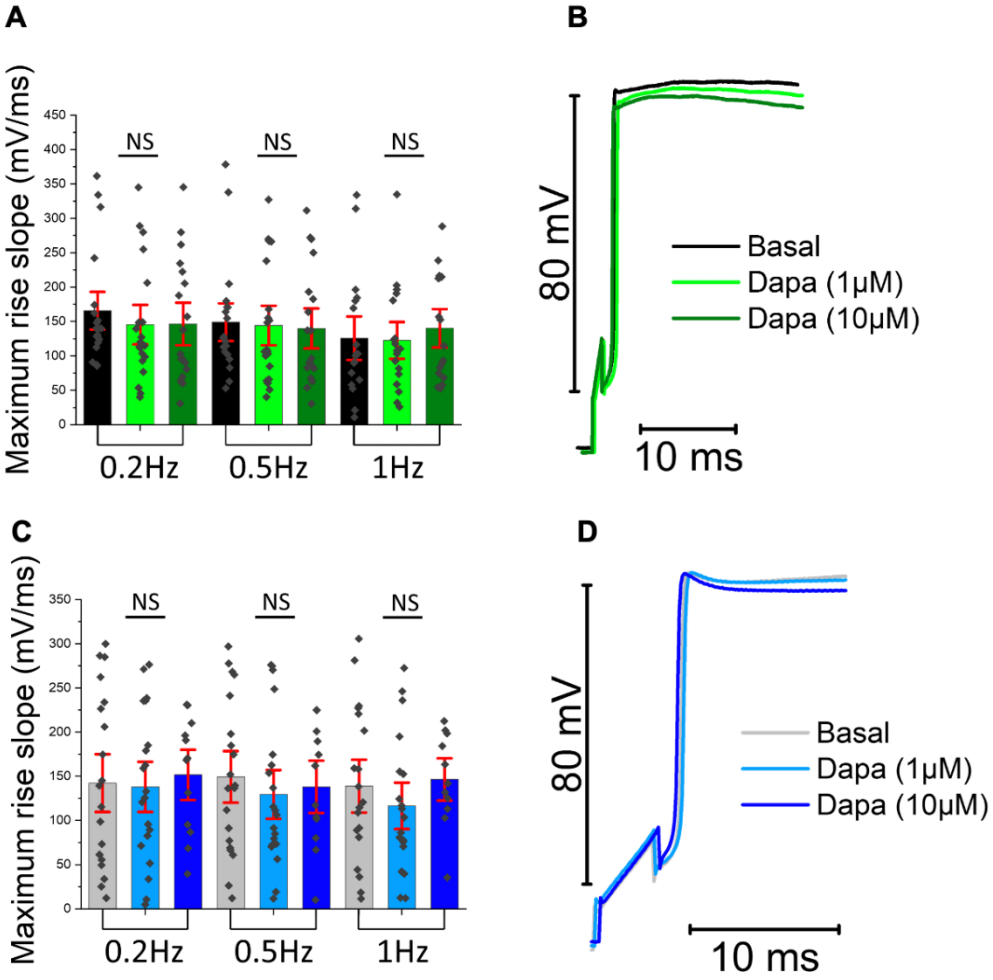

Figure 41: Effect of Dapagliflozin on maximum up stroke speed of action potential A) *Maximum upstroke speed of action potential recorded in ventricular cardiomyocytes from HCM patients at 0.2Hz, 0.5 and 1Hz, before and after exposure to different Dapagliflozin concentrations (1 µM and 10 µM). Mean ± SEM from 13 patients (20 cardiomyocytes). NS= Not Significant.* ***B)*** *Representative traces of maximum upstroke speed (mV/ms) of action potential recorded in ventricular cardiomyocytes from HCM patients at 0.2Hz, 0.5 and 1Hz, before and after exposure to different Dapagliflozin concentrations (1 µM and 10 µM).* ***C)*** *Maximum upstroke speed of action potential recorded in ventricular cardiomyocytes from AoS patients at 0.2Hz, 0.5 and 1Hz, before and after*

exposure to different Dapagliflozin concentrations (1µM and 10 µM). Mean ± SEM from 9 patients (19 cardiomyocytes). NS= Not Significant. ***D)*** *Representative traces of maximum upstroke speed (mV/ms) of action potential recorded in ventricular cardiomyocytes from AoS patients at 0.2Hz, 0.5 and 1Hz, before and after exposure to different Dapagliflozin concentrations (1 µM and 10 µM).*

Evaluation of the effects of Dapagliflozin on Na^+ current in HCM ventricular cardiomyocytes

In order to assess the molecular mechanisms behind the effects of Dapagliflozin on AP kinetics, we investigated the acute effects of the drug on Na^+ current. As shown above, late Na^+ current is markedly increased in HCM cardiomyocytes as compared to controls.

Our data show that Dapagliflozin is able to significantly reduce the late Na^+ current recorded at -20mV from a resting membrane potential of -120mV by patch- clamp measurements. The effect is dose-dependent, in that the observed reduction is larger when the drug is used at the concentration 10 µM with respect to 1 µM in *figure 42 A-B*. Instead, we observed no significant effects of the drug on peak Na^+ current in *figure 42 C-D.*

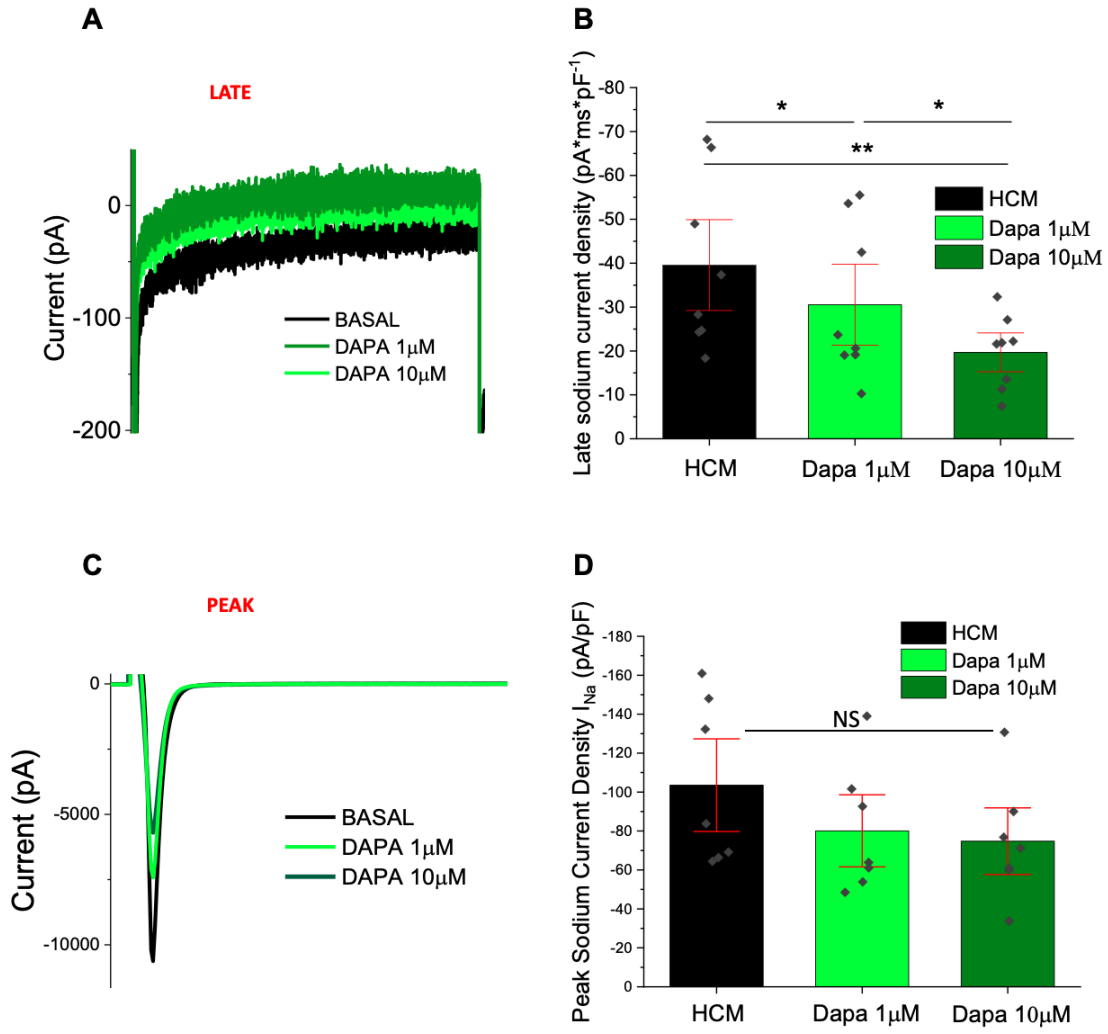

Figure 42: Effect of Dapagliflozin on late and peak Na^+ current density of ventricular cardiomyocytes isolated from HCM samples A) *Representative traces of late Na^+ current (I_{NaL}) recorded 50ms after the onset of the clamp pulse. Traces are elicited at -20mV from a resting potential of -120mV in basal condition (black), after the acute exposure to Dapagliflozin 1μM (light green) and to Dapagliflozin 10 μM (dark green).* ***B)*** *Average integral of the area of the current between 50 and 750 ms after onset of the −20 mV clamp pulse, normalized by cell capacitance, calculated in basal condition (black) and in the presence of Dapagliflozin (1μM in light green and 10μM in dark green). Mean ± SEM from 13 patients and 8 cells.* ***NS****= Not Significant.*

Evaluation of the effects of Dapagliflozin on sodium current in AoS ventricular cardiomyocytes

We performed the same voltage clamp experiment in aortic stenosis patients: our data show that Dapagliflozin, is able to significantly reduce the late Na^+ current in a dose-dependent manner, while peak Na^+ current is not affected. This is in line with the results observed in HCM cells.

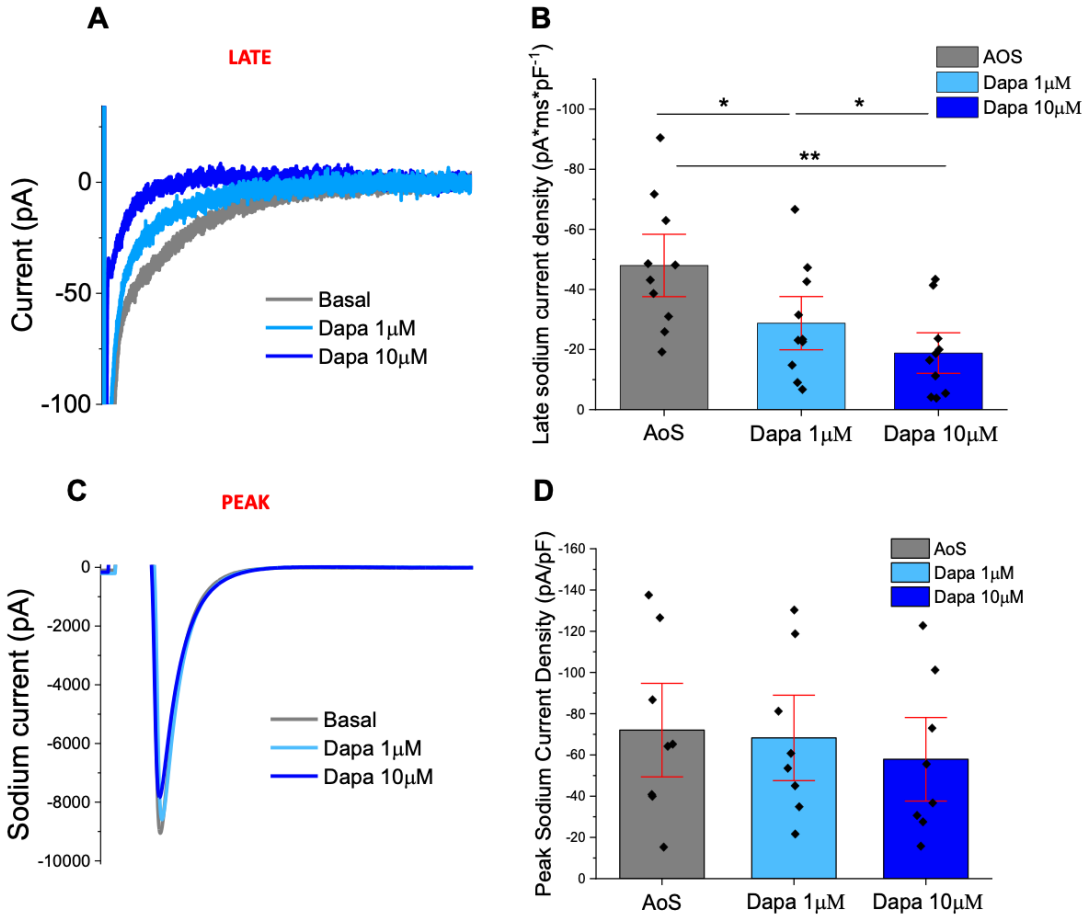

Figure 43: Effect of Dapagliflozin on late and peak Na^+ current density of ventricular cardiomyocytes isolated from AoS samples A) *Representative traces of late Na^+ current (I_{NaL}) recorded 50ms after the onset of the clamp pulse. Traces are elicited at -20mV from a resting potential of -120mV in basal condition (Grey), after the acute exposure to Dapagliflozin 1μM (light blue) and to Dapagliflozin 10 μM (blue)* ***B)*** *Average integral of the area of the current between 50 and 750 ms after onset of the −20 mV clamp pulse, normalized by cell capacitance, calculated in basal condition (Grey) and in the presence of Dapagliflozin (1μM in light blue and 10μM in blue). Single points represent single cell records. Mean ± SEM from 9 patients (10 cardiomyocytes).* ***C)*** *Representative peak Na^+ current ($I_{Na\text{-}peak}$) traces recorded at-20mV from a resting membrane potential of -120mV**;** in grey basal record, in light blue after the exposure to 1μM Dapagliflozin and in blue after 10μM Dapagliflozin.* ***D)*** *Average Peak Na^+ current recorded at -20mV from a resting*

potential of -120mV, normalized for cell capacitance at a stimulation rate of 1Hz in human ventricle cardiomyocytes isolated from AOS cardiac samples. In grey is the basal condition, in light blue after the exposure to 1 µM Dapagliflozin and in blue after 10 µM Dapagliflozin. Mean ± SEM from 9 patients (10 cardiomyocytes).

Considering the results obtained, we compared the percentage variation of action potential duration between HCM and AoS patients. Our results displayed in *figure 44)*, show that Dapagliflozin induces a significant reduction on action potential duration, in a dose-dependent manner in HCM compared to AoS patients, highlighting the major alterations in the primary hypertrophy.

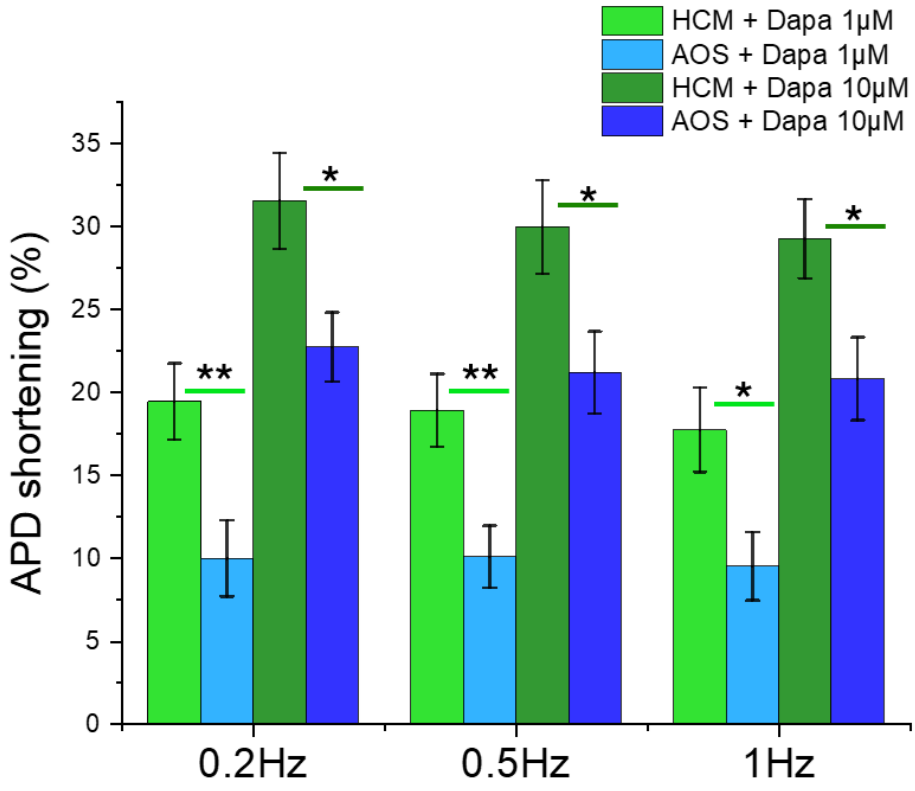

Figure 44: Comparison of the effect exerted by Dapagliflozin on action potential duration in ventricular cardiomyocytes isolated from HCM and AoS samples. *The figure shows the APD90 shortening (%) after the treatment whit Dapagliflozin (1µM and 10µM) recorded during stimulation at 0.2Hz, 0.5Hz and 1Hz in ventricular cardiomyocytes isolated from HCM and AoS samples. ** = p < 0.01. Mean ± SE*

In conclusion, our results show that Dapagliflozin is a promising drug for the treatment of HCM and AoS patients. In particular, is able to be reduced action potential duration, this is

evident on the light of the effect on the late Na^+ current in both groups, with a greater effect in primary hypertrophy.

4.4 Studies on human cardiac fibroblasts from hypertrophic myocardial samples

In the context of hypertrophy, fibroblasts are responsible for the generation of myocardial fibrosis; the abnormal, persistent activation of myofibroblasts is associated with the global pathological process that leads to cardiac remodelling. The appearance of fibrosis is a significant risk factor for the development of arrhythmias and heart failure. Fibrosis alters the architecture of cardiac tissue and impairs cardiac function, increasing susceptibility to severe cardiovascular complications and contributing to disease progression. To promote the proliferation and activation of fibroblast to myofibroblast, Ca^{2+} influx plays a crucial role. In this work, we tried to identify which channels are responsible for the activating Ca-influx influx and how their expression changes in the presence of HCM.

In particular, we focused on the contribution of L-type Ca^{2+} channel and TRP channels to the intracellular Ca^{2+} concentration in fibroblasts. TRP channels are mediators of myofibroblast differentiation: they form heterotrimeric channels and control Ca^{2+} influx levels in response to various stimuli including mechanical signals and oxidative stress (Lighthouse JK, 2016). Fibroblasts isolated from human cardiac HCM tissue samples and from a commercial control line, have been cultivated for at least a week and then labelled with Ca^{2+} sensitive fluorescent dyes. Subsequently, we analysed intracellular Ca^{2+} influx using a fluorescent microscope, as detailed in the materials and methods section.

Calcium fluxes analysis

We developed a protocol to analyse the Ca^{2+} fluxes in the fibroblasts. To characterize which channels are responsible for Ca^{2+} influx we used different blockers: Lacidipine (LACI) to block L-type channels and SKF to block TRP channels. To normalize the results obtained, we used ionomycin that induced the release of all the Ca^{2+} stores and normalized all fluorescent values using the maximal value obtained during perfusion with ionomycin. During all the experiments, cells were exposed to 1µM thapsigargin, to avoid the refill of SR and thus to isolate only the inward flux of Ca^{2+}ions from the plasmalemma. To evoke Ca^{2+} influx into fibroblasts, we increased the extracellular Ca^{2+} concentration (from 0 to 1.8 mM) in the presence or absence of drugs.

The protocol we designed is made of steps where we change the extracellular solution to induce different stimuli. Fibroblasts are previously loaded with Cal 520 for half an hour and then are suspended in Tyrode solution with thapsigargin (TYR). Cells are then placed in the microscope chamber where they are perfused with different solutions and stimuli. We then record the emitted fluorescent signals from Ca^{2+} ions in the fibroblasts cytosol, in response to the increase of extracellular Ca^{2+} concentration. The four steps we performed on each batch of cells are: (1) we first perform a baseline perfusion with Tyrode solution with [Ca^{2+}] 0, then we switch to (2) Tyrode solution with [Ca^{2+}]1.8mM (in order to get the basal inward Ca^{2+} flux peak in the absence of drugs), than we move back to (2.1)Tyrode solution without Ca^{2+}, when the signal goes back to the basal level, we move to (2.2) Tyrode with [Ca^{2+}] 0 containing the drug of interest (LACI or SKF), then we switch to (3) Tyrode with [Ca^{2+}]1.8mM containing the drug (where we observe the decreased inward flow due to the blocking effect of the drug), and finally we switch to (4) Tyrode with [Ca^{2+}]1.8mM and ionomycin to observe the maximal fluorescence and normalized all the previously measured values.

We first studied the effects of LACI and SKF in HCM vs. control fibroblasts. *Figure 45),* shows data collected from HCM fibroblasts. Representative traces in panel *45 A)* highlight the subsequent steps of our protocol. The first peak is induced by the extracellular Ca^{2+} concentration increment (from 0 to 1.8 mM) in the absence of the drug, the second peak is obtained by re-exposing the cells to [Ca^{2+}]1.8 mM in the presence of the drug; the last and largest peak observed is evoked by ionomycin; panel *B)* shows the percentage variation of Ca^{2+} transient amplitude after acute exposure to Lacidipine [10µM] or SKF [5µM], with respect to the first (baseline) peak. Lacidipine exposure reduces the basal Ca^{2+} peak by 34.8%, while SKF reduces Ca^{2+}-entry by 33.43%. The amount of reduction induced by the two drugs is comparable.

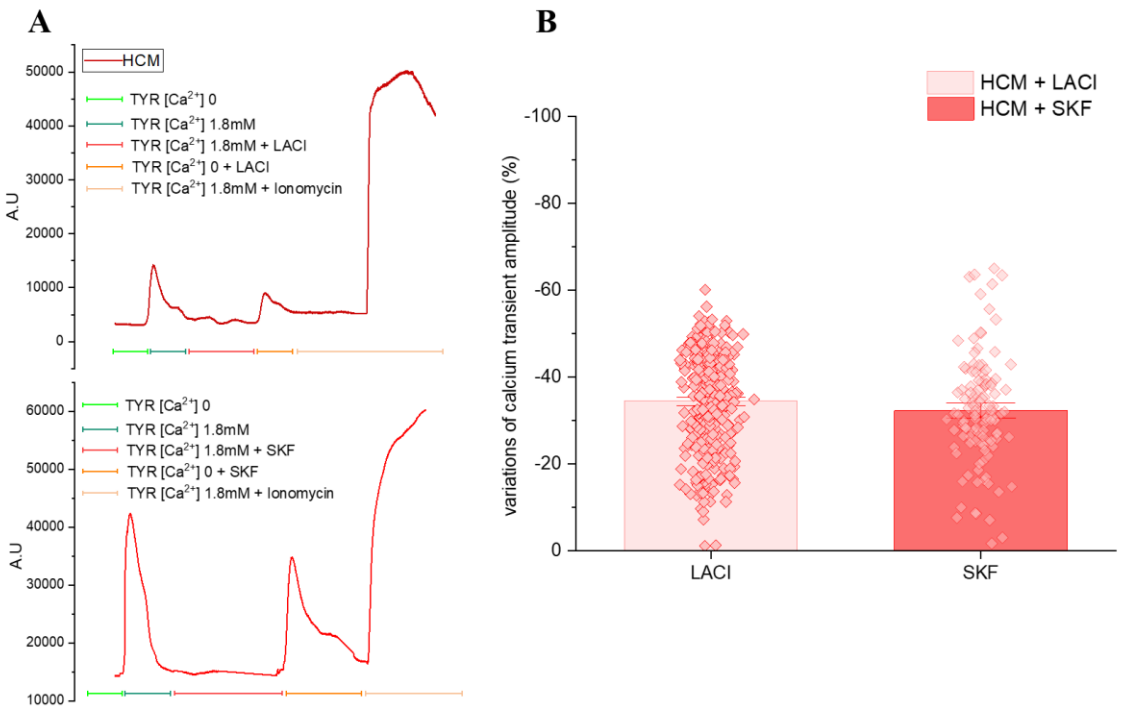

Figure 45: Evaluation of Ca^{2+} transient amplitude in HCM fibroblasts. A) *Representative traces of the protocol to measure Ca^{2+} entry in isolated cardiac fibroblasts; the line under the representative trace highlights the solution changes. Thapsigargin is used at 1µM, LCI at 10µM and SKF at 5µM.* ***B)*** *Variation of Ca^{2+} transient amplitude after exposure to LACI or SKF as percentage of the basal peak. Data from 123 HCM fibroblasts treated with SKF and 326 HCM fibroblasts treated with LACI. I (Bars are Means± S.E.M).*

As mentioned earlier, we performed the same experiment in control cardiac fibroblasts, in *figure 46*. Panel *B)* shows the percentage reduction of the basal Ca^{2+}-peak induced by exposure to LACI [10µM] or SKF [5µM]. LACI reduces the basal Ca^{2+} peak by 55.37%, while SKF reduces it by 52.53%. The reduction induced by the two drugs is comparable.

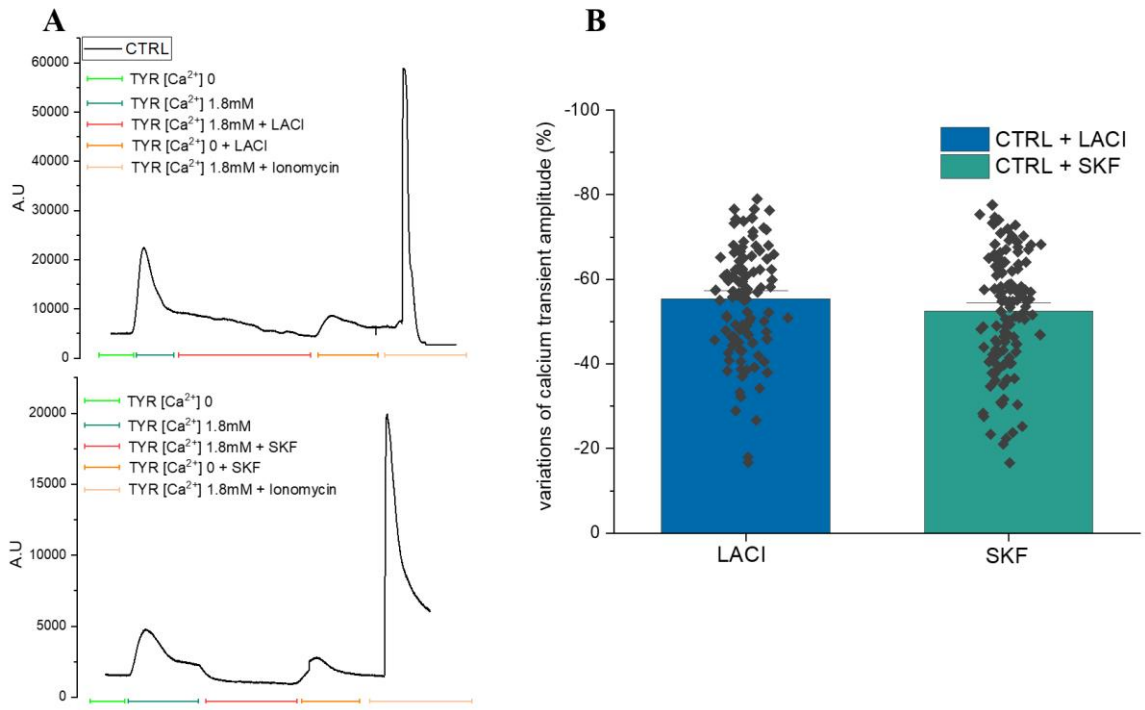

Figure 46: Evaluation of Ca^{2+} transient amplitude CTRL fibroblasts. A) *Representative traces.* ***B)*** *Variation of Ca^{2+} transient amplitude after exposure to LACI or SKF as a percentage of the basal peak, non-expose to drugs. Single points represent the single events, bars represent the mean. (Bars are Means± S.E.M).*

In *figure 47)* we compared the amplitude of the basal Ca^{2+}-entry peaks in CTRL vs HCM fibroblasts (after normalising based on the individual maximal values obtained with ionomycin). Notably, we observed that plasmalemmal Ca^{2+}entry was greater in fibroblasts derived from HCM patients compared to the controls; indeed, the mean amplitude is 31.35% of the ionomycin peak in HCM fibroblasts while it is only 17.53% in controls.

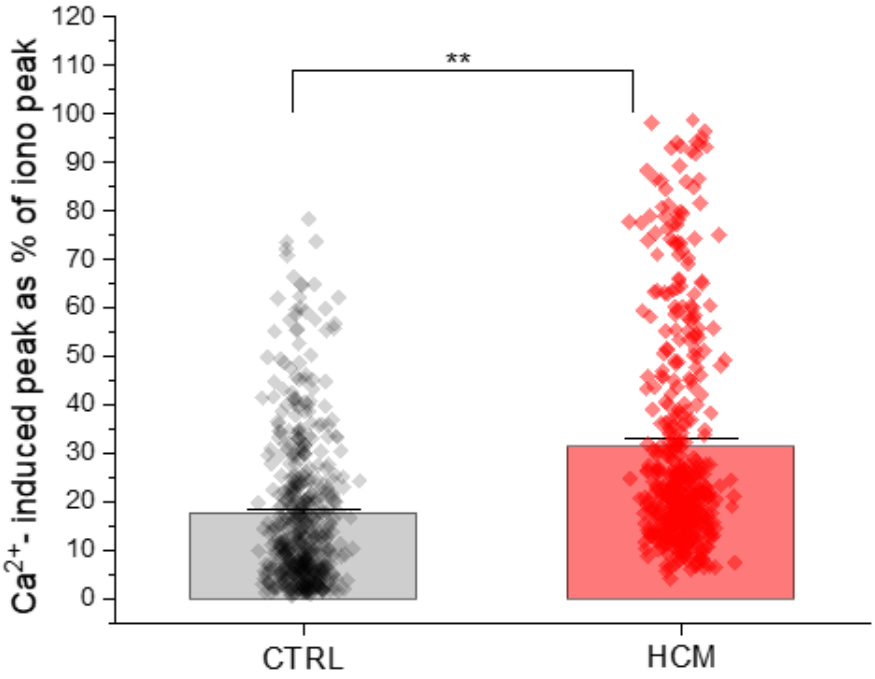

Figure 47: Comparison between Ca^{2+} transient amplitude in CTRL and HCM fibroblasts. *Evaluation of Ca^{2+}entry peaks induced by the increment of extracellular Ca^{2+} concentration, normalized by the amplitude of the transient evoked by ionomycin at the end of the experiment, in control and HCM fibroblast, without exposure to drugs. (Bars are Means± S.E.M,* ***** *= $p<0.01$).*

In *figure 48)* we compared the differences in the variation of Ca^{2+} entry peak amplitude after LACI or SKF exposure in control and HCM fibroblasts. We observed that in HCM fibroblasts the reduction of peak amplitude by the two drugs is significantly lower than that observed in control fibroblasts. Indeed, HCM fibroblasts treated with LACI shows a 34.80% reduction of peak amplitude, while the decrease of Ca-entry is 55.37% in control fibroblasts. Similarly, Ca^{2+} -peak reduction by SKF is 33.43% in HCM fibroblasts and 52.53% in control fibroblasts. This data highlight that the reduction induced by the two drugs is larger in control fibroblasts, despite the global Ca^{2+} influx is larger in HCM cells. This suggests that the increased Ca^{2+} entry in HCM fibroblasts is not caused by changes in the L-type Ca^{2+} current or in the expression of TRP channels.

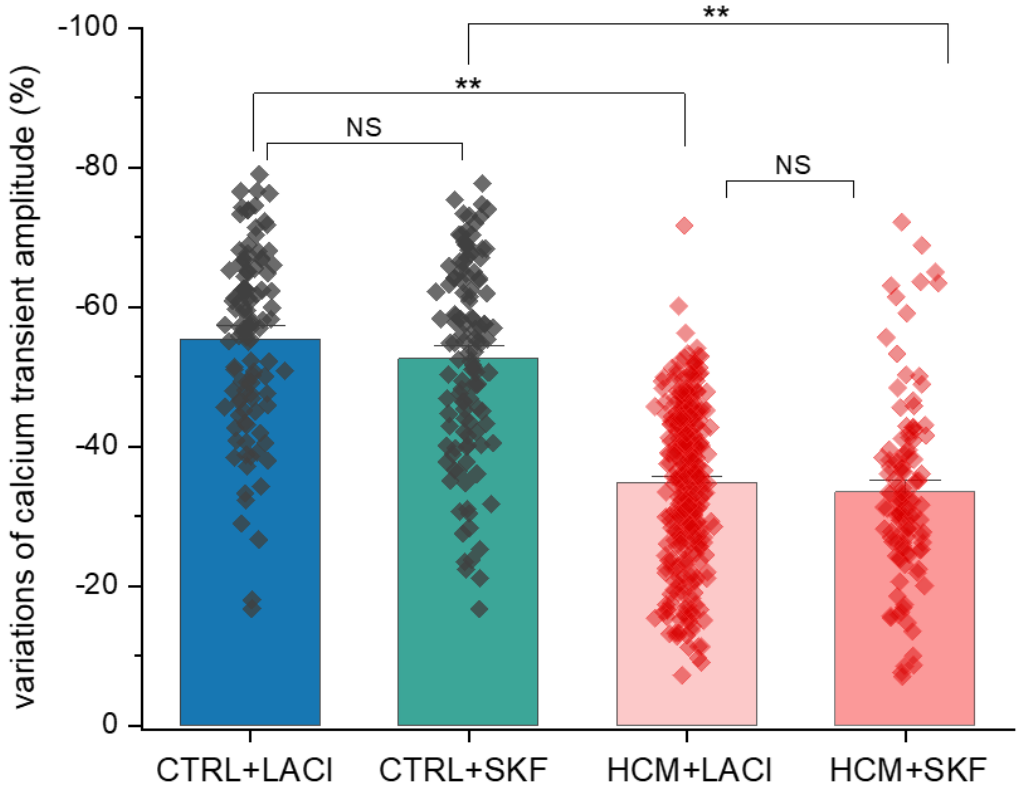

Figure 48: Comparison between Ca^{2+}transient amplitude in CTRL line and HCM fibroblasts in presences of the drugs. *Variation of Ca^{2+} transient amplitude after exposure to LACI or SKF as a percentage of the basal peak. (Bars are Means± S.E.M.* **** *=*** *$p<0.01$, NS: not significant).*

Finally, HCM fibroblasts were treated for 24 hours with TGF-β [10ng], a factor that stimulates cell growth and differentiation, promoting the production of ECM components. After 24h of pre-treatment with TGF-β, we performed the same protocol in the absence or presence of SKF. In panel *49 A)*, we report the amplitude of basal Ca^{2+} peaks normalized by ionomycin after incubation with TGF- β or with vehicle. The fibroblasts treated with TGF-β have a significant increment of Ca^{2+} entry with respect to the vehicle-treated HCM cells. In panel *B)* we reported data about the effects of SKF in vehicle-treated or in TGF-β-treated HCM fibroblasts. SKF reduces Ca^{2+}-peaks by 32.89% in vehicle-treated cells, while such reduction goes down to 28% in TGF- β-treated fibroblasts. Our results suggest that TGF- β does not increase global Ca^{2+}-entry in fibroblasts by increasing the expression of TRP channels.

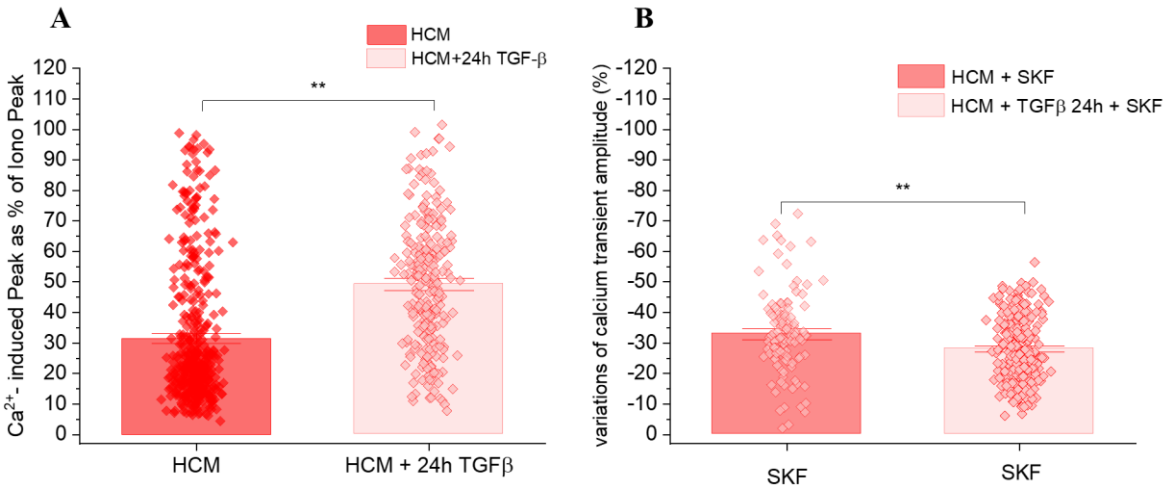

Figure 49: Effects of TGF-β 24h treatment on Ca^{2+} transient amplitude in HCM fibroblasts. A) *Evaluation of basal Ca^{2+} intracellular transient normalize on the amplitude of the transient evoked by ionomycin in HCM fibroblasts in absence (in red) and presence (light red) of the treatment with TGF-β.* ***B)*** *Evaluation of SKF effects on the Ca^{2+} transient variation, in HCM fibroblasts in absence (in red) and presence (light red) of pre-treatment with TGF-β. (Bars are Means± S.E.M.,* **** *= p<0.01).***

In conclusion, our results suggest that HCM fibroblasts show an increased Ca^{2+}-entry compared to the control fibroblasts in response to increased extracellular [Ca^{2+}]. Moreover, the drugs under investigation (LACI and SKF) on HCM and control fibroblasts, does not exert a larger reduction in HCM fibroblasts; suggesting that the increased Ca^{2+} influx is not promoted by L-type Ca^{2+} or TRP channels.

5.DISCUSSION

5.1 Electrophysiological evaluation of human ventricular cardiomyocytes from patient whit primary and secondary hypertrophy

We studied the pathological remodelling of cardiac tissue in patients with primary hypertrophy (HCM) and secondary hypertrophy due to AoS. Both conditions are characterized by distinct yet interrelated changes in the function and structure of left ventricle.

HCM is defined by an abnormal thickening of the left ventricular walls (maximal thickness > 15mm) in the absence of any hemodynamic abnormalities that may cause cardiac hypertrophy, often with asymmetric distribution across the different regions of the left ventricle (Nistri S. et al., 2006; Iacopo Olivotto et al., 2003).

AoS (Aortic Stenosis) is a valvular heart disease commonly caused by the calcification of a congenitally bicuspid or normal aortic valve. This calcification results in a progressive narrowing of the aortic valve orifice, creating a gradient (drop in pressure) that forces the ventricle to generate an higher ejection pressure. . This stress leads to significant remodelling of cardiac tissue, here cardiomyocytes increase in size to generate the required increase of force. However, such remodelling process also leads to myocardial fibrosis and dysregulation of Ca^{2+} handling and ion current balance within the affected cardiomyocytes. Over time, these alterations contribute to diastolic dysfunction and to an increased risk of heart failure, underlining the importance of understanding the pathophysiological mechanisms of AoS-induced LV hypertrophy and its effects on cardiac function.

The main cellular functional changes observed in primary hypertrophy and secondary hypertrophy are remarkably similar. In the myocardium from patients with both diseases, we observed significant alterations in Ca^{2+} handling, which has been proposed as a major pathogenic mechanism in all cardiac diseases. Ca^{2+} is a crucial ion in modulating the electrical and mechanical function of cardiomyocytes. Elevated levels of intracellular Ca^{2+} lead to activation of Ca^{2+}/calmodulin-dependent protein kinase II (CaMKII), which in turn increases the phosphorylation of its specific targets (Coppini et al., 2013). These alterations are closely associated with diastolic dysfunction and with an increased risk of arrhythmic events.

Electrophysiological evaluations were performed on human ventricular cardiomyocytes derived from myectomies obtained from hypertrophic patients with HCM or AoS, compared to control cardiomyocytes from non-failing non-hypertrophic patients with valvular

abnormalities. Patch-clamp investigations revealed a significant prolongation of action potential duration (APD90) in both HCM and AoS cells compared to control cardiomyocytes. These results highlight that the pathological remodelling associated with hypertrophy in both HCM and AoS leads to abnormalities in action potential kinetics. Furthermore, HCM cardiomyocytes exhibited a more pronounced prolongation of action potential duration when compared with cells from patients with AoS.

In order to assess Ca^{2+} handling, we used a specific fluorescent dye (Cal520) to visualize the movements of Ca^{2+} ions within the cytosol. Ca^{2+} transient kinetics evaluation revealed that the Ca^{2+} transient decay was significantly slower in HCM and AoS ventricular cardiomyocytes compared to control cells. Notably, this prolongation was more evident in HCM patients as compared with AoS samples. A similar prolongation was observed for the rising phase of Ca transients in cells from both the hypertrophic groups. Moreover, cardiomyocytes from both pathological groups exhibited increased diastolic Ca^{2+} concentration in response to increases in the rate of stimulation, highlighting that Ca^{2+} handling is significantly altered in HCM cardiomyocytes. Furthermore, we performed patch-clamp experiments to investigate the underlying changes of ion currents, specifically focusing on $Ca^{2+}$and late Na^{+} currents. Our results indicate an increase in both Ca^{2+} and Na^{+} currents in patients with HCM and AoS compared to controls, with a more pronounced effect observed in HCM patients. This suggests that the electrophysiological abnormalities seen in hypertrophic cardiomyocytes are not unique responses to specific diseases, but rather reflect common compensatory mechanisms associated with hypertrophic remodelling.

In conclusion, both primary hypertrophy and secondary hypertrophy, exhibit a similar range of functional and electrophysiological alterations, but the severity of these changes is significantly greater in HCM patients. The identified impairments in Ca^{2+} handling and action potential duration are essential to explain the pathophysiological basis of these cardiac conditions, providing novel insight for the development of targeted therapeutic strategies.

5.2 Evaluation of Cibenzoline in patients with HCM

HCM is a pathological condition characterized by significant electrophysiological abnormalities and Ca^{2+} handling. The most important feature is the prolongation of action potential duration, often associated with an increase frequency of early after depolarizations, contributing to a higher risk of ventricular tachyarrhythmias. These changes are primarily driven by the increase of late sodium current (I_{NaL}) and L-type calcium current (I_{CaL}), with a reduction of the repolarizing potassium currents, such as the inward rectifier current (I_{K1}) and the transient outward current (I_{to}) (Coppini et al, 2013).

These ionic current alterations result in slower Ca^{2+} transient kinetics and an elevated diastolic Ca^{2+} concentration; several mechanisms are responsible for this alteration in Ca^{2+} handling. The reduced density of T-tubules in HCM cardiomyocytes impairs the efficiency of excitation-contraction coupling by causing asynchronous Ca^{2+} release from the SR. Furthermore, Ca^{2+} overload within the SR can trigger spontaneous Ca^{2+} release during diastolic phase, raising diastolic Ca^{2+} levels and contributing to the arrhythmogenic potential. The Na^{+}/Ca^{2+} exchanger (NCX) also plays a key role, as the increased intracellular Na^{+} levels force NCX to more favourably work in its “reverse mode" (Ca flows in, Na flows out) while reducing the rate of its “forward mode” (Ca^{2+} out, Na^{+} in), further contributing to elevate intracellular Ca^{2+}concentrations. Additionally, reduced expression of the SERCA pump and altered phospholamban phosphorylation impairs the reuptake of Ca^{2+}into the SR (Kranias EG. et al., 2012).

Currently, no pharmacological agents specifically target the electrophysiological alterations underlying oHCM, such as the excessive I_{NaL} current and the impaired Ca^{2+} homeostasis. While surgical interventions like septal myectomy are performed for patients who do not respond adequately to drug treatment, these procedures are invasive and may not be suitable for all patients. Cibenzoline, an antiarrhythmic drug, has recently emerged as a potential candidate for treating oHCM, the mechanism of this drug suggests that it could be effective in reducing the electrophysiological abnormalities in the HCM myocardium, such as the excessive I_{NaL} influx. Our previous studies have shown that antiarrhythmic drugs, such as Disopyramide, have a beneficial effect in cardiomyocytes from patients with oHCM; Disopyramide is able to shorten action potential duration, reduce the I_{NaL} current, and normalize intracellular Ca^{2+} handling in HCM cardiomyocytes (Coppini et al., 2019). Given the promising effects observed with Disopyramide, Cibenzoline is an excellent candidate due to its comparatively lower incidence of adverse effects. Cibenzoline has the potential to

similarly modulate I_{NaL} current and restore Ca^{2+} handling abnormalities, representing an effective and safe pharmacological option for patients with oHCM (Hamada M. et al., 2021). Cibenzoline is a racemic compound. Previous studies suggested that the two stereoisomers may have different pharmacological profiles. Here we tested the s stereoisomer of Cibenzoline (CT-G20) in comparison with the racemate mixture (CT-G11)

In particular, our results show that CT-G20 is a potent blocker of late and peak Na^+ currents, within increased potency on late over peak Na^+ current in human ventricular cardiomyocytes from oHCM patients. The ratio of CT-G20 potency on late vs. peak current inhibition is about 4. Consistent with the use-dependence exhibited by several class-I antiarrhythmic agents, the inhibitory effects of CT-G20 on Na^+ current showed pronounced rate-dependency, becoming increasingly significant with higher rates of current activation. This property represents a notable advantage of CT-G20 over racemic Cibenzoline, which demonstrates no particular selectivity between late and peak Na^+ currents and exhibits reduced inhibitory efficacy at equivalent concentrations. As mentioned above, late Na^+ current plays a direct role in determining action potential duration ad repolarization in HCM cardiomyocytes. Instead, the peak Na^+ current is responsible for the action potential upstroke and determine electrical conduction velocity within the ventricular wall. Consistent with the greater potency of CT-G20 on late $I_{Na}{}^+$ rather than on peak $I_{Na}{}^+$, our observations indicate that CT-G20 shows greater efficacy in shortening the action potential duration rather than in slowing the action potential upstroke. In a direct comparison between the two drugs, CT-G20 (s-stereoisomer) demonstrated a significantly higher effect on shortening action potential duration compared to CT-G11 (racemate), when tested at equivalent concentrations. At the hypothetical therapeutic concentration of CT-G20 (approximately 1 μM), the compound effectively reduces action potential duration in ventricular cardiomyocytes derived from HCM patients, while causing only a minimal reduction in action potential upstroke velocity. This result is significant because highlight the safety of the drug, as an excessive slowing of conduction velocity could result in arrhythmic events.

Moreover, the evaluation of Ca^{2+} transient amplitude shows that CT-G20 is able to reduce the amplitude of Ca^{2+} transients in HCM ventricular cardiomyocytes in dose-dependent manner. In parallel, diastolic Ca^{2+} is reduced in a similar dose-dependent fashion. CT-G11 reduces Ca^{2+} transients in a similar dose-dependent manner, though it exhibits slightly lower potency when compared with CT-G20. Unlike CT-G20, however, CT-G11 does not produce any notable positive effects on Ca^{2+} transient kinetics.

In conclusion, CT-G20 represents a therapeutic option for the treatment of HCM; the drug demonstrated a lower inhibitory activity on muscarinic receptors (when compared with Disopyramide) and is very rarely associated whit anticholinergic side effects such as dry mouth and constipation (which are common with Disopyramide). Additionally, it does not prolong the QT interval. The ability to block late Na^+ current represents a key feature for the reduction of action potential duration in human ventricular HCM cardiomyocytes. This reduction of action potential duration, as well as the amelioration of Ca handling, has a beneficial effect in this context, where the diastolic dysfunction is a prominent clinical feature that plays an important role in symptom manifestation and disease progression.

5.3 Evaluation of Dapagliflozin in patients with HCM and AoS

HCM is the most common hereditary cardiomyopathy. Early diagnosis and treatments are important, because is the most common cause of sudden cardiac death in young people (Marian A. J. and Brauwald E., 2017). Today, drug treatment is limited to relieving symptoms such as heart failure, chest pain and shortness of breath. The most common clinical interventions are focused on the symptoms mitigation and include angiotensin II receptor blockers, Ca^{2+} inhibitors or β-blockers treatment.

AoS is a common cardiac disease, characterized by valve narrowing and calcification causing obstruction and hypertrophic changes in the left ventricle. The reduction of the aortic valve orifice alters the physiology of the heart in proportion with the severity of stenosis. In patients with AoS, hypertrophy represents a gradual adaptive process occurring in response to the chronic pressure overload, fundamental to normalize the LV ejection fraction. However, compensatory hypertrophy globally affects cardiac function in affected patients. The symptoms related to AoS are dyspnoea, angina pectoris, pulmonary congestion (Freeman RV. et al., 2005). The treatment for patients with severe AoS is surgery, where the aortic valve is replaced. As an alternative, symptoms can be addressed with diuretics and ACE inhibitors. Notwithstanding the different etiological features, HCM and AoS share a fundamental anatomic abnormality, that is left ventricular hypertrophy. This common anatomical feature makes it possible to investigate novel drugs that could result in benefits for both patients with HCM and AoS, with the goal of improving their quality of life.

Recent studies have shown that the inhibitors of the sodium-glucose 2 (SGLT2) co-transported (gliflozins) produce long term benefits in patients with heart failure. Gliflozins are a new class of oral drugs that were shown to reduce HF-related mortality and the risk of

hospitalization in patients with HF (EMPEROR-Reduced trial). Although SGLT2-inhibitors were developed for the treatment of type two diabetes, additional clinical trials revealed beneficial cardiovascular effect in patients without diabetes, although the specific mechanisms o are still unclear. We here tested Dapagliflozin, one of the clinically available SGLT2-inhibitors, in ventricular cardiomyocytes derived from HCM and AoS patients, at two different concentrations (1 and 10 μM).

Our results show a reduction in action potential duration in both patient groups, with a more pronounced shortening observed in HCM patients. This difference is likely attributable to the more advanced degree of hypertrophic remodelling in HCM. Furthermore, increasing the drug concentration from 1 μM to 10 μM led to a further reduction in action potential duration, demonstrating a clear dose-dependent effect. This highlights that the pharmacological response is directly correlated with the administered dose and its impact on action potential duration depends on the severity of myocardial remodelling in different patient groups.

However, the smaller effect observed in cardiomyocytes from patients with secondary hypertrophy can be explained by considering that HCM cardiomyocytes show a larger late Na^+ current when compared with AoS patients. To better understand the observed effects on action potential kinetics, we therefore investigated two components of the Na^+ current: the late and peak currents.

Dapagliflozin is able to selectively reduce late Na^+ current without affecting the peak Na^+ current, the latter being is essential for the initial phase of action potential. This selective action makes it a safer drug, as it does not interfere with the critical phase of depolarization, thus reducing the risk of triggering arrhythmic events that could lead to sudden cardiac death. Further studies are needed to better understand the complete mechanisms of gliflozins in the heart. Nonetheless, these results are a starting point for understanding how Dapagliflozin exerts its cardioprotective effects.

5.4 Studies on human cardiac fibroblasts from hypertrophic myocardial samples

In the context of hypertrophic hearts, the fibrosis process is closely linked to alterations in the extracellular matrix, as pro-inflammatory cytokines induce the production of extracellular components. Following myocardial infarction, necrotic cardiomyocytes are

replaced through the deposition of collagen, a process mediated by fibroblasts which differentiate into myofibroblasts, thus resulting in an overproduction of type I collagen. Consequently, ischemic injury leads to the formation of fibrotic scars and diastolic dysfunction (Liu M. et al, 2021).

Cardiac fibrosis occurs in many cardiac pathologies, including those discussed in this thesis, i.e. HCM and AoS. Excessive collagen production by myofibroblasts leads to increased stiffness of the matrix and abnormal cardiac function, impairing the heart's filling capacity and consequently resulting in heart failure with reduced ejection fraction (Hinderer S. et al, 2019).

To date, cardiac fibrosis remains an unresolved issue in heart diseases. Our interest is to study the channels responsible for increased Ca^{2+} influx through the fibroblast membrane, as this mechanism is one of the triggers of myofibroblast activation. The influx of Ca^{2+} into fibroblast is essential to modulate their function in response to pathological and physiological stimuli, as it partially regulates target genes dependent on the nuclear factor of activated T-cells (NFAT).

In particular we investigated the role of TRP channels and Ca^{2+} channel type L in activating Ca influx. In cardiac fibroblasts, the TRP channels influence their activation and their differentiation into myofibroblasts, that cause excessive collagen formation in the myocardium. Ca^{2+} influx through TRP channels is essential for the activation of key transcriptional regulators such as NFATs that control fibrotic gene expression. According to the literature, in cardiac fibroblasts Ca^{2+} influx mediated by TRP channels is essential for the worsening of fibrosis. For instance, activation of TRPC3 leads to an increase in the production of ROS and the activation of RhoA signalling pathways, which collectively contribute to fibrous remodelling in the heart (Falcón D. et al, 2019).

L-type Ca^{2+} channels are also implicated in the regulation of Ca^{2+} influx, playing a role in modulating fibroblast activation and the progression of fibrosis. In particular, previous studies highlighted that L-type Ca^{2+} channels blockers can reduce fibrosis by attenuating Ca^{2+} -mediated activation of fibrogenic factors such as TGF-β (Chen Q. et al, 2024). Moreover, recent evidence suggests that its over-expression in failing hearts could affect fibrotic pathways. This suggest that Ca^{2+}signalling proteins could serve as targets for therapeutic interventions aimed at managing or preventing fibrosis.

We studied the mechanisms of Ca^{2+} influx in fibroblasts isolated from human samples from HCM and control patients. We used specific inhibitors to discriminate which channels

facilitate the entry of Ca^{2+}: Lacidipine, targeting L-type Ca^{2+}channels, and SKF, targeting TRPC. Additionally, we used TGF-β to assess its effects on the influx of Ca^{2+}into fibroblasts. This approach allowed us to delineate the contributions of these different channel types to the overall dynamics of Ca^{2+} within these cells.

Initially, the effects of LACI [10μM] and SKF [5μM] on Ca^{2+} influx in HCM and control fibroblast were examined. Here, both agents were able to reduce the amplitude of transients Ca^{2+} in both lines. In particular, we observed a significantly higher reduction of Ca^{2+} inflow in the control line as compared to HCM fibroblasts, when treated with SKF or LACI. Afterwards, we evaluated the Ca^{2+} influx in the absence of drugs and we observed that in HCM fibroblasts we have an increased Ca^{2+} influx, which might contribute to the pathophysiology of the disease by impairing Ca^{2+} homeostasis and enhancing fibroblast activation. Our results suggest that the increase of Ca^{2+} influx in HCM vs. control fibroblasts is not caused by alterations of the TRP or of the L-type Ca^{2+} channels but is probably determined by different channels that remain to be identified. Indeed, the reduction induced by the two blockers in control or HCM fibroblasts is comparable.

Further, we explored the effects of TGF-β, a growth factor known to stimulate cell growth and differentiation and to promote ECM component production. Treatment of HCM fibroblasts with TGF-β for 24 hours prior to the Ca^{2+} influx evaluation, showed a significant increase in Ca^{2+} entry compared to untreated cells. Then, we evaluated the effect of SKF in the presence or absence of TGF-β in HCM fibroblasts; the results show that the reduction in Ca^{2+} influx, mediated by SKF, was less pronounced in TGF-β-treated compared to untreated cells, indicating that TGF-β modifies cellular responsiveness to Ca^{2+} by modulating TRPC. These results highlight the complexity of Ca^{2+} signalling in fibroblast, especially in the presence of cardiomyopathy, where alterations in Ca^{2+} handling can significantly influence the cellular environment, potentially exacerbating the disease phenotype.

REFERENCES

- *Al Ghorani H, Kulenthiran S, Lauder L, Böhm M, Mahfoud F. Hypertension trials update. J Hum Hypertens. 2021 May;35(5):398-409. doi: 10.1038/s41371-020-00477-1. Epub 2021 Jan 12. PMID: 33437020; PMCID: PMC8134044.*
- *Alcaide P, Kallikourdis M, Emig R, Prabhu SD. Myocardial Inflammation in Heart Failure With Reduced and Preserved Ejection Fraction. Circ Res. 2024 Jun 7;134(12):1752-1766. doi: 10.1161/CIRCRESAHA.124.323659. Epub 2024 Jun 6. PMID: 38843295; PMCID: PMC11160997.*
- *Antunes MO, Scudeler TL. Hypertrophic cardiomyopathy. Int J Cardiol Heart Vasc. 2020 Mar 25 ;27 :100503. doi: 10.1016/j.ijcha.2020.100503. Erratum in : Int J Cardiol Heart Vasc. 2020 Nov 18 ;31 :100676. doi: 10.1016/j.ijcha.2020.100676. PMID : 32309534 ; PMCID : PMC7154317.*
- *Arbelo E, Protonotarios A, Gimeno JR, Arbustini E, Barriales-Villa R, Basso C, Bezzina CR, Biagini E, Blom NA, de Boer RA, De Winter T, Elliott PM, Flather M, Garcia-Pavia P, Haugaa KH, Ingles J, Jurcut RO, Klaassen S, Limongelli G, Loeys B, Mogensen J, Olivotto I, Pantazis A, Sharma S, Van Tintelen JP, Ware JS, Kaski JP ; ESC Scientific Document Group. 2023 ESC Guidelines for the management of cardiomyopathies. Eur Heart J. 2023 Oct 1;44(37):3503-3626. doi: 10.1093/eurheartj/ehad194. PMID: 37622657.*
- *Arimont M, Sun SL, Leurs R, Smit M, de Esch IJP, de Graaf C. Structural Analysis of Chemokine Receptor-Ligand Interactions. J Med Chem. 2017 Jun 22;60(12):4735-4779. doi: 10.1021/acs.jmedchem.6b01309. Epub 2017 Mar 10. PMID: 28165741; PMCID: PMC5483895.*
- *Backs J, Song K, Bezprozvannaya S, Chang S, Olson EN. CaM kinase II selectively signals to histone deacetylase 4 during cardiomyocyte hypertrophy. J Clin Invest. 2006 Jul;116(7):1853-64. doi: 10.1172/JCI27438. Epub 2006 Jun 8. PMID: 16767219; PMCID: PMC1474817.*
- *Barker TH, Engler AJ. The provisional matrix: setting the stage for tissue repair outcomes. Matrix Biol. 2017 Jul;60-61:1-4. doi: 10.1016/j.matbio.2017.04.003. PMID: 28527902; PMCID: PMC5831186.*

- *Bartekova M, Radosinska J, Jelemensky M, Dhalla NS. Role of cytokines and inflammation in heart function during health and disease. Heart Fail Rev. 2018 Sep;23(5):733-758. doi: 10.1007/s10741-018-9716-x. PMID: 29862462.*
- *Bass-Stringer S, Tai CMK, McMullen JR. IGF1-PI3K-induced physiological cardiac hypertrophy: Implications for new heart failure therapies, biomarkers, and predicting cardiotoxicity. J Sport Health Sci. 2021 Dec;10(6):637-647. doi: 10.1016/j.jshs.2020.11.009. Epub 2020 Nov 24. PMID: 33246162; PMCID: PMC8724616.*
- *Bernardo BC, Weeks KL, Pretorius L, McMullen JR. Molecular distinction between physiological and pathological cardiac hypertrophy: experimental findings and therapeutic strategies. Pharmacol Ther. 2010 Oct;128(1):191-227. doi: 10.1016/j.pharmthera.2010.04.005. Epub 2010 May 12. PMID: 20438756.*
- *Bers DM. Cardiac sarcoplasmic reticulum calcium leak: basis and roles in cardiac dysfunction. Annu Rev Physiol. 2014; 76:107-27. doi: 10.1146/annurev-physiol-020911-153308. Epub 2013 Nov 13. PMID: 24245942.*
- *Bersell K, Arab S, Haring B, Kühn B. Neuregulin1/ErbB4 signaling induces cardiomyocyte proliferation and repair of heart injury. Cell. 2009 Jul 23;138(2):257-70. doi: 10.1016/j.cell.2009.04.060. PMID: 19632177.*
- *Bhullar SK, Dhalla NS. Angiotensin II-Induced Signal Transduction Mechanisms for Cardiac Hypertrophy. Cells. 2022 Oct 22;11(21):3336. doi: 10.3390/cells11213336. PMID: 36359731; PMCID: PMC9657342.*
- *Bondi CD, Manickam N, Lee DY, Block K, Gorin Y, Abboud HE, Barnes JL. NAD(P)H oxidase mediates TGF-beta1-induced activation of kidney myofibroblasts. J Am Soc Nephrol. 2010 Jan;21(1):93-102. doi: 10.1681/ASN.2009020146. Epub 2009 Nov 19. PMID: 19926889; PMCID: PMC2799274.*
- *Borg TK, Rubin K, Carver W, Samarel A, Terracio L. The cell biology of the cardiac interstitium. Trends Cardiovasc Med. 1996 Feb;6(2):65-70. doi: 10.1016/1050-1738(96)00005-9. PMID: 21232277.*
- *Braunwald E, Mann DL, Zipes DP, Libby P, Bonow RO. (2016) Malattie del cuore di Braunwald - Trattato di medicina cardiovascolare.*
- *Braunwald E. Gliflozins in the Management of Cardiovascular Disease. N Engl J Med. 2022 May 26;386(21):2024-2034. doi: 10.1056/NEJMra2115011. PMID: 35613023.*

- *Camelliti P, Borg TK, Kohl P. Structural and functional characterisation of cardiac fibroblasts. Cardiovasc Res. 2005 Jan 1;65(1):40-51. doi: 10.1016/j.cardiores.2004.08.020. PMID: 15621032.*
- *Campbell P, Rutten FH, Lee MM, Hawkins NM, Petrie MC. Heart failure with preserved ejection fraction: everything the clinician needs to know. Lancet. 2024 Mar 16;403(10431):1083-1092. doi: 10.1016/S0140-6736(23)02756-3. Epub 2024 Feb 14. Erratum in: Lancet. 2024 Mar 16;403(10431):1026. doi: 10.1016/S0140-6736(24)00494-X. PMID: 38367642.*
- *Carabello BA, Paulus WJ. Aortic stenosis. Lancet. 2009 Mar 14;373(9667):956-66. doi: 10.1016/S0140-6736(09)60211-7. Epub 2009 Feb 21. PMID: 19232707.*
- *Chen Q, Pan Y, Hu Y, Chen G, Chen X, Xie Y, Wang M, Li Z, Huang J, Shi Y, Huang H, Zhang T, Wang M, Zeng P, Wang S, Chen R, Zheng Y, Zhong L, Yang H, Liang D. An L-type calcium channel blocker nimodipine exerts anti-fibrotic effects by attenuating TGF-β1 induced calcium response in an in vitro model of thyroid eye disease. Eye Vis (Lond). 2024 Sep 6;11(1):37. doi: 10.1186/s40662-024-00401-5. PMID: 39237996; PMCID: PMC11378575.*
- *Choudhury L, Elliott P, Rimoldi O, Ryan M, Lammertsma AA, Boyd H, McKenna WJ, Camici PG. Transmural myocardial blood flow distribution in hypertrophic cardiomyopathy and effect of treatment. Basic Res Cardiol. 1999 Feb;94(1):49-59. doi: 10.1007/s003950050126. PMID: 10097830.*
- *Chu PY, Mariani J, Finch S, McMullen JR, Sadoshima J, Marshall T, Kaye DM. Bone marrow-derived cells contribute to fibrosis in the chronically failing heart. Am J Pathol. 2010 Apr;176(4):1735-42. doi: 10.2353/ajpath.2010.090574. Epub 2010 Feb 11. PMID: 20150435; PMCID: PMC2843465.*
- *Cleutjens JP, Verluyten MJ, Smiths JF, Daemen MJ. Collagen remodeling after myocardial infarction in the rat heart. Am J Pathol. 1995 Aug;147(2):325-38. PMID: 7639329; PMCID: PMC1869816.*
- *Coppini R, Ferrantini C, Pioner JM, Santini L, Wang ZJ, Palandri C, Scardigli M, Vitale G, Sacconi L, Stefàno P, Flink L, Riedy K, Pavone FS, Cerbai E, Poggesi C, Mugelli A, Bueno-Orovio A, Olivotto I, Sherrid MV. Electrophysiological and Contractile Effects of Disopyramide in Patients with Obstructive Hypertrophic Cardiomyopathy: A Translational Study. JACC Basic Transl Sci. 2019 Oct*

9;4(7):795-813. doi: 10.1016/j.jacbts.2019.06.004. PMID: 31998849; PMCID: PMC6978554.

- *Coppini R, Ferrantini C, Yao L, Fan P, Del Lungo M, Stillitano F, Sartiani L, Tosi B, Suffredini S, Tesi C, Yacoub M, Olivotto I, Belardinelli L, Poggesi C, Cerbai E, Mugelli A. Late sodium current inhibition reverses electromechanical dysfunction in human hypertrophic cardiomyopathy. Circulation. 2013 Feb 5;127(5):575-84. doi: 10.1161/CIRCULATIONAHA.112.134932. Epub 2012 Dec 27. PMID: 23271797.*
- *Cowie B. The Preoperative Patient With a Systolic Murmur. Anesth Pain Med. 2015 Dec 5;5(6): e32105. doi: 10.5812/aapm.32105. PMID: 26705529; PMCID: PMC4688819.*
- *Falcón D, Galeano-Otero I, Calderón-Sánchez E, Del Toro R, Martín-Bórnez M, Rosado JA, Hmadcha A, Smani T. TRP Channels: Current Perspectives in the Adverse Cardiac Remodeling. Front Physiol. 2019 Mar 1; 10:159. doi: 10.3389/fphys.2019.00159. PMID: 30881310; PMCID: PMC6406032.*
- *Feldman MD, Copelas L, Gwathmey JK, Phillips P, Warren SE, Schoen FJ, Grossman W, Morgan JP. Deficient production of cyclic AMP: pharmacologic evidence of an important cause of contractile dysfunction in patients with end-stage heart failure. Circulation. 1987 Feb;75(2):331-9. doi: 10.1161/01.cir.75.2.331. PMID: 2433073.*
- *Ferrara N. Vascular endothelial growth factor: basic science and clinical progress. Endocr Rev. 2004 Aug;25(4):581-611. doi: 10.1210/er.2003-0027. PMID: 15294883.*
- *Fidziańska A, Bilińska ZT, Walczak E, Witkowski A, Chojnowska L. Autophagy in transition from hypertrophic cardiomyopathy to heart failure. J Electron Microsc (Tokyo). 2010;59(2):181-3. doi: 10.1093/jmicro/dfp048. Epub 2009 Sep 30. PMID: 19797323.*
- *Finocchiaro G, Sheikh N, Biagini E, Papadakis M, Maurizi N, Sinagra G, Pelliccia A, Rapezzi C, Sharma S, Olivotto I. The electrocardiogram in the diagnosis and management of patients with hypertrophic cardiomyopathy. Heart Rhythm. 2020 Jan;17(1):142-151. doi: 10.1016/j.hrthm.2019.07.019. Epub 2019 Aug 10. PMID: 31349064.*

- *Fox PR. Endomyocardial fibrosis and restrictive cardiomyopathy: pathologic and clinical features. J Vet Cardiol. 2004 May;6(1):25-31. doi: 10.1016/S1760-2734(06)70061-3. PMID: 19083301.*
- *Frangogiannis NG. Cardiac fibrosis. Cardiovasc Res. 2021 May 25;117(6):1450-1488. doi: 10.1093/cvr/cvaa324. PMID: 33135058; PMCID: PMC8152700.*
- *Freeman RV, Otto CM. Spectrum of calcific aortic valve disease: pathogenesis, disease progression, and treatment strategies. Circulation. 2005 Jun 21;111(24):3316-26. doi: 10.1161/CIRCULATIONAHA.104.486738. PMID: 15967862.*
- *Fulghum KL, Smith JB, Chariker J, Garrett LF, Brittian KR, Lorkiewicz PK, McNally LA, Uchida S, Jones SP, Hill BG, Collins HE. Metabolic signatures of pregnancy-induced cardiac growth. Am J Physiol Heart Circ Physiol. 2022 Jul 1;323(1):H146-H164. doi: 10.1152/ajpheart.00105.2022. Epub 2022 May 27. PMID: 35622533; PMCID: PMC9236881.*
- *Garg R, Yusuf S. Overview of randomized trials of angiotensin-converting enzyme inhibitors on mortality and morbidity in patients with heart failure. Collaborative Group on ACE Inhibitor Trials. JAMA. 1995 May 10;273(18):1450-6. Erratum in: JAMA 1995 Aug 9;274(6):462. PMID: 7654275.*
- *Gersh BJ, Maron BJ, Bonow RO, Dearani JA, Fifer MA, Link MS, Naidu SS, Nishimura RA, Ommen SR, Rakowski H, Seidman CE, Towbin JA, Udelson JE, Yancy CW. 2011 ACCF/AHA guideline for the diagnosis and treatment of hypertrophic cardiomyopathy: executive summary: a report of the American College of Cardiology Foundation/American Heart Association Task Force on Practice Guidelines. J Am Coll Cardiol. 2011 Dec 13;58(25):2703-38. doi: 10.1016/j.jacc.2011.10.825. Epub 2011 Nov 8. PMID: 22075468.*
- *Geske JB, Ommen SR, Gersh BJ. Hypertrophic Cardiomyopathy: Clinical Update. JACC Heart Fail. 2018 May;6(5):364-375. doi: 10.1016/j.jchf.2018.02.010. Epub 2018 Apr 11. PMID: 29655825.*
- *Gistri R, Cecchi F, Choudhury L, Montereggi A, Sorace O, Salvadori PA, Camici PG. Effect of verapamil on absolute myocardial blood flow in hypertrophic cardiomyopathy. Am J Cardiol. 1994 Aug 15;74(4):363-8. doi: 10.1016/0002-9149(94)90404-9. PMID: 8059699.*

- *Gogiraju R, Bochenek ML, Schäfer K. Angiogenic Endothelial Cell Signaling in Cardiac Hypertrophy and Heart Failure. Front Cardiovasc Med. 2019 Mar 6;6:20. doi: 10.3389/fcvm.2019.00020. PMID: 30895179; PMCID: PMC6415587.*
- *Green EM. Wakimoto H, Anderson RL, Evanchik MJ, Gorham JM, Harrison BC, Henze M, Kawas R, Oslob JD, Rodriguez HM, Song Y, Wan W, Leinwand LA, Spudich JA, McDowell RS, Seidman JG, Seidman CE. A small-molecule inhibitor of sarcomere contractility suppresses hypertrophic cardiomyopathy in mice. Science. 2016 Feb 5;351(6273):617-21. doi: 10.1126/science. aad3456. PMID: 26912705; PMCID: PMC4784435.*
- *Grimard BH, Larson JM. Aortic stenosis: diagnosis and treatment. Am Fam Physician. 2008 Sep 15;78(6):717-24. PMID: 18819236*
- *Grossman W, Jones D, McLaurin LP. Wall stress and patterns of hypertrophy in the human left ventricle. J Clin Invest. 1975 Jul;56(1):56-64. doi: 10.1172/JCI108079. PMID: 124746; PMCID: PMC436555.*
- *Grossman W, Paulus WJ. Myocardial stress and hypertrophy: a complex interface between biophysics and cardiac remodeling. J Clin Invest. 2013 Sep;123(9):3701-3. doi: 10.1172/JCI69830. Epub 2013 Sep 3. PMID: 23999445; PMCID: PMC3754273.*
- *Gupta M, Rao S, Manek G, Fonarow GC, Ghosh RK. The Role of Dapagliflozin in the Management of Heart Failure: An Update on the Emerging Evidence. Ther Clin Risk Manag. 2021 Aug 12; 17:823-830. doi: 10.2147/TCRM.S275076. PMID: 34408424; PMCID: PMC8367215*
- *Gupta S, Das B, Sen S. Cardiac hypertrophy: mechanisms and therapeutic opportunities. Antioxid Redox Signal. 2007 Jun;9(6):623-52. doi: 10.1089/ars.2007.1474. PMID: 17511580*
- *Gupta S, Ge Y, Singh A, Gräni C, Kwong RY. Multimodality Imaging Assessment of Myocardial Fibrosis. JACC Cardiovasc Imaging. 2021 Dec;14(12):2457-2469. doi: 10.1016/j.jcmg.2021.01.027. Epub 2021 May 19. PMID: 34023250.*
- *Hamada M, Ikeda S, Shigematsu Y. Advances in medical treatment of hypertrophic cardiomyopathy. J Cardiol. 2014 Jul;64(1):1-10. doi: 10.1016/j.jjcc.2014.02.022. Epub 2014 Apr 13. Erratum in: J Cardiol. 2014 Oct;64(4):330. PMID: 24735741.*
- *Hamada M, Shigematsu Y, Ikeda S, Ohshima K, Ogimoto A. Impact of cibenzoline treatment on left ventricular remodelling and prognosis in hypertrophic obstructive*

cardiomyopathy. ESC Heart Fail. 2021 Dec;8(6):4832-4842. doi: 10.1002/ehf2.13672. Epub 2021 Oct 29. PMID: 34713615; PMCID: PMC8712831

- *Hamdani N, Paulus WJ, van Heerebeek L, Borbély A, Boontje NM, Zuidwijk MJ, Bronzwaer JG, Simonides WS, Niessen HW, Stienen GJ, van der Velden J. Distinct myocardial effects of beta-blocker therapy in heart failure with normal and reduced left ventricular ejection fraction. Eur Heart J. 2009 Aug;30(15):1863-72. doi: 10.1093/eurheartj/ehp189. Epub 2009 May 31. PMID: 19487234.*
- *Hensley N, Dietrich J, Nyhan D, Mitter N, Yee MS, Brady M. Hypertrophic cardiomyopathy: a review. Anesth Analg. 2015 Mar;120(3):554-569. doi: 10.1213/ANE.0000000000000538. PMID: 25695573.*
- *Hill JA, Olson EN. Cardiac plasticity. N Engl J Med. 2008 Mar 27;358(13):1370-80. doi: 10.1056/NEJMra072139. PMID: 18367740.*
- *Hinderer S, Schenke-Layland K. Cardiac fibrosis - A short review of causes and therapeutic strategies. Adv Drug Deliv Rev. 2019 Jun; 146:77-82. doi: 10.1016/j.addr.2019.05.011. Epub 2019 May 31. PMID: 31158407*
- *Hoshijima M. Mechanical stress-strain sensors embedded in cardiac cytoskeleton: Z disk, titin, and associated structures. Am J Physiol Heart Circ Physiol. 2006 Apr;290(4):H1313-25. doi: 10.1152/ajpheart.00816.2005. PMID: 16537787; PMCID: PMC3241960.*
- *Hudmon A, Schulman H. Structure-function of the multifunctional Ca2+/calmodulin-dependent protein kinase II. Biochem J. 2002 Jun 15;364(Pt 3):593-611. doi: 10.1042/BJ20020228. PMID: 11931644; PMCID: PMC1222606.*
- *Ingles J, Goldstein J, Thaxton C, Caleshu C, Corty EW, Crowley SB, Dougherty K, Harrison SM, McGlaughon J, Milko LV, Morales A, Seifert BA, Strande N, Thomson K, Peter van Tintelen J, Wallace K, Walsh R, Wells Q, Whiffin N, Witkowski L, Semsarian C, Ware JS, Hershberger RE, Funke B. Evaluating the Clinical Validity of Hypertrophic Cardiomyopathy Genes. Circ Genom Precis Med. 2019 Feb;12(2):e002460. doi: 10.1161/CIRCGEN.119.002460. PMID: 30681346; PMCID: PMC6410971.*
- *Ionita MG, Arslan F, de Kleijn DP, Pasterkamp G. Endogenous inflammatory molecules engage Toll-like receptors in cardiovascular disease. J Innate Immun. 2010;2(4):307-15. doi: 10.1159/000314270. Epub 2010 Apr 30. PMID: 20431283.*

- *Izumiya Y, Shiojima I, Sato K, Sawyer DB, Colucci WS, Walsh K. Vascular endothelial growth factor blockade promotes the transition from compensatory cardiac hypertrophy to failure in response to pressure overload. Hypertension. 2006 May;47(5):887-93. doi: 10.1161/01.HYP.0000215207.54689.31. Epub 2006 Mar 27. PMID: 16567591; PMCID: PMC3132898.*
- *January CT, Wann LS, Alpert JS, Calkins H, Cigarroa JE, Cleveland JC Jr, Conti JB, Ellinor PT, Ezekowitz MD, Field ME, Murray KT, Sacco RL, Stevenson WG, Tchou PJ, Tracy CM, Yancy CW; American College of Cardiology/American Heart Association Task Force on Practice Guidelines. 2014 AHA/ACC/HRS guideline for the management of patients with atrial fibrillation: a report of the American College of Cardiology/American Heart Association Task Force on Practice Guidelines and the Heart Rhythm Society. J Am Coll Cardiol. 2014 Dec 2;64(21):e1-76. doi: 10.1016/j.jacc.2014.03.022. Epub 2014 Mar 28. Erratum in: J Am Coll Cardiol. 2014 Dec 2;64(21):2305-7. PMID: 24685669.*
- *Juni RP, Kuster DWD, Goebel M, Helmes M, Musters RJP, van der Velden J, Koolwijk P, Paulus WJ, van Hinsbergh VWM. Cardiac Microvascular Endothelial Enhancement of Cardiomyocyte Function Is Impaired by Inflammation and Restored by Empagliflozin. JACC Basic Transl Sci. 2019 Sep 4;4(5):575-591. doi: 10.1016/j.jacbts.2019.04.003. PMID: 31768475; PMCID: PMC6872802.*
- *Kanwar A, Thaden JJ, Nkomo VT. Management of Patients With Aortic Valve Stenosis. Mayo Clin Proc. 2018 Apr;93(4):488-508. doi: 10.1016/j.mayocp.2018.01.020. PMID: 29622096.*
- *Kawase Y, Ly HQ, Prunier F, Lebeche D, Shi Y, Jin H, Hadri L, Yoneyama R, Hoshino K, Takewa Y, Sakata S, Peluso R, Zsebo K, Gwathmey JK, Tardif JC, Tanguay JF, Hajjar RJ. Reversal of cardiac dysfunction after long-term expression of SERCA2a by gene transfer in a pre-clinical model of heart failure. J Am Coll Cardiol. 2008 Mar 18;51(11):1112-9. doi: 10.1016/j.jacc.2007.12.014. PMID: 18342232.*
- *Klocko DJ, Hanifin C. Cardiac auscultation: Using physiologic maneuvers to further identify heart murmurs. JAAPA. 2019 Dec;32(12):21-25. doi: 10.1097/01.JAA.0000604856.33701.ad. PMID: 31714345.*
- *Koziris LP, Hickson RC, Chatterton RT Jr, Groseth RT, Christie JM, Goldflies DG, Unterman TG. Serum levels of total and free IGF-I and IGFBP-3 are increased and*

maintained in long-term training. J Appl Physiol (1985). 1999 Apr;86(4):1436-42. doi: 10.1152/jappl.1999.86.4.1436. PMID: 10194233.

- *Kranias EG, Hajjar RJ. Modulation of cardiac contractility by the phospholamban/SERCA2a regulatome. Circ Res. 2012 Jun 8;110(12):1646-60. doi: 10.1161/CIRCRESAHA.111.259754. PMID: 22679139; PMCID: PMC3392125.*
- *Krittanawong C, Rodriguez M, Lui M, Misra A, Tang WHW, Bozkurt B, Yancy CW. Misconceptions and Facts about Heart Failure with Reduced Ejection Fraction. Am J Med. 2023 May;136(5):422-431. doi: 10.1016/j.amjmed.2023.01.024. Epub 2023 Feb 3. PMID: 36740210.*
- *Li J, Zhou L, Gong H. New insights and advances of sodium-glucose cotransporter 2 inhibitors in heart failure. Front Cardiovasc Med. 2022 Sep 15; 9:903902. doi: 10.3389/fcvm.2022.903902. PMID: 36186974; PMCID: PMC9520058.*
- *Lighthouse JK, Small EM. Transcriptional control of cardiac fibroblast plasticity. J Mol Cell Cardiol. 2016 Feb; 91:52-60. doi: 10.1016/j.yjmcc.2015.12.016. Epub 2015 Dec 22. PMID: 26721596; PMCID: PMC4764462.*
- *Lindman BR, Clavel MA, Mathieu P, Iung B, Lancellotti P, Otto CM, Pibarot P. Calcific aortic stenosis. Nat Rev Dis Primers. 2016 Mar 3; 2:16006. doi: 10.1038/nrdp.2016.6. PMID: 27188578; PMCID: PMC5127286.*
- *Liu M, López de Juan Abad B, Cheng K. Cardiac fibrosis: Myofibroblast-mediated pathological regulation and drug delivery strategies. Adv Drug Deliv Rev. 2021 Jun; 173:504-519. doi: 10.1016/j.addr.2021.03.021. Epub 2021 Apr 5. PMID: 33831476; PMCID: PMC8299409*
- *Lourenço AP, Leite-Moreira AF, Balligand JL, Bauersachs J, Dawson D, de Boer RA, de Windt LJ, Falcão-Pires I, Fontes-Carvalho R, Franz S, Giacca M, Hilfiker-Kleiner D, Hirsch E, Maack C, Mayr M, Pieske B, Thum T, Tocchetti CG, Brutsaert DL, Heymans S. An integrative translational approach to study heart failure with preserved ejection fraction: a position paper from the Working Group on Myocardial Function of the European Society of Cardiology. Eur J Heart Fail. 2018 Feb;20(2):216-227. doi: 10.1002/ejhf.1059. Epub 2017 Nov 16. PMID: 29148148.*
- *Lyu L, Wang H, Li B, Qin Q, Qi L, Nagarkatti M, Nagarkatti P, Janicki JS, Wang XL, Cui T. A critical role of cardiac fibroblast-derived exosomes in activating renin angiotensin system in cardiomyocytes. J Mol Cell Cardiol. 2015 Dec;89(Pt B):268-*

79. doi: 10.1016/j.yjmcc.2015.10.022. Epub 2015 Oct 20. PMID: 26497614; PMCID: PMC4988239.

- *M. Vinciguerra, M.P. Santini,W.C. Claycomb, A.G. Ladurner, N. Rosenthal, Local IGF-1 isoform protects cardiomyocytes from hypertrophic and oxidative stresses via SirT1 activity, Aging (Albany NY) 2 (2010) 43–62.*
- *Malik R, Maron MS, Rastegar H, Pandian NG. Hypertrophic cardiomyopathy with right ventricular outflow tract and left ventricular intracavitary obstruction. Echocardiography. 2014 May;31(5):682-5. doi: 10.1111/echo.12543. Epub 2014 Mar 20. PMID: 24649889.*
- *Mandeş L, Roşca M, Ciupercă D, Popescu BA. The role of echocardiography for diagnosis and prognostic stratification in hypertrophic cardiomyopathy. J Echocardiogr. 2020 Sep;18(3):137-148. doi: 10.1007/s12574-020-00467-9. Epub 2020 Apr 16. PMID: 32301048; PMCID: PMC7473965.*
- *Marian AJ, Braunwald E. Hypertrophic Cardiomyopathy: Genetics, Pathogenesis, Clinical Manifestations, Diagnosis, and Therapy. Circ Res. 2017 Sep 15;121(7):749-770. doi: 10.1161/CIRCRESAHA.117.311059. PMID: 28912181; PMCID: PMC5654557.*
- *Marian AJ. Contemporary treatment of hypertrophic cardiomyopathy. Tex Heart Inst J. 2009;36(3):194-204. PMID: 19568388; PMCID: PMC2696493.*
- *Maron BJ, Epstein SE. Hypertrophic cardiomyopathy: a discussion of nomenclature. Am J Cardiol. 1979 Jun;43(6):1242-4. doi: 10.1016/0002-9149(79)90160-7. PMID: 571671.*
- *Maron BJ, Maron MS. Hypertrophic cardiomyopathy. Lancet. 2013 Jan 19;381(9862):242-55. doi: 10.1016/S0140-6736(12)60397-3. Epub 2012 Aug 6. PMID: 22874472.*
- *Maron BJ, Towbin JA, Thiene G, Antzelevitch C, Corrado D, Arnett D, Moss AJ, Seidman CE, Young JB; American Heart Association; Council on Clinical Cardiology, Heart Failure and Transplantation Committee; Quality of Care and Outcomes Research and Functional Genomics and Translational Biology Interdisciplinary Working Groups; Council on Epidemiology and Prevention. Contemporary definitions and classification of the cardiomyopathies: an American Heart Association Scientific Statement from the Council on Clinical Cardiology, Heart Failure and Transplantation Committee; Quality of Care and Outcomes*

Research and Functional Genomics and Translational Biology Interdisciplinary Working Groups; and Council on Epidemiology and Prevention. Circulation. 2006 Apr 11;113(14):1807-16. doi: 10.1161/CIRCULATIONAHA.106.174287. Epub 2006 Mar 27. PMID: 16567565.

- *Maron BJ. Sudden death in young athletes. N Engl J Med. 2003 Sep 11;349(11):1064-75. doi: 10.1056/NEJMra022783. PMID: 12968091.*
- *Maron MS. The current and emerging role of cardiovascular magnetic resonance imaging in hypertrophic cardiomyopathy. J Cardiovasc Transl Res. 2009 Dec;2(4):415-25. doi: 10.1007/s12265-009-9136-3. Epub 2009 Nov 7. PMID: 20560000.*
- *Marx SO, Reiken S, Hisamatsu Y, Jayaraman T, Burkhoff D, Rosemblit N, Marks AR. PKA phosphorylation dissociates FKBP12.6 from the calcium release channel (ryanodine receptor): defective regulation in failing hearts. Cell. 2000 May 12;101(4):365-76. doi: 10.1016/s0092-8674(00)80847-8. PMID: 10830164.*
- *McMurray JJV, Solomon SD, Inzucchi SE, Køber L, Kosiborod MN, Martinez FA, Ponikowski P, Sabatine MS, Anand IS, Bělohlávek J, Böhm M, Chiang CE, Chopra VK, de Boer RA, Desai AS, Diez M, Drozdz J, Dukát A, Ge J, Howlett JG, Katova T, Kitakaze M, Ljungman CEA, Merkely B, Nicolau JC, O'Meara E, Petrie MC, Vinh PN, Schou M, Tereshchenko S, Verma S, Held C, DeMets DL, Docherty KF, Jhund PS, Bengtsson O, Sjöstrand M, Langkilde AM; DAPA-HF Trial Committees and Investigators. Dapagliflozin in Patients with Heart Failure and Reduced Ejection Fraction. N Engl J Med. 2019 Nov 21;381(21):1995-2008. doi: 10.1056/NEJMoa1911303. Epub 2019 Sep 19. PMID: 31535829.*
- *Merovci A, Solis-Herrera C, Daniele G, Eldor R, Fiorentino TV, Tripathy D, Xiong J, Perez Z, Norton L, Abdul-Ghani MA, DeFronzo RA. Dapagliflozin improves muscle insulin sensitivity but enhances endogenous glucose production. J Clin Invest. 2014 Feb;124(2):509-14. doi: 10.1172/JCI70704. Epub 2014 Jan 27. Erratum in: J Clin Invest. 2014 May 1;124(5):2287. PMID: 24463448; PMCID: PMC3904617.*
- *Mesquita T, Lin YN, Ibrahim A. Chronic low-grade inflammation in heart failure with preserved ejection fraction. Aging Cell. 2021 Sep;20(9):e13453. doi: 10.1111/acel.13453. Epub 2021 Aug 12. PMID: 34382743; PMCID: PMC8441359.*
- *Mewton N, Liu CY, Croisille P, Bluemke D, Lima JA. Assessment of myocardial fibrosis with cardiovascular magnetic resonance. J Am Coll Cardiol. 2011 Feb*

22;57(8):891-903. doi: 10.1016/j.jacc.2010.11.013. PMID: 21329834; PMCID: PMC3081658.

- *Moravsky G, Ofek E, Rakowski H, Butany J, Williams L, Ralph-Edwards A, Wintersperger BJ, Crean A. Myocardial fibrosis in hypertrophic cardiomyopathy: accurate reflection of histopathological findings by CMR. JACC Cardiovasc Imaging. 2013 May;6(5):587-96. doi: 10.1016/j.jcmg.2012.09.018. Epub 2013 Apr 10. PMID: 23582356.*
- *Mukherjee D, Sen S. Alteration of cardiac collagen phenotypes in hypertensive hypertrophy: role of blood pressure. J Mol Cell Cardiol. 1993 Feb;25(2):185-96. doi: 10.1006/jmcc.1993.1021. PMID: 8474126.*
- *Nag AC. Study of non-muscle cells of the adult mammalian heart: a fine structural analysis and distribution. Cytobios. 1980;28(109):41-61. PMID: 7428441.*
- *Nagueh SF, Zoghbi WA. Prognostic value of stress echocardiography in stable angina or after myocardial infarction. Curr Opin Cardiol. 1996 Nov;11(6):627-34. doi: 10.1097/00001573-199611000-00012. PMID: 8968679.*
- *Nakamura, M., Sadoshima, J. Mechanisms of physiological and pathological cardiac hypertrophy. Nat Rev Cardiol 15, 387–407 (2018). 19 April 2018 Doi: 10.1038/s41569-018-0007-y*
- *Nambu H, Takada S, Fukushima A, Matsumoto J, Kakutani N, Maekawa S, Shirakawa R, Nakano I, Furihata T, Katayama T, Yamanashi K, Obata Y, Saito A, Yokota T, Kinugawa S. Empagliflozin restores lowered exercise endurance capacity via the activation of skeletal muscle fatty acid oxidation in a murine model of heart failure. Eur J Pharmacol. 2020 Jan 5; 866:172810. doi: 10.1016/j.ejphar.2019.172810. Epub 2019 Nov 15. PMID: 31738936.*
- *Nassif ME, Windsor SL, Borlaug BA, Kitzman DW, Shah SJ, Tang F, Khariton Y, Malik AO, Khumri T, Umpierrez G, Lamba S, Sharma K, Khan SS, Chandra L, Gordon RA, Ryan JJ, Chaudhry SP, Joseph SM, Chow CH, Kanwar MK, Pursley M, Siraj ES, Lewis GD, Clemson BS, Fong M, Kosiborod MN. The SGLT2 inhibitor dapagliflozin in heart failure with preserved ejection fraction: a multicenter randomized trial. Nat Med. 2021 Nov;27(11):1954-1960. doi: 10.1038/s41591-021-01536-x. Epub 2021 Oct 28.*

- *New SE, Aikawa E. Molecular imaging insights into early inflammatory stages of arterial and aortic valve calcification. Circ Res. 2011 May 27;108(11):1381-91. doi: 10.1161/CIRCRESAHA.110.234146. PMID: 21617135; PMCID: PMC3139950.*
- *Nistri S, Olivotto I, Betocchi S, Losi MA, Valsecchi G, Pinamonti B, Conte MR, Casazza F, Galderisi M, Maron BJ, Cecchi F. Prognostic significance of left atrial size in patients with hypertrophic cardiomyopathy (from the Italian Registry for Hypertrophic Cardiomyopathy). Am J Cardiol. 2006 Oct 1;98(7):960-5. doi: 10.1016/j.amjcard.2006.05.013. Epub 2006 Aug 14. PMID: 16996883*
- *Oikonomou E, Zografos T, Papamikroulis GA, Siasos G, Vogiatzi G, Theofilis P, Briasoulis A, Papaioannou S, Vavuranakis M, Gennimata V, Tousoulis D. Biomarkers in Atrial Fibrillation and Heart Failure. Curr Med Chem. 2019;26(5):873-887. doi: 10.2174/0929867324666170830100424. PMID: 28875838.*
- *Oldfield CJ, Duhamel TA, Dhalla NS. Mechanisms for the transition from physiological to pathological cardiac hypertrophy. Can J Physiol Pharmacol. 2020 Feb;98(2):74-84. doi: 10.1139/cjpp-2019-0566. PMID: 31815523.*
- *Olivotto I, Cecchi F. The epidemiologic evolution and present perception of hypertrophic cardiomyopathy. Ital Heart J. 2003 Sep;4(9):596-601. PMID: 14635376.*
- *Olivotto I, Oreziak A, Barriales-Villa R, Abraham TP, Masri A, Garcia-Pavia P, Saberi S, Lakdawala NK, Wheeler MT, Owens A, Kubanek M, Wojakowski W, Jensen MK, Gimeno-Blanes J, Afshar K, Myers J, Hegde SM, Solomon SD, Sehnert AJ, Zhang D, Li W, Bhattacharya M, Edelberg JM, Waldman CB, Lester SJ, Wang A, Ho CY, Jacoby D; EXPLORER-HCM study investigators. Mavacamten for treatment of symptomatic obstructive hypertrophic cardiomyopathy (EXPLORER-HCM): a randomised, double-blind, placebo-controlled, phase 3 trial. Lancet. 2020 Sep 12;396(10253):759-769. doi: 10.1016/S0140-6736(20)31792-X. Epub 2020 Aug 29. Erratum in: Lancet. 2020 Sep 12;396(10253):758. doi: 10.1016/S0140-6736(20)31872-9. PMID: 32871100.*
- *Ommen SR, Mital S, Burke MA, Day SM, Deswal A, Elliott P, Evanovich LL, Hung J, Joglar JA, Kantor P, Kimmelstiel C, Kittleson M, Link MS, Maron MS, Martinez MW, Miyake CY, Schaff HV, Semsarian C, Sorajja P. 2020 AHA/ACC Guideline for the Diagnosis and Treatment of Patients With Hypertrophic Cardiomyopathy: Executive Summary: A Report of the American College of Cardiology/American*

Heart Association Joint Committee on Clinical Practice Guidelines. Circulation. 2020 Dec 22;142(25): e533-e557. doi: 10.1161/CIR.0000000000000938. Epub 2020 Nov 20. PMID: 33215938.

- *Pagourelias ED, Alexandridis GM, Vassilikos VP. Fibrosis in hypertrophic cardiomyopathy: role of novel echo techniques and multi-modality imaging assessment. Heart Fail Rev. 2021 Nov;26(6):1297-1310. doi: 10.1007/s10741-020-10058-6. Epub 2021 May 15. PMID: 33990907.*
- *Palandri C, Santini L, Argirò A, Margara F, Doste R, Bueno-Orovio A, Olivotto I, Coppini R. Pharmacological Management of Hypertrophic Cardiomyopathy: From Bench to Bedside. Drugs. 2022 Jun;82(8):889-912. doi: 10.1007/s40265-022-01728-w. Epub 2022 Jun 13. PMID: 35696053; PMCID: PMC9209358.*
- *Paulus WJ, Tschöpe C. A novel paradigm for heart failure with preserved ejection fraction: comorbidities drive myocardial dysfunction and remodeling through coronary microvascular endothelial inflammation. J Am Coll Cardiol. 2013 Jul 23;62(4):263-71. doi: 10.1016/j.jacc.2013.02.092. Epub 2013 May 15. PMID: 23684677.*
- *Pawade TA, Newby DE, Dweck MR. Calcification in Aortic Stenosis: The Skeleton Key. J Am Coll Cardiol. 2015 Aug 4;66(5):561-77. doi: 10.1016/j.jacc.2015.05.066. PMID: 26227196.*
- *Peled Y, Ducharme A, Kittleson M, Bansal N, Stehlik J, Amdani S, Saeed D, Cheng R, Clarke B, Dobbels F, Farr M, Lindenfeld J, Nikolaidis L, Patel J, Acharya D, Albert D, Aslam S, Bertolotti A, Chan M, Chih S, Colvin M, Crespo-Leiro M, D'Alessandro D, Daly K, Diez-Lopez C, Dipchand A, Ensminger S, Everitt M, Fardman A, Farrero M, Feldman D, Gjelaj C, Goodwin M, Harrison K, Hsich E, Joyce E, Kato T, Kim D, Luong ML, Lyster H, Masetti M, Matos LN, Nilsson J, Noly PE, Rao V, Rolid K, Schlendorf K, Schweiger M, Spinner J, Townsend M, Tremblay-Gravel M, Urschel S, Vachiery JL, Velleca A, Waldman G, Walsh J. International Society for Heart and Lung Transplantation Guidelines for the Evaluation and Care of Cardiac Transplant Candidates-2024. J Heart Lung Transplant. 2024 Oct;43(10):1529-1628.e54. doi: 10.1016/j.healun.2024.05.010. Epub 2024 Aug 8. PMID: 39115488.*
- *Peltonen T, Näpänkangas J, Ohtonen P, Aro J, Peltonen J, Soini Y, Juvonen T, Satta J, Ruskoaho H, Taskinen P. (Pro)renin receptors and angiotensin converting enzyme*

2/angiotensin-(1-7)/Mas receptor axis in human aortic valve stenosis. Atherosclerosis. 2011 May;216(1):35-43. doi: 10.1016/j.atherosclerosis.2011.01.018. Epub 2011 Jan 21. PMID: 21316680.

- *Porter KE, Turner NA. Cardiac fibroblasts: at the heart of myocardial remodeling. Pharmacol Ther. 2009 Aug;123(2):255-78. doi: 10.1016/j.pharmthera.2009.05.002. Epub 2009 May 19. PMID: 19460403.*
- *Qiu Y, Pan X, Chen Y, Xiao J. Hallmarks of exercised heart. J Mol Cell Cardiol. 2022 Mar;164:126-135. doi: 10.1016/j.yjmcc.2021.12.004. Epub 2021 Dec 14. PMID: 34914934.*
- *Reiser PJ, Portman MA, Ning XH, Schomisch Moravec C. Human cardiac myosin heavy chain isoforms in fetal and failing adult atria and ventricles. Am J Physiol Heart Circ Physiol. 2001 Apr;280(4):H1814-20. doi: 10.1152/ajpheart.2001.280.4.H1814. PMID: 11247796.*
- *Rockey DC, Bell PD, Hill JA. Fibrosis--a common pathway to organ injury and failure. N Engl J Med. 2015 Mar 19;372(12):1138-49. doi: 10.1056/NEJMra1300575. PMID: 25785971.*
- *Roger VL, Go AS, Lloyd-Jones DM, Adams RJ, Berry JD, Brown TM, Carnethon MR, Dai S, de Simone G, Ford ES, Fox CS, Fullerton HJ, Gillespie C, Greenlund KJ, Hailpern SM, Heit JA, Ho PM, Howard VJ, Kissela BM, Kittner SJ, Lackland DT, Lichtman JH, Lisabeth LD, Makuc DM, Marcus GM, Marelli A, Matchar DB, McDermott MM, Meigs JB, Moy CS, Mozaffarian D, Mussolino ME, Nichol G, Paynter NP, Rosamond WD, Sorlie PD, Stafford RS, Turan TN, Turner MB, Wong ND, Wylie-Rosett J; American Heart Association Statistics Committee and Stroke Statistics Subcommittee. Heart disease and stroke statistics--2011 update: a report from the American Heart Association. Circulation. 2011 Feb 1;123(4): e18-e209. doi: 10.1161/CIR.0b013e3182009701. Epub 2010 Dec 15. Erratum in: Circulation. 2011 Feb 15;123(6):e240. Erratum in: Circulation. 2011 Oct 18;124(16): e426. PMID: 21160056; PMCID: PMC4418670.*
- *Rosing DR, Kent KM, Maron BJ, Condit J, Epstein SE. Verapamil therapy: a new approach to pharmacologic treatment of hypertrophic cardiomyopathy. Chest. 1980 Jul;78(1 Suppl):239-47. doi: 10.1378/chest.78.1_supplement.239. PMID: 6995039.*
- *Salvatore T, Galiero R, Caturano A, Rinaldi L, Di Martino A, Albanese G, Di Salvo J, Epifani R, Marfella R, Docimo G, Lettieri M, Sardu C, Sasso FC. An Overview of*

the Cardiorenal Protective Mechanisms of SGLT2 Inhibitors. Int J Mol Sci. 2022 Mar 26;23(7):3651. doi: 10.3390/ijms23073651. PMID: 35409011; PMCID: PMC8998569

- *Seth M, Zhang ZS, Mao L, Graham V, Burch J, Stiber J, Tsiokas L, Winn M, Abramowitz J, Rockman HA, Birnbaumer L, Rosenberg P. TRPC1 channels are critical for hypertrophic signaling in the heart. Circ Res. 2009 Nov 6;105(10):1023-30. doi: 10.1161/CIRCRESAHA.109.206581. Epub 2009 Sep 24. PMID: 19797170; PMCID: PMC2881555.*
- *Shah AK, Bhullar SK, Elimban V, Dhalla NS. Oxidative Stress as A Mechanism for Functional Alterations in Cardiac Hypertrophy and Heart Failure. Antioxidants (Basel). 2021 Jun 8;10(6):931. doi: 10.3390/antiox10060931. PMID: 34201261; PMCID: PMC8228897.*
- *Shah SJ, Lam CSP, Svedlund S, Saraste A, Hage C, Tan RS, Beussink-Nelson L, Ljung Faxén U, Fermer ML, Broberg MA, Gan LM, Lund LH. Prevalence and correlates of coronary microvascular dysfunction in heart failure with preserved ejection fraction: PROMIS-HFpEF. Eur Heart J. 2018 Oct 1;39(37):3439-3450. doi: 10.1093/eurheartj/ehy531. Erratum in: Eur Heart J. 2019 Feb 7;40(6):541. doi: 10.1093/eurheartj/ehy804. PMID: 30165580; PMCID: PMC6927847.*
- *Shahim A, Hourqueig M, Donal E, Oger E, Venkateshvaran A, Daubert JC, Savarese G, Linde C, Lund LH, Hage C. Predictors of long-term outcome in heart failure with preserved ejection fraction: a follow-up from the KaRen study. ESC Heart Fail. 2021 Oct;8(5):4243-4254. doi: 10.1002/ehf2.13533. Epub 2021 Aug 10. PMID: 34374216; PMCID: PMC8497206.*
- *Sherrid MV, Pearle G, Gunsburg DZ. Mechanism of benefit of negative inotropes in obstructive hypertrophic cardiomyopathy. Circulation. 1998 Jan 6-13;97(1):41-7. doi: 10.1161/01.cir.97.1.41. Erratum in: Circulation 1998 Mar 17;97(10):1026. PMID: 9443430.*
- *Shimizu I, Minamino T. Physiological and pathological cardiac hypertrophy. J Mol Cell Cardiol. 2016 Aug; 97:245-62. doi: 10.1016/j.yjmcc.2016.06.001. Epub 2016 Jun 2. PMID: 27262674.*
- *Slivnick J, Lampert BC. Hypertension and Heart Failure. Heart Fail Clin. 2019 Oct;15(4):531-541. doi: 10.1016/j.hfc.2019.06.007. Epub 2019 Jul 31. PMID: 31472888.*

- *Spirito P, Seidman CE, McKenna WJ, Maron BJ. The management of hypertrophic cardiomyopathy. N Engl J Med. 1997 Mar 13;336(11):775-85. doi: 10.1056/NEJM199703133361107. PMID: 9052657.*
- *Stella JA, Sacks MS. On the biaxial mechanical properties of the layers of the aortic valve leaflet. J Biomech Eng. 2007 Oct;129(5):757-66. doi: 10.1115/1.2768111. PMID: 17887902.*
- *Stenmark KR, Yeager ME, El Kasmi KC, Nozik-Grayck E, Gerasimovskaya EV, Li M, Riddle SR, Frid MG. The adventitia: essential regulator of vascular wall structure and function. Annu Rev Physiol. 2013; 75:23-47. doi: 10.1146/annurev-physiol-030212-183802. Epub 2012 Dec 3. PMID: 23216413; PMCID: PMC3762248.*
- *Tallquist MD. Cardiac Fibroblast Diversity. Annu Rev Physiol. 2020 Feb 10; 82:63-78. doi: 10.1146/annurev-physiol-021119-034527. PMID: 32040933; PMCID: PMC10939057.*
- *Tanjore R, Rangaraju A, Vadapalli S, Remersu S, Narsimhan C, Nallari P. Genetic variations of β-MYH7 in hypertrophic cardiomyopathy and dilated cardiomyopathy. Indian J Hum Genet. 2010 May;16(2):67-71. doi: 10.4103/0971-6866.69348. PMID: 21031054; PMCID: PMC2955954.*
- *Teekakirikul P, Zhu W, Huang HC, Fung E. Hypertrophic Cardiomyopathy: An Overview of Genetics and Management. Biomolecules. 2019 Dec 16;9(12):878. doi: 10.3390/biom9120878. PMID: 31888115; PMCID: PMC6995589.*
- *Tomasoni D, Adamo M, Lombardi CM, Metra M. Highlights in heart failure. ESC Heart Fail. 2019 Dec;6(6):1105-1127. doi: 10.1002/ehf2.12555. PMID: 31997538; PMCID: PMC6989277.*
- *Verdecchia P, Murdolo G, Coiro S, Santucci A, Notaristefano F, Angeli F, Cavallini C. Therapy of Type 2 diabetes: more gliflozines and less metformin? Eur Heart J Suppl. 2023 Apr 21;25(Suppl B):B171-B176. doi: 10.1093/eurheartjsupp/suad098. PMID: 37091638; PMCID: PMC10120941.)*
- *Verma S, Rawat S, Ho KL, Wagg CS, Zhang L, Teoh H, Dyck JE, Uddin GM, Oudit GY, Mayoux E, Lehrke M, Marx N, Lopaschuk GD. Empagliflozin Increases Cardiac Energy Production in Diabetes: Novel Translational Insights into the Heart Failure Benefits of SGLT2 Inhibitors. JACC Basic Transl Sci. 2018 Aug 26;3(5):575-587. doi: 10.1016/j.jacbts.2018.07.006. PMID: 30456329; PMCID: PMC6234616.*

- *Weber KT, Sun Y, Bhattacharya SK, Ahokas RA, Gerling IC. Myofibroblast-mediated mechanisms of pathological remodelling of the heart. Nat Rev Cardiol. 2013 Jan;10(1):15-26. doi: 10.1038/nrcardio.2012.158. Epub 2012 Dec 4. PMID: 23207731.*
- *Wei K, Nguyen HN, Brenner MB. Fibroblast pathology in inflammatory diseases. J Clin Invest. 2021 Oct 15;131(20): e149538. doi: 10.1172/JCI149538. PMID: 34651581; PMCID: PMC8516469.*
- *Wilkins BJ, Molkentin JD. Calcium-calcineurin signaling in the regulation of cardiac hypertrophy. Biochem Biophys Res Commun. 2004 Oct 1;322(4):1178-91. doi: 10.1016/j.bbrc.2004.07.121. PMID: 15336966.*
- *Wiviott SD, Raz I, Bonaca MP, Mosenzon O, Kato ET, Cahn A, Silverman MG, Zelniker TA, Kuder JF, Murphy SA, Bhatt DL, Leiter LA, McGuire DK, Wilding JPH, Ruff CT, Gause-Nilsson IAM, Fredriksson M, Johansson PA, Langkilde AM, Sabatine MS; DECLARE–TIMI 58 Investigators. Dapagliflozin and Cardiovascular Outcomes in Type 2 Diabetes. N Engl J Med. 2019 Jan 24;380(4):347-357.*
- *Yan GX, Wu Y, Liu T, Wang J, Marinchak RA, Kowey PR. Phase 2 early afterdepolarization as a trigger of polymorphic ventricular tachycardia in acquired long-QT syndrome: direct evidence from intracellular recordings in the intact left ventricular wall. Circulation. 2001 Jun 12;103(23):2851-6. doi: 10.1161/01.cir.103.23.2851. PMID: 11401944.*
- *Yoshida T, Delafontaine P. Mechanisms of IGF-1-Mediated Regulation of Skeletal Muscle Hypertrophy and Atrophy. Cells. 2020 Aug 26;9(9):1970. doi: 10.3390/cells9091970. PMID: 32858949; PMCID: PMC7564605.*
- *Yue Y, Meng K, Pu Y, Zhang X. Transforming growth factor beta (TGF-β) mediates cardiac fibrosis and induces diabetic cardiomyopathy. Diabetes Res Clin Pract. 2017 Nov; 133:124-130. doi: 10.1016/j.diabres.2017.08.018. Epub 2017 Sep 1. PMID: 28934669.*
- *Zhang J, Tao R, Campbell KF, Carvalho JL, Ruiz EC, Kim GC, Schmuck EG, Raval AN, da Rocha AM, Herron TJ, Jalife J, Thomson JA, Kamp TJ. Functional cardiac fibroblasts derived from human pluripotent stem cells via second heart field progenitors. Nat Commun. 2019 May 20;10(1):2238. doi: 10.1038/s41467-019-09831-5. PMID: 31110246; PMCID: PMC6527555.*